The Thesis Committee for Eric Carl Dierks
Certifies that this is the approved version of the following thesis:

Design of an Electromagnetic Vibration Energy Harvester for Structural Health Monitoring of Bridges Employing Wireless Sensor Networks

APPROVED BY
SUPERVISING COMMITTEE:

Supervisor:

Kristin L. Wood

Richard H. Crawford

Design of an Electromagnetic Vibration Energy Harvester for Structural Health Monitoring of Bridges Employing Wireless Sensor Networks

by

Eric Carl Dierks, BSME

Thesis

Presented to the Faculty of the Graduate School of

The University of Texas at Austin

in Partial Fulfillment

of the Requirements

for the Degree of

Master of Science in Engineering

The University of Texas at Austin

August 2011

Acknowledgements

I would like to thank Dr. Kris Wood, Dr. Dan Jensen, Dr. Sharon Wood, and Dr. Rich Crawford for providing me this great research opportunity, financial support and for their guidance and advice over the past year and a half. I am grateful of the institutions responsible for the creation of the project: the Office of the Secretary of Defense: Corrosion Policy, the National Institute for Standards and Technology: Technology Innovation Program, the Department of Mechanical Engineering at The University of Texas at Austin, and the Department of Engineering Mechanics at the United States Air Force Academy. The Civil and Electrical Engineering professors and students who continue to participate in the project were also a great resource: Dr. Todd Helwig, Jeremiah Fasl, Matt Riechenbach, Vasilis Vasamaras, Dr. Dean Niekirk, and Dr. Praveen Pasupathy. I am also very thankful for Dr. Preston Wilson and Dr. Eric Farenthold, who gave technical advice and lent lab equipment in his free time. Mark Phillips was very helpful in lending additional electronic lab equipment and overseeing SLS printing, and Danny Jares always provided great machining advice throughout the prototype development. Scott Allen was also very helpful in procuring raw materials for the prototype. I would also like to thank my fellow Mechanical Engineering students: Sumedh Inamdar, Jason Weaver, Scott Dale, Katie Carpenter, Mikko Ponkala, Jorge Flores and Travis McEvoy, who contributed in various ways. Finally, I would like to thank my parents for graciously helping every time I needed them, supporting my decision to attend graduate school and their contribution to my understanding and enjoyment of the way things work.

August 12, 2011

Abstract

Design of an Electromagnetic Vibration Energy Harvester for Structural Health Monitoring of Bridges Employing Wireless Sensor Networks

Eric Carl Dierks, MSE

The University of Texas at Austin, 2011

Supervisor: Kristin L. Wood

Energy harvesting is playing an increasingly important role in supplying power to monitoring and automation systems such as structural health monitoring using wireless sensor networks. This importance is most notable when the structures to be monitored are in rural, hazardous, or limited access environments such as busy highway bridges where traffic would be greatly disrupted during maintenance, inspection, or battery replacement. This thesis provides an overview of energy harvesting technologies and details the design, prototyping, testing, and simulation of an energy harvester which converts the vibrations of steel highway bridges into stored electrical energy through the use of a translational electromagnetic generator, to power a wireless sensor network for bridge structural health monitoring. An analysis of bridge vibrations, the use of nonlinear and linear harvester compliance, resonant frequency tuning, and bandwidth widening to maximize the energy harvested is presented. The design approach follows broad and

focused background research, functional analysis, broad and focused concept generation and selection, early prototyping, parametric modeling and simulation, rapid prototyping with selective laser sintering, and laboratory testing with replicated bridge vibration. The key outcomes of the work are: a breadth of conceptual designs, extensive literature review, a prototype which harvests an average of 80μW under bridge vibration, a prototype which provides quick assembly, mounting and tuning, and the conclusion that a linear harvester out performs a nonlinear harvester with stiffening magnetic compliance for aperiodic vibrations such as those from highway bridges.

Table of Contents

List of Tables

List of Figures

Chapter 1: Introduction

1.1: Need For the Project

The structural integrity of our nation's infrastructure is constantly decreasing due to fatigue and corrosion, with a direct impact on the public's safety and their pocket book. According to the Federal Highway Administration (FHA), 146,633 (24.2%) of the 604,474 total bridges in the United States are structurally deficient as of December 2010 (Federal Highway Administration, 2010). Figure 1 shows the distribution of a portion of these bridges. The current strategy in Texas is to manually inspect the bridges that are deemed fracture critical every five years, with the inspection interval decreasing to every two years in the near future. This approach may sound acceptable, but recent failures and collapses of bridges which were serviced within this interval provide evidence to the contrary. For instance, the I-35W Mississippi River Bridge in Minnesota which collapsed in 2007, only one year after manual inspection (National Transportation Safety Board, 2007).

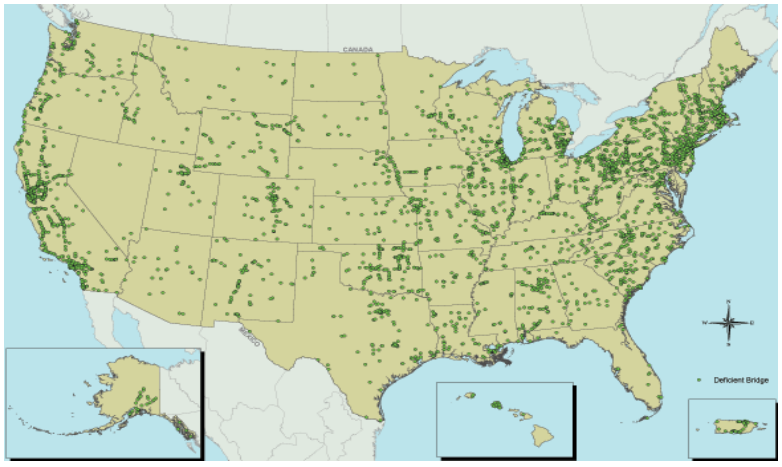

Figure 1. Distribution of structurally deficient bridges across the U.S. (RITA, 2007).

Inspections of bridges, new and old, every two years take large budgetary and human resources. The manual inspections often require closing off traffic to allow inspection trucks access to the bridge structure using what are called Snoopers, as shown in Figure 2 (Missouri Department of Transportation, 2011). Additionally, the FHA has reported that manual inspections following the National Bridge Inspection Standard often result in unreliable and subjective assessment, and that more detailed inspection of deficient bridges are not likely to deliver a more concrete assessment using current methods (Turner-Fairbank Highway Research Center: Federal Highway Administration, 2001).

Figure 2. Equipment in use during manual bridge inspection (Missouri Department of Transportation, 2011).

These challenges may be mitigated with the use of a structural health monitoring system employing sensors and wireless communications to relay measurements to offsite operators. Monitoring may then be performed frequently and with higher precision than manual inspections while limiting human-related errors and investment of human resources. Such a system could eventually pay for itself with a reduction of manual inspections as the reliability and safety of monitoring is proven over long-term use. A

basic schematic of a wireless structural health monitoring system is shown in Figure 3, where wireless sensor network (WSN) nodes collect, pre-process, and transmit data to a WSN gateway (aka receiver unit) through either a structured network utilizing dedicated WSN routers (aka relays), or in an unstructured, ad-hoc network where the sensor nodes relay data from other nodes to the gateway. The gateway performs additional data processing before transmitting to the host computer through an Ethernet cable or long-range wireless network.

Figure 3. Example wireless sensor network configuration for remote monitoring (National Instruments, 2011).

There is an ever-growing need for monitoring and automating processes and structures throughout many industrial domains, with strong progress in the past ten years as shown in Figure 4 (Google, 2010). In combination, these factors produce an area of great need and promise for future expansion as government and industry wish to increase safety and efficiency while adding precision and reducing human-related error (Duderstadt, 2005; Pisano & Shih, 2009).

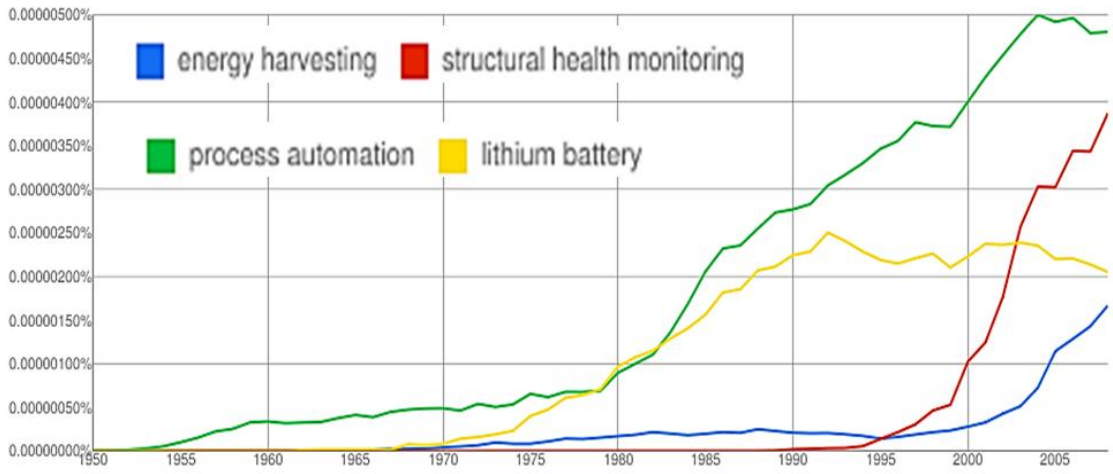

Figure 4. Relevant research trends over the past sixty years (Google, 2010).

Five approaches may be considered for a power source: grid electricity, pre-charged batteries, generative power sources such as combustion-based generators, continuous energy harvesting without storage, and energy harvesting with storage. Hard wiring power from the grid to each component of the network for thousands of bridges would incur large installation costs in addition to the cost to power the system for several decades. Rural bridges would incur additional costs as connection to the electrical grid is not convenient. For these reasons wireless power sources are preferred. Pre-charged batteries are the next logical step but batteries powering each WSN component may have to be replaced frequently depending upon the respective power consumption. Replacement of batteries every few years in each monitoring component on thousands of bridges would be very labor and cost intensive (Weaver, Crawford, & K. L. Wood, 2010). Additionally, monitoring of remote or hazardous locations make batteries even less attractive. Gas generators could similarly take the place of the grid for each bridge but with similar problems faced by batteries, as a constant fuel supply is needed.

Energy harvesting power supplies able to operate for decades at a time, dependent only upon ambient energy sources such as light, wind, heat, water, or vibration could give these wireless systems true and far-reaching potential. Energy harvesters may be connected directly to the load to deliver power in a continuous fashion or may charge a storage system which delivers power to the load. A continuous system would likely be simpler and cheaper but at the cost of limited harvesters which can supply adequate power continuously. Most harvesters utilize a storage system such as a battery to accumulate the harvested energy and deliver it to the load often at higher power levels than the harvester can supply directly. This allows a broader range of energy sources and harvesting techniques to be used which harvest at low power over long periods of time, then deliver at high power over short periods of time. The benefits of energy harvesting power supplies is evident in the rapid increase of work in industry and academia on energy harvesting over the past ten years, as was shown in Figure 4. This figure was generated using Google Labs' Ngram Viewer, which is a free tool that plots the percentage of all websites and books in Google's index containing the given search terms over time. The figure shows increasing work on energy harvesting is likely in response to the growth of process automation and structural health monitoring, and possibly the slowing of growth in lithium-ion battery related work.

Finally, it is interesting to note here that the automation of structural health monitoring through wireless networks and energy harvesting is just one of many examples of Altshuller's laws concerning the evolution of technical systems (Altshuller, 1984). One such law is the law of increasing the idealness of the system, which is represented by the desire for the bridge itself to notify operators when a problem arises, provide the operators with data to explain the problem, and do so under its own power. A second relevant law is the law of increasing the S-Field involvement, which describes the

evolution of systems from mechanical to electro-magnetic components often with increased interlinking between components and increased system responsiveness.

1.2: PROJECT DESCRIPTION

The National Institute for Standards and Technology's (NIST) Technology Innovation Program (TIP) has funded a five year research project to address the need for energy harvesting wireless structural health monitoring of highway bridges. NIST has deemed structural health monitoring of failing infrastructure an area of critical need with nation-wide societal impact (NIST Technology Innovation Program, 2008). The Office of the Secretary of Defense: Office of Corrosion Policy and Oversight has also provided some funding through collaboration of the author with cadets in the senior design course at the United States Air Force Academy.

The NIST project group is an interdisciplinary team composed of professors and graduate students in the Civil, Electrical, and Mechanical Engineering departments at The University of Texas at Austin (UT), as well as National Instruments (NI) and Wiss, Janney, Elstner Associates (WJE). NI is contributing the wireless communications system, while WJE is contributing advice on structural instrumentation from their experience in industry. The Electrical Engineering group is developing passive corrosion sensors which are not connected to the wireless system and are powered by a passing inspection vehicle, while the Mechanical Engineering group is developing energy harvesting solutions. The Civil Engineering group provides instrumentation of bridges, sensor selection and testing, sensor data processing, and serves as overall project management.

1.2.1: Bridge Types

Three types of bridges are targeted for inspections by the project: Box Girder, I-Girder, and Truss. An example of each is given in Figures 5 and 6 with desired sensor locations indicated. A successful system will consider all three types, but priority will be given to I-Girder bridges as the box girder design's status as fracture critical is under debate, and truss bridges are much less common.

(a) (b)

Figure 5 External (a) and internal (b) views of a typical box girder bridge.

(a) (b)

Figure 6. Underside of a typical I-Girder bridge (a), and typical truss bridge (b).

1.2.2: Monitoring System Description

The monitoring system proposed is represented by the schematic shown in Figure 7. Several strain gages and crack propagation gages are wired to each NI Wireless Sensor Network node. These nodes contain a LabVIEW Real-Time target (Field Programmable Gate Array) to perform data acquisition and initial processing using LabVIEW (National Instruments, 2011). The coded system will regulate the power usage, such as sleep mode to reduce power demand, as well as data transmission to the WSN router. The router is identical to a node but does not enter sleep mode such that all incoming transmissions may be relayed to the WSN gateway. The gateway is very similar to an NI CompactRIO, and is used to process and send the data to the host computer (aka host controller) offsite through a cellular telephone network. The gateway is located at one end of the bridge, where hard-wire access is easiest. An energy harvester will power one to several nodes, while one to several harvesters may be needed to power the router. The gateway will be powered by solar panels due to its high power demand and location at the bridge end away from under-passing traffic. The collected data will be processed to determine the state of stress of the girders (S. L. Wood & Dean, 2007).

1.2.3: Energy and Power Requirements

Calculation of average power usage by the WSN node and router were presented in Weaver, Crawford, & Wood, 2010 as part of this project. The major results are shown in Table 1 and Figure 8. In summary, the long-term average power usage of the WSN node is about 0.5 mW, while the router and gateway require about 200 mW and 5-10 W respectively. These values were calculated based upon the current commercially available NI WSN system components, but future generations under development are likely to require less power as the efficiencies, algorithms, and protocols are improved.

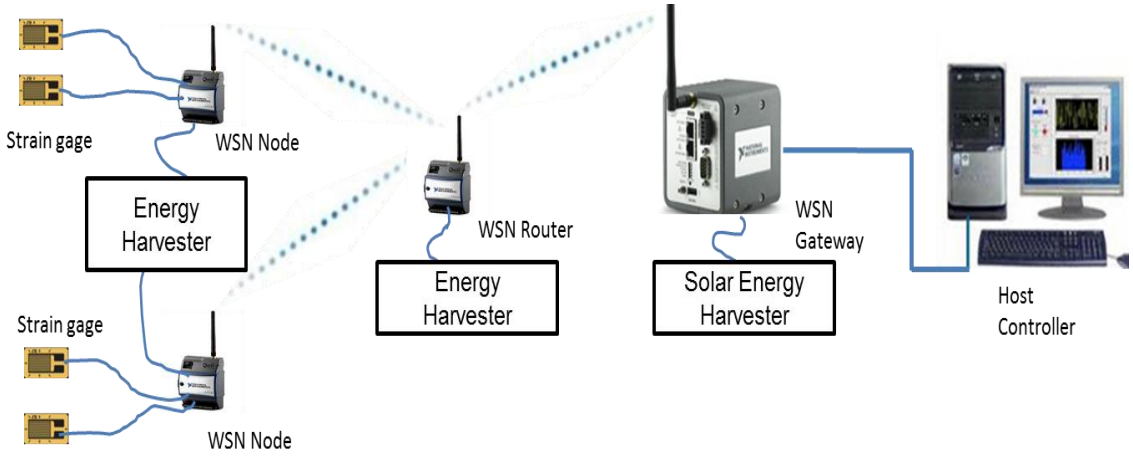

Figure 7. Schematic of wireless monitoring system.

Table 1. WSN node average power consumption and duration by function (Weaver et al., 2010).

Function	Power (mW)	Δt (ms)
Power-up	200	12.4
Settle power	52.5	14.5
Measure analog	73.4	13.0
Prepare data	37.9	12.0
Radio activity	207	29.0
Total – active period	154 (average)	81
Sleep period	0.3	variable

1.2.4: Energy Harvester Customer Needs

A detailed specification sheet was created to define the properties a successful energy harvester must have to satisfy the customers, which for now are the Civil Engineers involved in the project. They were interviewed to gain an understanding of their preferences, and a portion of the questions and responses of this interview is available in Appendix A. The specification sheet was split into two components which define the functional requirements and constraints, respectively. The most significant functional requirements are noted with a star and concern the average energy generation per year, instantaneous power level during continuous sampling, and the DC output voltage

required to power a WSN node. The third and fourth requirements listed concern the router and gateway, respectively. Ideally a single harvester will be designed to meet the energy needs of the node, router, and gateway while upholding the constraints, but is not likely in the initial phase of this project. The first step is to meet the requirements of the node, then progress to the other, higher power components. Noteworthy constraints are also starred in Tables B2 and B3 of Appendix B, and include prohibited traffic interference, damage and theft protection, ease and speed of installation, allowable bridge alterations, installation locations, and long lifespan between maintenance.

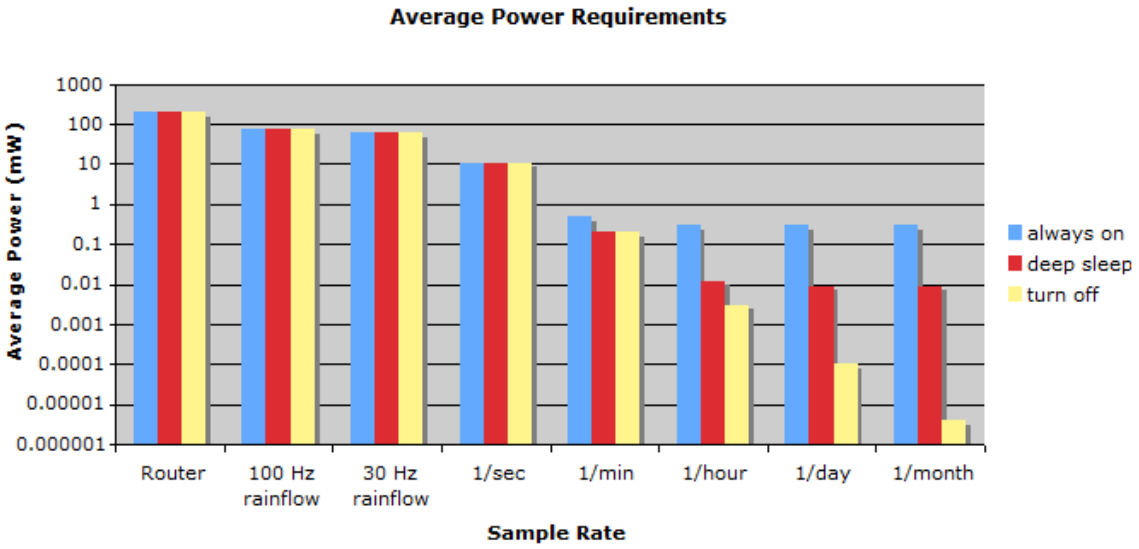

Figure 8. Average power requirements of WSN node for various sample rates (Weaver et al., 2010).

Table 2. Functional requirements of successful energy harvester.

Demand or Wish	Specification		Test / Verification
Functional Requirements			
★ **D**	Generate long-term energy level of	> 104 Wh/year (375 kJ/year)	analytical models, field testing
★ **D**	Provide power level continuously for 2 weeks of	> 61 mW	analytical models, field testing
W	Provide continuous power for router of	> 207 mW (1.8 kWh/year, 6.5 MJ/year)	analytical models, field testing
W	Provide continuous power to gateway like CompactRio	> 10 W (88 kWh/year, 315 MJ/year)	analytical models, field testing
D	Store enough energy to go two weeks with no harvesting input	> 20 Wh (75 kJ)	analytical models, field testing
★ **D**	Provide DC voltage	6 V DC, constant	analytical models, field testing
D	Provide DC current	200 mA, max pulse	analytical models, field testing
W	Communicate to central node	*lack of power, *malfunction	analytical models, field testing

1.3: CHALLENGES AND OPPORTUNITIES

The specification sheet points out several challenges and opportunities concerning the development of energy harvesters for this application. Many solutions may be infeasible because traffic cannot be interrupted or disturbed, and the harvester may not hang below girders where traffic passes beneath. Damage from hail, vandalism, theft, and birds, as well as corrosion push the harvesters to be self-contained, strongly attached, and possibly disguised into the bridge environment. At this time the alteration of the bridge structure is prohibited, restricting welding, bolting, and potentially unsafe mounting via epoxy or magnets. Of greatest importance is the relatively high average power levels the harvesters must provide to the monitoring system. Previous work at Clarkson University showed a low power sensor node could be powered from bridge vibrations, but the

current project's requirements take the demand to a new level (Sazonov, Curry, & P. Pillay, 2009).

If bridge vibration is considered as a viable energy source, careful study of its characteristics is important as harvesting ambient vibration is more complex than harvesting constant, small frequency range vibrations common in vibration harvesting research (Beeby, M J Tudor, & N M White, 2006). The challenges and opportunities are caused by the low acceleration amplitude (peaks less than +-0.2g), low frequency, and multi-frequency vibrations which are dependent upon location, temperature, traffic load and speed, and bridge age. Technically, the bridge vibration is classified as aperiodic, non-stationary, and non-ergodic, meaning the vibration is relatively random with a shift in frequencies over time, and measurements recorded at different times do not have equal RMS values. The real challenge appears in interpreting this data to make decisions for the successful design of robust yet powerful vibration energy harvesters.

1.4: HYPOTHESIS AND RESEARCH OBJECTIVES

The hypothesis of this thesis is as follows:

> *A vibration energy harvester using electromagnetic induction is capable of powering an NI WSN node with the functional requirements and constraints stated in the specification sheet.*

The objectives of this research are as follows:

- *Generate concepts of electromagnetic vibration energy harvesters for bridge applications*
- *Create a lumped-parameter model of the selected harvester*
- *Perform numerical simulations of the model to predict performance*
- *Design and build a prototype of the selected concept*

- *Test the prototype to evaluate power generation and compare results with the simulations*
- *Suggest a next generation design using the insights gained from the process*

1.5: THESIS ORGANIZATION

The remainder of this thesis begins with a review of energy harvesting technologies in chapter 2. Chapter 3 presents the results of concept generation of several types of energy harvesters for the given application, the decision to pursue vibration harvesting using induction, and the subsequent measurement and analysis of bridge vibrations to define the scope for further design. Chapter 4 then provides a focused literature review on electromagnetic vibration energy harvesting, amassing the required information for focused conceptual design in chapter 5. This chapter first presents generated concepts, the selection of one to prototype, an analytical model of the harvester, its embodiment and numerical model. The prototype fabrication, initial parameter measurement, testing, and comparison with simulation follow in chapter 6. Chapter 7 then presents a refined prototype with added functionality. The thesis concludes with a summary and discussion of future work to be carried by another graduate student on the project.

Chapter 2: Review of Energy Harvesting

Energy harvesting is an emerging technological field with potential to find its way into the everyday life of the public, across markets, socioeconomic backgrounds, and geographical locations. It is a broad field, defined by IDTechEx's report for the *Energy Harvesting Journal* as "the use of ambient energy to provide electrical power for small electronic and electrical devices making them self-sufficient – often for decades. The technologies employed variously convert human power, body fluids, heat differences, vibration or other movement, dirt, vegetation, ultraviolet, visible light or infrared to electricity" (Harrop, 2009)[1].

Some of the prominent energy harvesting technologies include capturing solar radiation through photovoltaic cells and heat engines, wind and water flow through turbines and aeroelastic flutter, mechanical vibration through piezoelectric, electrostatic, and electromagnetic transducers, heat through thermoelectric ceramics, turbines, and Stirling engines, human power through hand cranks and vibration methods, and ambient radio waves acquired by antennae. A sub-category of energy harvesting is energy scavenging, which involves capturing ambient energy that is either not regularly predictable with ease, only available in short emissions over long time periods, or would otherwise be lost as waste heat or noise (Priya & Inman, 2008). An example of energy scavenging is the concept of a vehicle detection system in a rural or military environment where wireless communications are powered by the vibrations of the passing vehicles. These scavengers could lie dormant for years until activated, consuming no energy until needed.

[1] This chapter contains many figures from the sources under review, with citations to the original source. The author of this thesis does not claim copyright on any figures or tables with a citation in the caption.

Energy harvesting has grown in popularity as the demand for more information in more locations with less human involvement has increased (Google, 2010). This growth is shown by the following needs for energy harvesting (Dierks, 2011; Weaver, 2010):

- *Manufacturers desire to reduce downtime caused by machine failure without cluttering the building with wires.*
- *Oil and gas pipeline operators wish to reduce inspections on remote locations.*
- *Infrastructure and aerospace structures need to be monitored for structural weakness.*
- *The shipping industry desires higher resolution tracking of trucks, packages, and equipment.*
- *Users demand laptops with longer battery life.*
- *Facility owners wish to reduce lighting installation costs.*
- *Militaries desire long distance tracking of unconventional, mobile threats.*
- *Rural undeveloped communities need light at night.*
- *Cities desire lower costs by picking up trash only when it is full.*

The increasing prominence of smart electronic devices and low power wireless networks coupled with the ever-decreasing energy usage of CPUs, actuators, circuitry, and software is enabling even further application diversity.

2.1: ENERGY SOURCES

Many energy sources exist for a given application. A visualization of many found in a search of literature and commercial products is given in Figure 9 in the form of a mind map (Dierks, 2011; Weaver, 2010). In this mind map, the energy domain is given as a node and the sub-domains and their energy sources are given as branches from the node. The sources are grouped into four main energy domains: mechanical, chemical,

electromagnetic, and thermal, with mechanical being subdivided into solid, liquid, and gas motion. Biological sources form a subdivision of the chemical domain since a chemical process is at the heart of every biological system. In a similar manner, nuclear energy sources contribute to the thermal and electromagnetic domains. Although the figure does represent a comprehensive survey-identifying every possible source of energy for harvesting—it does span a large segment of the available energy sources pertaining to energy harvesting. This mind map, and those found throughout this thesis, serve to give a broad overview of the possibilities that may be chosen for investigation as a solution to a given application.

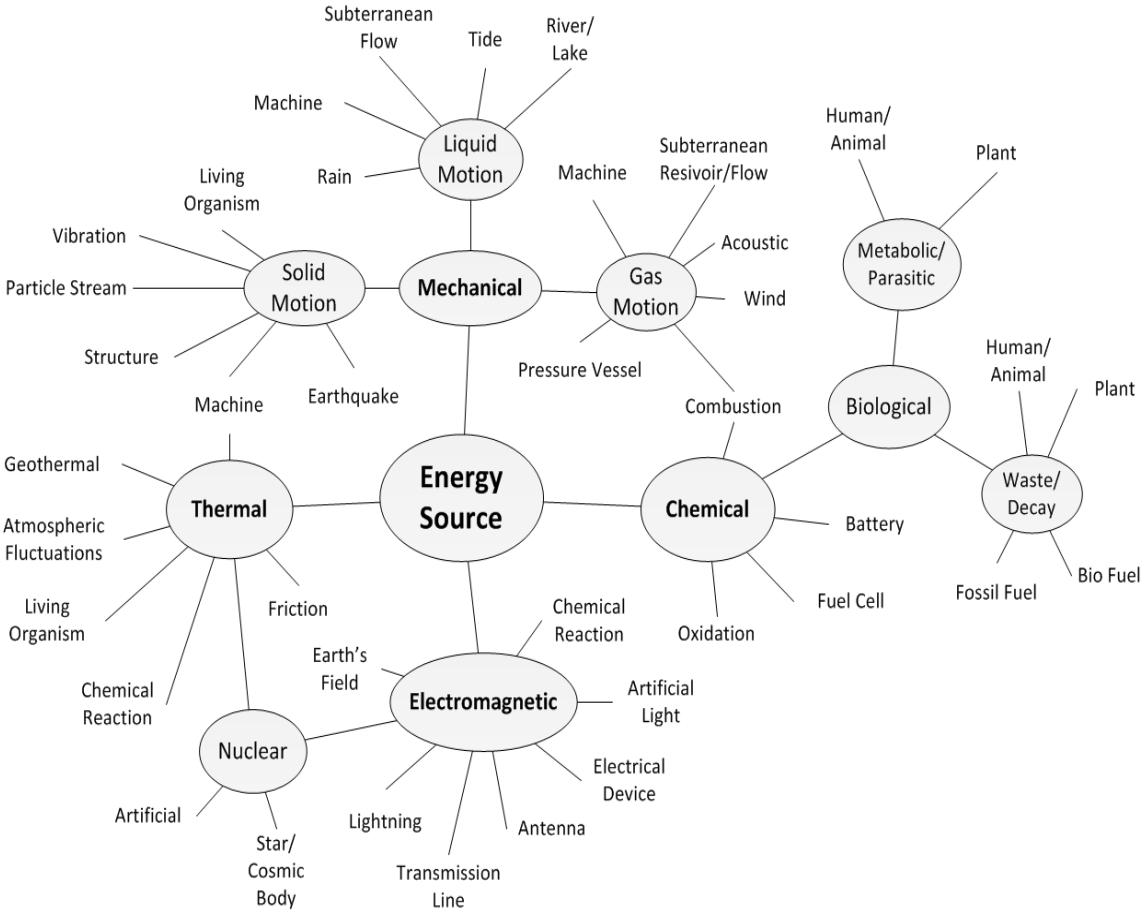

Figure 9. Mind map of energy sources organized by energy domain.

Some of the sources may require additional explanation for clarity, such as Particle Stream, under Solid Motion. A harvester exists which uses radiated atomic particles building up on a cantilevered beam, deflecting the beam until dislodging, causing the beam to spring upward and oscillate (Beeby et al., 2006). Additionally, Metabolic/Parasitic refers to extracting metabolic energy from living matter, such as plants or animals, in a parasitic manner but without killing the organism. A commercially available harvester exists which claims to be powered from tree roots for forest fire monitoring (Voltree Power, 2009).

To narrow the scope of possible solutions, it is necessary to determine which, if any, of the categories of harvesters are feasible given current technology and the operating conditions of the application. One area of feasibility determination is the harvester's ability to provide sufficient power for a given application load. The first step in determining power feasibility is an understanding of the environmental energy available for harvesting. Because energy harvesters may be scaled up or down to match the required power, a useful metric for comparison is power density. This metric is the power the system can provide, normalized by area, volume, or mass depending upon the system and information available. The theoretical maximum power density can be determined from the fundamental equations or models describing each environmental process. These theoretical maximums must also be compared to the actual power densities observed in baseline commercial and experimental energy harvesters to be fully reliable. A brief summary of the power densities of some energy harvesting technologies was created by Weaver, et al., and is presented in Table 3. The simplified calculations are based upon the primary power equations for each domain, which are used to predict theoretical and practical maximums with common parameters. Several more possibilities of harvesters exist than are given in Table 3. For example, studies of energy harvesting

from the human body are not included, but are available in the following sources (Annalisa Bonfiglio & Danilo De Rossi, 2010; Saez, 2004; Starner, 1996).

Table 3. Power densities of several energy harvesting sources (Roundy, Wright, & Rabaey, 2004).

Model	Theoretical Max	Practical Max	Parameters
$P=\eta EA$	100 mW/cm^2	3,750 μW/cm^2	1 kW/m^2 irrad., 15% eff., 6 hr. insol.
$P=0.5\rho Sv^3C$	4.45 mW/cm^2	380 μW/cm^2	5 m/s, 5% conversion eff.
$P=m\zeta_e A^2/4\omega\zeta_T^2$	19 mW/cm^3	300 μW/cm^3	Tungsten mass, 1 Hz, .01 ζ_e, .02 ζ_t
$P=0.5\rho Sv^3C$	3.7 W/cm^2	67 μW/cm^2	5 m/s, 5% conversion eff.
$P=\eta_C k\Delta T/L$	117 mW/cm^2	40 μW/cm^2	5°C differential, silicon, 1 cm length
$P=\eta EA$	5 mW/cm^2	10 μW/cm^2	Shade reduces both irrad. & eff.
$\Delta E=mR\Delta T$	17 μW/cm^3	3 μW/cm^3	helium, 10°C temp change/day
$P=P_0\lambda^2/4\pi R^2$	50 μW/receiver	2 μW/receiver	1 W transmitter, 5 m away, 2.4 GHz
$P=A_cE_e$	1.6x10^6 W/cm^3	0.52 μW/cm^3	^{63}Ni activating an oscillator
$I=P_{ac}/4\pi R^2$	0.96 μW/cm^2	0.1 μW/cm^2	100 dB

2.2: Energy Conversion

Figure 10 provides a mind map of energy conversions between domains. The domains are represented as nodes and the mechanisms or processes for converting between domains are represented as lines linking the nodes. The choice of conversion mechanism will affect the power density for the harvester, so a careful study of the advantages and disadvantages particular to the application should be included when considering energy-conversion choices. A brief introduction to most of these conversions as well as the energy sources of Figure 9 follows, with emphasis on those most commonly used today. Links to manufacturers of many kinds of energy harvesters and accessories, as well as more detailed information may be found in the Energy Harvesting

Forum and Energy Harvesting Journal (Energy Harvesting Forum, 2011; IDTechEx, 2011).

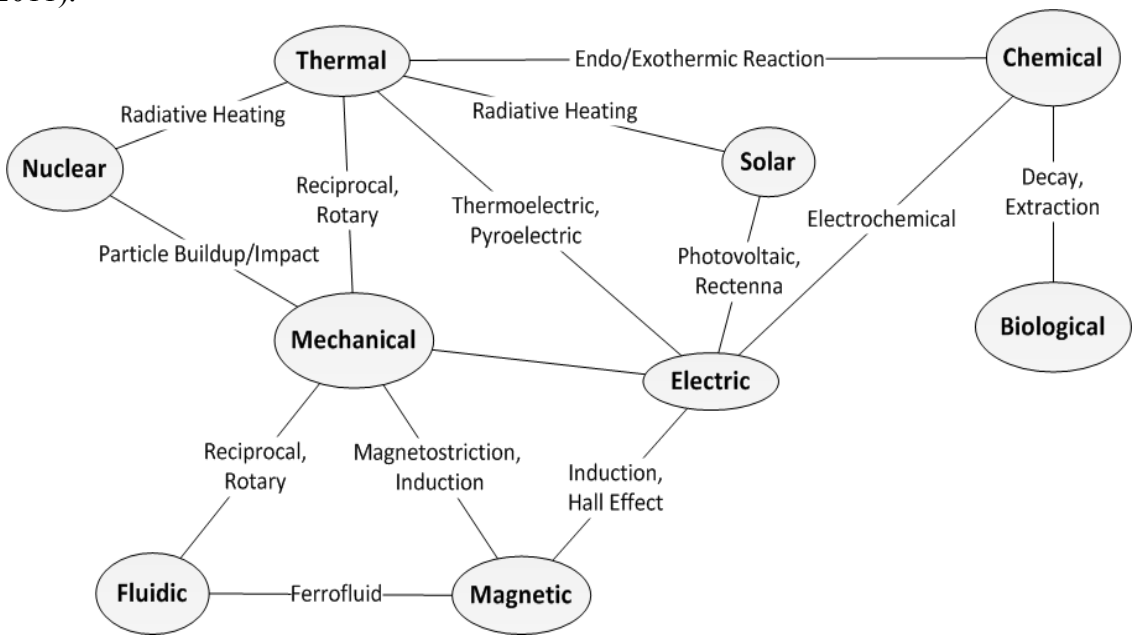

Figure 10. A map of transduction mechanisms and processes for converting between energy domains.

2.2.1: Solar Energy Harvesting

As shown in Table 3, photovoltaic (PV) solar power is by far the most power dense, surpassing wind and vibration by an order of magnitude. The power available from solar irradiation is governed by the relationship:

$$P = \eta E A_{cell} \tag{2.1}$$

where P is the power output (W), η is the efficiency, E is the solar irradiation (W/m^2), and A_{cell} is the area of the photovoltaic cell (m^2). The current maximum efficiencies for PV technologies are 25% for single-crystal silicon, 20% for thin-film silicon, and claims of more than 40% for multiple-junction cells (Solar Panel Center, 2011). Most economical PV panels use poly-crystalline, thin-film, or amorphous silicon and exhibit efficiencies ranging from 5% to 15%. Recently, flexible photovoltaic cells have been

developed and are now commercially available, allowing a decrease in required storage volume (Silicon Solar, 2011). One advantage of photovoltaic cells, besides the high power density, is no rectification circuit is needed as the voltage out is DC.

The most significant parameter in characterizing a solar energy source is solar irradiance, measured in watts per square meter. Long-term levels of solar energy are described by comparing the total irradiance per day to an equivalent number of hours at a constant irradiance of 1,000 W/m^2. This relationship is called the solar insolation. Solar irradiance is commonly measured with a lux meter. Long-term average insolation is available in the literature for most major U.S. cities for both summer and winter (Sundance Power Systems Inc., 2011). Levels of solar irradiation vary in the short-term due to weather patterns and seasonal variation, but long-term average levels are reasonably consistent and well documented (Sundance Power Systems Inc., 2011). This makes sizing a system for a given power output a straightforward process of gathering data on irradiation in the area, determining voltage and current needs, and specifying the appropriate size of solar panels and battery.

Solar technology does have several shortcomings concerning some applications. A first concern is maintenance. Solar panels designed for outdoor use often have estimated lives of twenty years or more, but they may require periodic cleaning or other maintenance. In many circumstances occasional rain is sufficient to remove dust, but panels may be subject to much higher levels of debris ranging from grease and dirt to animal droppings, bird nests, and litter. Precaution should also be used in environments where hail occurs regularly. A second concern is the need for direct sunlight to operate at peak capacity. In the shade, both the available irradiation and the panel efficiency itself drastically decrease. For example, measurements taken as part of this research showed irradiation levels of 1,132 W/m^2 in direct sunlight, but only 3-15 W/m^2 in the shade.

Because of this result, the use of solar panels is largely confined to locations where direct sunlight is regularly available.

A solar nantenna is a nanometer-scale antenna and rectifier array which captures light in a manner similar to reception of radio waves by a car's antenna. Light delivers more energy than radio waves since the energy contained in an electromagnetic wave increases with the frequency of the wave. At this time, this device is not practical as diodes for rectification have not yet been able to operate at such high frequencies (Kotter, Novack, Slafer, & Pinhero, 2008). Future implementations of nantennas are expected to be very power dense, and continuing research is progressing to make them a reality.

2.2.2: Wind Energy Harvesting

Small-scale wind-turbines have not yet found widespread use compared to large power generation turbines. The power available from the kinetic energy of wind is governed by the relationship

$$P = \tfrac{1}{2}\rho S v^3 C_p \tag{2.2}$$

where P is the power output (W), ρ is the density of the air (kg/m^3), S is the effective cross-sectional area of the turbine (m^2), v is the initial velocity of the air entering the turbine (m/s), and C_p is the efficiency of the system. Betz's Law limits this efficiency to a maximum of 59.3%, with large-scale turbines often operating in the range of 30-50% (Khaligh & Onar, 2009). Small-scale turbines usually have much lower efficiencies, usually around 5-10% (Khaligh & Onar, 2009). Since wind is often intermittent, the average power harvested by a wind turbine should be adjusted for its environment. The capacity factor is a common way to evaluate the level at which the turbine is performing in its environment, and is defined as the ratio of actual output power to output power at full capacity, over a set time period. Typical wind farms have capacity factors ranging

from 20-40% (Renewable Energy Research Laboratory: University of Massachusetts at Amherst, 2011).

Rotational turbines are available in two main categories: horizontal axis wind turbines (HAWTs) and vertical axis wind turbines (VAWTs) (Khaligh & Onar, 2009; New Energy Watch, 2011). HAWTs rotate about axes parallel to the airflow. They are more efficient, but only operate in one direction without a yaw mechanism to turn the blades towards the wind, as shown on the left of Figure 11. VAWTs rotate about axes perpendicular to the airflow. Such turbines are slightly less efficient, but they are omnidirectional; their effectiveness is not dependent on wind direction so they are therefore better suited for variable wind directions. In addition, many can operate at lower wind speeds than HAWTs. VAWTs come in many varieties, such as those shown on the right of Figure 11. In addition to these two turbine types, an airfoil may be used which flutters in the wind, allowing vibration harvesting methods to be used to further capture the energy in a compact volume (Humdinger Wind Energy LLC, 2011).

(a) (b) (c) (d)

Figure 11. Examples of some commercially available wind turbines (Helix Wind, 2011; Sunforce Products Inc., 2011; Wikipedia Contributors, 2005; Windspire Energy, 2011).

The potential limitations of using wind turbines are similar to those presented by photovoltaic panels. Maintenance is a key issue, even more so than with solar panels as turbines have exposed moving parts which can easily be damaged or clogged. Designing a small, inexpensive turbine that can reliably last many years without maintenance may be difficult. Also, like solar panels, wind turbines are dependent on the predictable availability of power. Some may be in locations where wind is channeled in predictable and relatively constant patterns but others may only sporadically encounter wind. Ducting may be used to guide the wind through the turbine, but usually at the cost of becoming more directional. Power derived from the wind is proportional to the velocity cubed, so brief but powerful gusts may be preferable over constant but weak breezes. Thus, the feasibility of using wind power must be evaluated on a location-by-location basis by evaluating wind speeds with experimentation, such as extended data collection using an anemometer. Hourly, daily, and long-term average wind velocities are also available for many geographic locations in the literature (National Climatic Data Center, 2011).

2.2.3: Vibration Energy Harvesting

The conversion between mechanical vibration and electricity has been used for some time in microphones, speakers, accelerometers, geophones, and seismographs; however synthesis and optimization of this technology for energy harvesting is a relatively recent development. The fundamental relationship describing the theoretical power available in a vibration harvesting system with a simple sinusoidal input acceleration at mechanical resonance is

$$P = \frac{m\zeta_E a^2}{4\omega\left(\zeta_E + \zeta_M\right)^2} \tag{2.3}$$

where P is the power output, m is the vibrating mass in the harvester, a is the magnitude of acceleration experienced by the mass, ω is the frequency of the acceleration (with the

harvester designed to vibrate at the same natural frequency), and ζ_E and ζ_M are the electrical and mechanical damping coefficients. This equation shows the general need to maximize mass and amplitude, minimize the difference between the harvester natural frequency and the lowest excitation frequency with appreciable amplitude, and minimize mechanical damping (Beeby et al., 2006).

The three most common methods of vibration energy harvesting are electromagnetic, piezoelectric, and electrostatic. Electromagnetic harvesting operates using Faraday's Law of Induction: a changing magnetic flux will induce a voltage in a closed loop of conductor. In practice, this is usually accomplished by moving a magnet and coil relative to each other to produce an AC voltage in the coil. This technology is currently used with great success in motion-powered flashlights and watches, as well as commercially available and research vibration harvesters as shown in Figure 12. Inductive transducers are preferred in low frequency applications as the impedance of inertial/inductive systems is directly proportional to frequency. This translates to relatively low voltage and high current outputs, compared to piezoelectric and electrostatic transducers.

In a piezoelectric harvester, an applied mechanical strain in the piezoelectric material separates electric charges in the material, producing a voltage across its electric terminals. The typical embodiment is a cantilever beam with a mass at the tip and piezoelectric ceramic or polymer film attached to the upper and lower faces of the beam such as in Figure 13 (Mide, 2011). As the beam vibrates, the films undergo cyclical tension and compression, generating a relatively high AC voltage and low current due to the capacitive impedance – inversely proportional to frequency. Piezoelectric energy

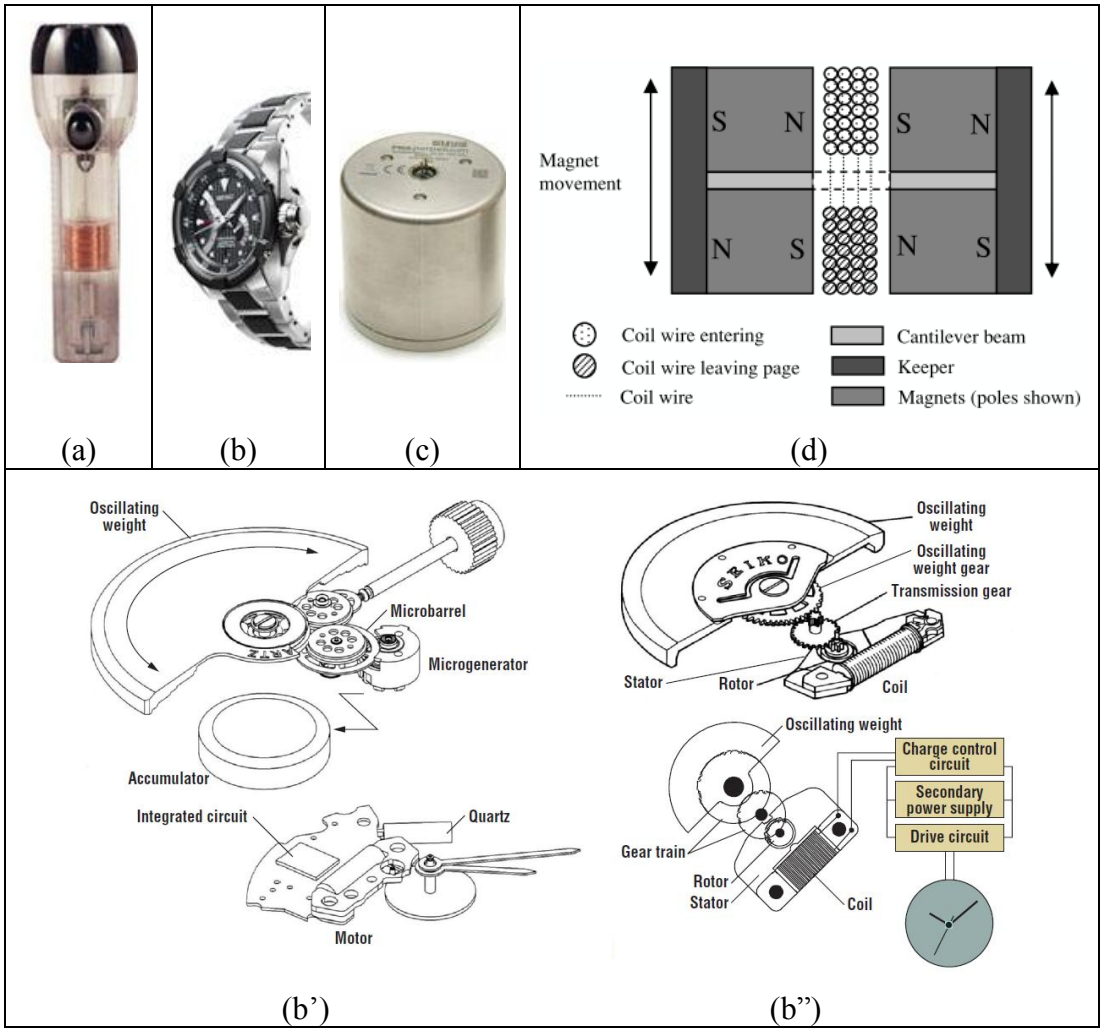

Figure 12. Examples of electromagnetic vibration harvesting, including (a) motion powered flashlights, (b) kinetic watches (such as (b') the ETA Autoquartz design and (b") the Seiko AGS generator), (c) commercial inductive energy harvester, and (d) concept of an inductive energy harvester (Beeby et al., 2007; Joseph A. Paradiso, 2005; Perpetuum, 2011; Seiko, 2011; ToolStore, 2011).

harvesters are often used instead of inductive harvesters when one of the following conditions is true:

- *The application is too small to economically manufacture an electromagnetic system.*

- *The input vibration frequency is in the hundreds or thousands of Hz (piezoelectric systems are difficult to design to resonate at low frequencies due to their high stiffness and high impedance at low frequencies).*
- *The vibrations are intermittent such as isolated impacts or shocks (which give high strain rates).*
- *The environmental conditions may be matched as an input to high impedance performance of a piezoelectric system.*

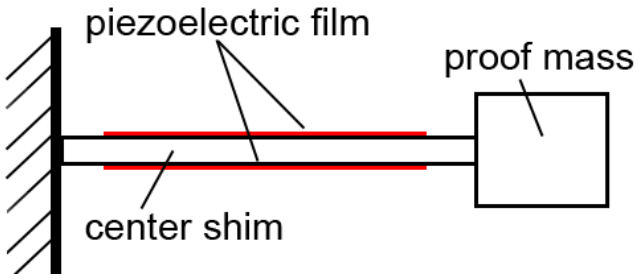

Figure 13. Bimorph cantilever piezoelectric harvester.

Electrostatic harvesters are capacitors which change either the gap distance or normal area of opposite electrically charged plates as shown in the schematic of Figure 14a (Beeby et al., 2006). The output is similar to a piezoelectric transducer, with impedance inversely proportional to frequency, giving relatively high voltages and low currents. Most require a polarization voltage to be applied to the plates before energy may be harvested, which is a significant disadvantage, but electrets may be used to supply this voltage without an external source. The electret substance is deposited upon the plates during manufacture and provides the polarization voltage eliminating this disadvantage (Baxter, 1996). Electret microphones have existed for some time but application to energy harvesting has not yet been found as part of this research.

Other less common methods of vibration harvesting are the use of magnetostrictive and electrostrictive materials as well as magnetostrictive-piezoelectric hybrids. Magnetostrictive and electrostrictive materials strain when exposed to varying magnetic or electric fields, respectively (Z. L. Wang & Kang, 1998). A simple magnetostrictive harvester contains a bar of Terfenol-D surrounded by a coil across which a voltage is induced when the straining bar changes the magnetic field in the coil (Ueno, Summers, Wun-Fogle, & Higuchi, 2008). In a slight alteration a magnetostrictive-piezoelectric hybrid delivers a voltage from a piezoelectric crystal which is strained by the magnetostrictive material when it is exposed to a moving magnet such as shown in the schematic of Figure 14b (Beeby et al., 2006). These devices are not typically used in low frequency applications due to their impedance characteristics which are similar to piezoelectrics.

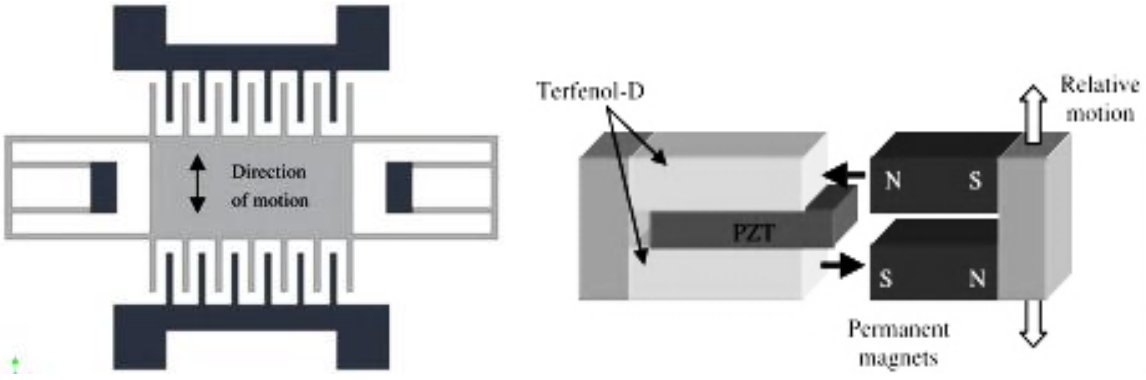

(a) (b)

Figure 14. Electrostatic (a) and magnetostrictive-piezoelectric (b) harvester schematics (Beeby et al., 2006).

2.3: ENERGY STORAGE

The harvested energy may be stored in a number of ways. A visualization of results from a search of literature and available commercial products is given in Figure 15

in the form of a mind map. After considering the many possible methods to store the harvested energy, the best choice must be made by considering the power and energy required by the load as well as the maximum allowable volume. A storage method may be energy dense, but if that energy cannot be delivered at the desired power level then the method cannot be successfully used. An appropriate approach to determine which methods are suitable is to compare their power and energy densities, which will allow the user to estimate the volume that will be required. Figure 16 presents both values for common storage methods. The values for compressed air are lacking in Figure 16 but may be found in the literature (Paloheimo & Omidiora, 2009).

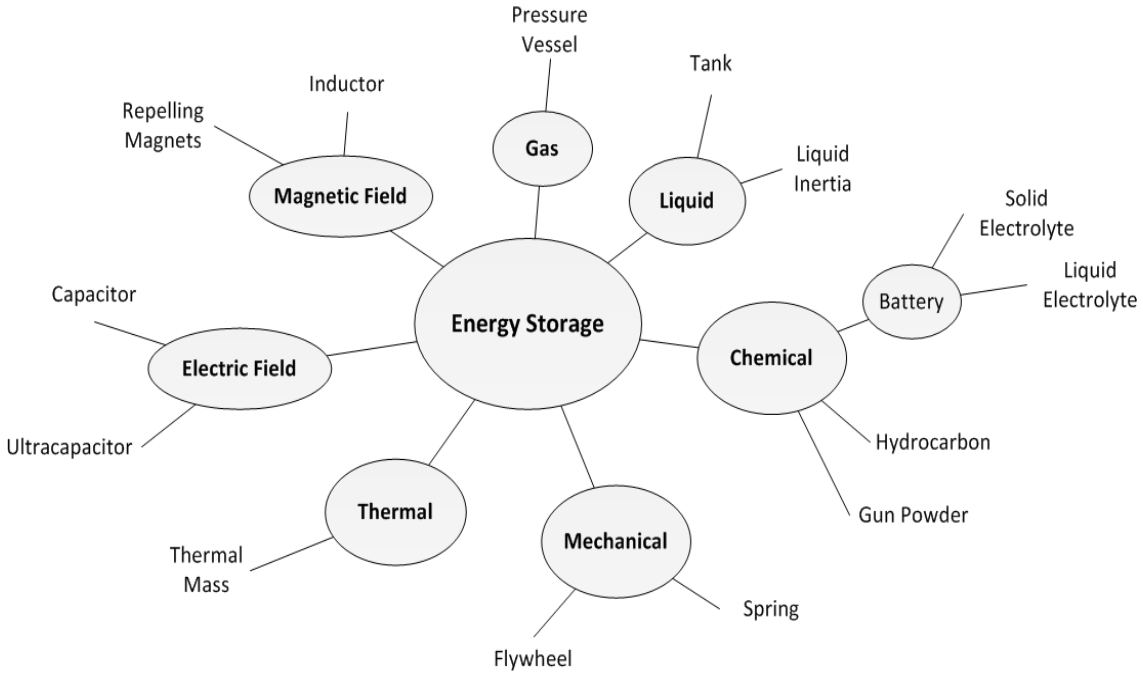

Figure 15. Mind map of energy storage methods by energy domain.

An extensive study of energy storage methods may be found in the text by Huggins (Huggins, 2010). The most commonly used method is the liquid electrolyte battery such as the typical Lithium-ion or Nickel Metal-Hydride battery available from

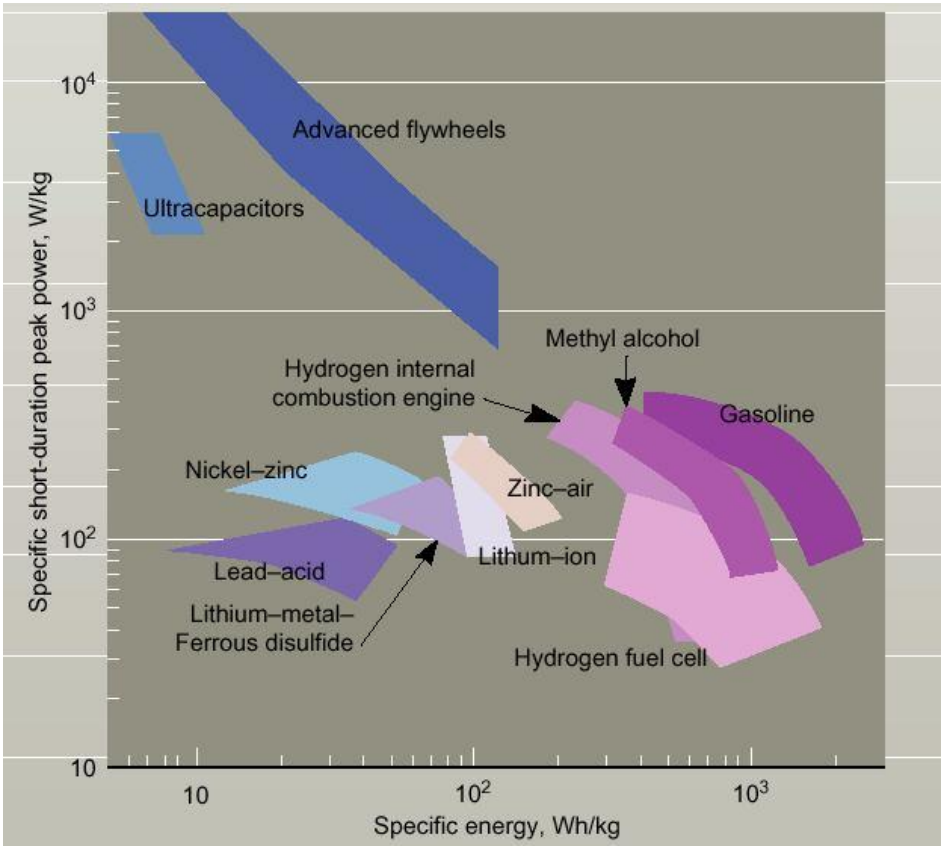

Figure 16. Power density of various energy storage methods (Rutman, 2004).

SAFT (SAFT, 2007) or A123 (A123 Systems, 2007). Table 4 provides a comparison between the various types of batteries currently on the market. Lead acid batteries are used in gasoline-powered cars, while Ni-MH and Li-ion are more common in consumer electronics. Lithium-ion batteries necessitate protection circuitry because they can be ruined and no longer hold a charge if they are either discharged completely or over-heated the battery could be ruined and no longer hold a charge (Pistoia, 2005). Therefore an additional chip must be used to manage the charge and temperature of the battery, but these are often included with the battery system. Solid state lithium ion batteries—which are not included in any of the figures of this chapter—have a solid electrolyte and offer significantly longer life but are still fairly small in capacity. Infinite Power Solutions

(Infinitie Power Solutions, 2010) and Cymbet (Cymbet, 2011) sell the new batteries utilizing nanometer-scale channels which prevent the cathode and anode from contacting via dendrites which build up over time, rendering a battery unable to hold charge.

Table 4. Battery Performance Comparison (Electric-Auto, 2011).

Items	Li-ion	Ni-MH	Lead-acid
Working voltage (V)	3.7	1.2	2.0
Gravimetric energy density (Wh/kg)	130~200	60~90	30~40
Volumetric energy density (Wh/L)	340~400	200~250	130~180
Cycle life (cycles)	500	400	300
Capacity self discharge rate (% per month)	5%	30%	10%
Memory effect	None	40%	None
Energy efficiency ($C_{discharge}/C_{charge}$)	99%	70%	75%
Weight comparison for the same capacity	1	2	4
Size comparison for the same capacity	1	1.8	3.5
Reliability	High	Low	High

Figure 17 compares the energy densities and power densities of additional battery types to those of regular electrolytic capacitors and double layer ultracapacitors (aka supercapacitors), which are missing from Table 4. Ultracapacitors are attractive because they charge and discharge quickly and have a longer cycle life. Maxwell is one manufacturer of ultracapacitors for all uses (Burke, 2000).

2.4: Future Innovations

Future innovations may be in the hybrid use of several energy harvesting/scavenging technologies collaboratively in one package, as well as systems of harvesters in separate packages which network to capture energy in a more efficient, strategic, or constant manner. Solar cells and wind turbines may supply energy when it is available with electromagnetic generators supplying a continuous flow. Solutions which include new functions like pre-harvesting preparation, adaptation to changes in the

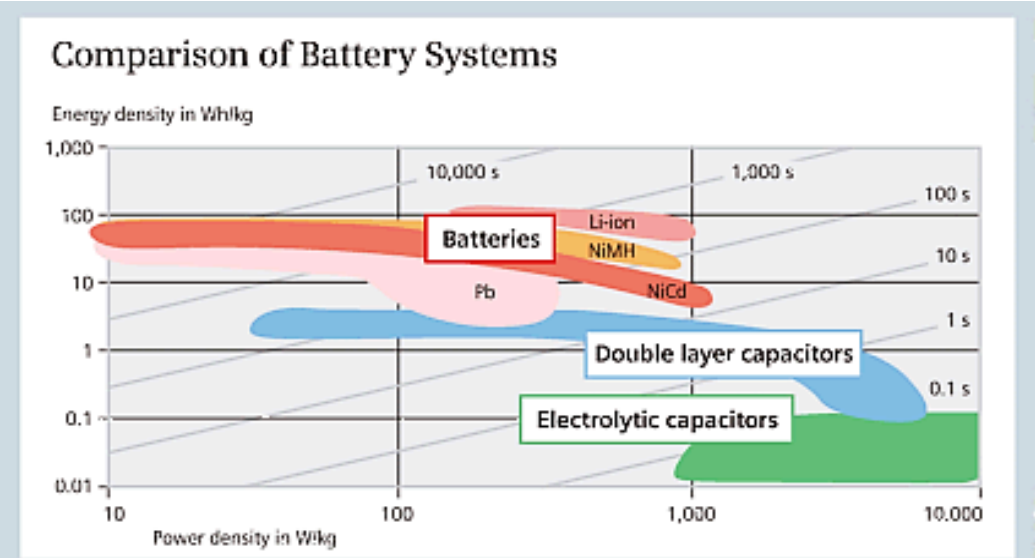

Battery type	Energy density Wh/kg	Power density W/kg	Service life in cycles / years
Lead-acid battery	30 – 50	150 – 300	300 –1,000 / 3 – 5
Nickel-metal hydride battery	60 – 80	200 – 300	>1,000 / >5
Lithium-ion battery	90 – 150	500 – >2,000	>2,000 / 5 – 10
Supercaps (double layer capac.)	3 – 5	2,000 – 10,000	1,000,000 / unlimited

Figure 17. Comparison of capacitors and batteries (Gerl, 2007).

source, robust handling of uncertainty, built-in sensing, and protection would have significant impact on the field. Solar cells may be fitted with concentrating lenses, sun-tracking equipment, and adaptive protection while vibration harvesters may be fitted with self-tuning and bandwidth widening capabilities (Zhu, Michael J Tudor, & Beeby, 2010). With core technologies being developed to increasingly optimized levels, significant innovations will occur in the system-level design and its customization for particular applications. It's not all about reinventing the wheel. The novel use of technology and supporting functions are innovations, beyond discovering the next revolutionary material or technology.

2.5: CHAPTER SUMMARY

Energy harvesting and scavenging is a field with great potential for future mobile, quick-install, and remote applications, enabling growth in wireless sensing applications. There are many energy sources and types of harvesters to consider for any application, and the number is growing rapidly. Solar, wind, and vibration harvesters possess the highest power densities of those reviewed, with solar being most attractive with a power density one order of magnitude above wind and vibration. Vibration harvesting possesses one very important trait—the ability to be sealed from the environment and protected from intentional or accidental damage—whereas solar and wind harvesters must interact with the elements directly. Properly matching the impedance characteristics of the energy conversion mechanism to those of the energy source must not be overlooked, and this requires careful study of the ambient energy source. Furthermore, conditioning and storing the harvested electrical energy are as important to the overall success of the harvester as capturing and converting the energy, so care must be taken in the design of these subsystems. The average number of lifecycles, operating conditions, and self-discharge of storage devices must be considered for successful delivery to the load. Capacitors, ultracapacitors, and lithium-ion batteries are at the top of the storage options, due to their high energy density, easy electrical monitoring, and growing research focus. Ultracapacitors may be used to rapidly collect bursts of energy, and then deliver this energy to a more efficient long-term storage source, such as ceramic capacitors or lithium-ion batteries. The near future will see solid-electrolyte lithium-ion batteries with increased storage capacity, allowing implementation in energy harvesting applications where their 100,000+ cycle life will help maintenance-free operation for decades.

Chapter 3: Broad Conceptual Design and Field Measurements

This chapter begins with conceptual design of energy harvesters of various types in a broad sense with no imposed limitations on the concept generation process. This is followed with the selection of one with which to focus in all future chapters. The energy source specific to this harvester type is then quantified by measurements in the field and analyzed in order to gain an understanding of its characteristics. With this information, a focused literature review is performed in Chapter 4 with a better-defined scope in attempt to generate superior conceptual designs in Chapter 5.

3.1: Concept Generation

The conceptual design process began with unconstrained concept generation open to all energy harvesters, regardless of the functional requirements and constraints listed in the specification sheet. This approach was taken to generate a breadth of ideas and to be sure that an innovative solution was not overlooked. Concepts were sketched and a mind map was formed of all generated concepts. Mounting concepts were also generated for the fastening of a generic harvester to a Box-girder and I-girder bridge. These concepts were constrained to the requirements set by the project, as high importance was placed upon mounting-specific requirements. Following this, a patent search was performed to identify idea generators as well as to discover what has already been done. A qualitative evaluation of the advantages and disadvantages of each harvester type resulted in the selection of harvester type for focused concept generation.

3.1.1: Harvester Concepts

Concept generation focused on a set of key functions, which a generic energy harvester should perform:

- *Interface with environment*
- *Direct energy from environment*
- *Separate energy*
- *Transform energy*
- *Convert energy*
- *Store energy short term*
- *Store electrical energy long term*
- *Supply energy to electric load*
- *Interface with user*
- *Divert debris, theft, vandalism*
- *Adapt to changing environment*

Detailed functional modeling of energy harvesters and the insights gained from the critical functions was performed by fellow graduate student on this project, Jason Weaver, and are included in his publication (Weaver, K. L. Wood, & Crawford, 2011).

Sketches of some of the generated concepts are given in Figures 18-22. Figure 18 shows a design by analogy concept which is based upon the road hose counters that are currently used to track vehicle traffic. A vehicle would drive over the elastomer hose, causing hydraulic fluid inside the hose to flow through a nozzle to increase the velocity. The motion would be converted to electricity by either a permanent magnet in a solenoid coil or a turbine attached to an alternator. The turbine could be driven continuously by rectifying the fluid flow through one way valves, or could be driven in an oscillatory manner similar to the solenoid. A wire mesh could be embedded in the hose to prevent pinching.

The “windbelt” uses aeroelastic flutter to convert wind into vibrations, as shown in Figure 19. In this concept, strips of piezoelectric ceramic or polymer are attached to the top and bottom surfaces of an elastic fabric in a cross-hatch pattern. The fabric is tensioned with turnbuckles attached to a structural member. Turbulent wind causes the fabric to flutter, straining the piezoelectric elements which generate a voltage to an electric load. This type of wind harvester is thought to be better suited for the bridge application than a HAWT or VAWT as it does not need to hang below the girders, which

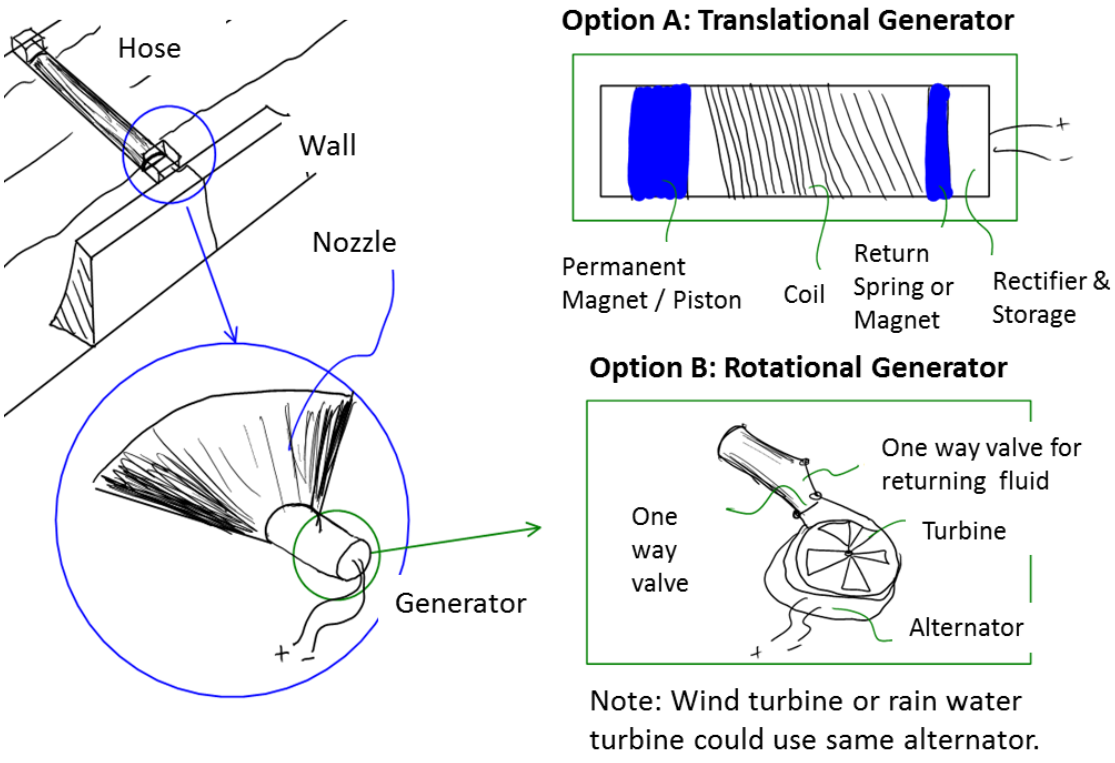

Figure 18. Road hose concept.

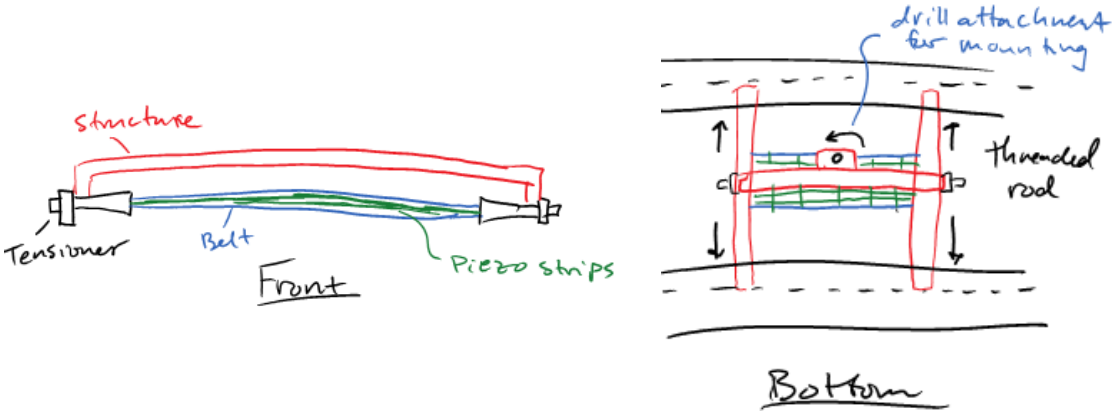

Figure 19. Aeroelastic "windbelt" concept.

is a particularly limiting design constraint for other turbines. The windbelt could actually benefit from the turbulence caused by the girders obstructing the airflow, whereas other

turbines are hindered by this obstruction. The harvester would be mounted by extending threaded rods between girders. The rods could be tightened using a power drill with an extension so the operator could install the system from the ground.

In an attempt to eliminate some of the disadvantages of photovoltaic panels, a concept was generated in which panels are mounted facing down between two girders while mirrors direct sunlight underneath the bridge[2], as shown in Figure 20. In this manner the panels would not be exposed to all of the elements, and the mirrors could possibly be positioned such that minimal surface extends beyond the side of the bridge. Given that photovoltaics have a power density an order of magnitude higher than wind turbines, sufficient power *might* still be harvested without direct exposure. Also shown in Figure 20 is the basic idea of using piezoelectric ceramics in the bridge's preexisting expansion joints. The joints are exposed to very large forces which could theoretically be harvested, but the expansion and contraction is at a very slow rate. This makes it very difficult to harvest energy with either vibration method.

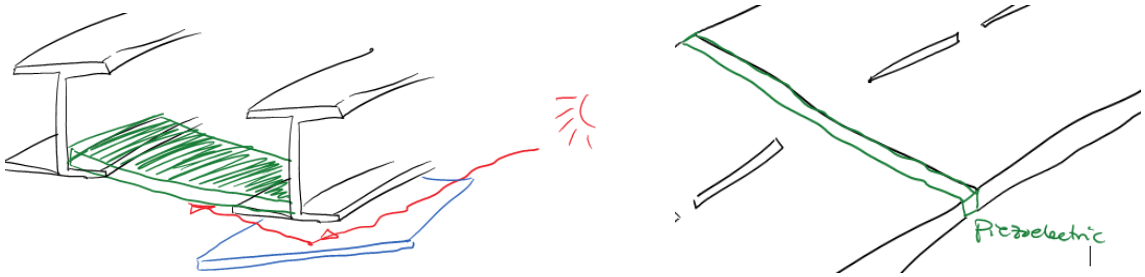

(a) (b)

Figure 20. Reflected solar concept (a), and expansion joint concept (b).

Two vibration harvester concepts are shown in Figure 21: a geophone/seismometer type electromagnetic harvester, and a spring loaded impact

[2] This exploits the *Direct energy from environment* and *Divert debris, theft, and vandalism* functions.

piezoelectric harvester. The electromagnetic harvester uses an iron structure suspended from a helical extension spring to concentrate magnetic flux across a coil. The piezoelectric harvester makes use of the piezoelectric material's strain-rate dependent voltage and poor performance at low frequency by periodically impacting the ceramic with a spring loaded slug. The spring is compressed by the relative motion of the chassis and weighted arm during vibration through a simple clutch and rack and pinion. Frictional losses would have to be a focus in detailed design.

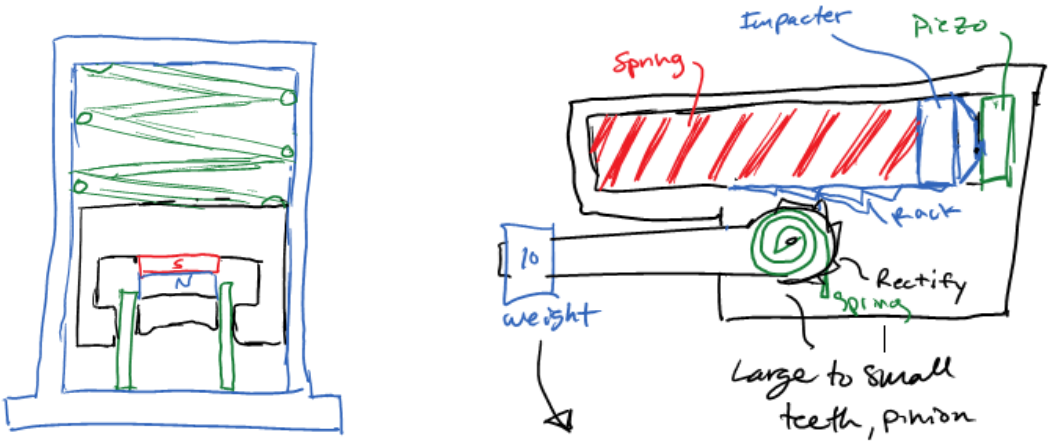

(a) (b)

Figure 21. Electromagnetic vibration concept (a), and impact piezoelectric concept (b).

Since a vibration harvester delivers the greatest power when its resonant frequency matches the excitation frequency, tuning is an important function which may be included to ensure high power output[3]. The previous electromagnetic vibration harvester concept was expanded to include an active measurement and tuning system, Figure 22. The extension spring is attached to a disk which has static pin supports to allow the disk to bend easily, with small stiffness. The disk is held in place by a

[3] Tuning is covered by the *Adapt to changing environment* function in the previous bulleted list.

piezoelectric clamp and teeth to increase its stiffness similar to the way a snare drum is tuned. As part of this concept, a comparator circuit would be contained in the harvester to activate the piezoelectric clamps when the output voltage of the coil is below a threshold. The teeth would hold the disk in place allowing the piezoelectric clamps to be used only to increase or decrease the clamping force, so to minimize power usage. An additional feature is a magnet at the bottom of the harvester to act as a soft alternative to a mechanical stop in limiting the displacement of the translating magnet structure. The concept's main drawback is the low sensitivity of the coupled springs; doubling the disk stiffness results in only a 15% increase in the combined, equivalent stiffness. As with any harvester which tunes by changing the spring stiffness, the increase must be by a factor of four to double the resonant frequency.

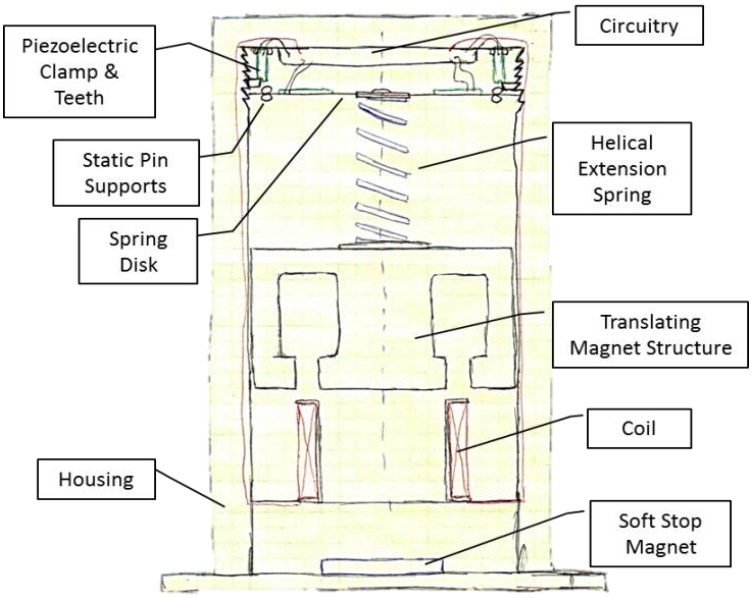

Figure 22. Concept of an active coupled-spring tuning system for an electromagnetic vibration energy harvester.

Several other concepts which were generated in less detail are illustrated in Appendix C as a mind map, sorted by energy source.

3.1.2: Mounting Concepts

Some concepts for mounting a generic energy harvester to I-girder and box-girder bridges were generated by referring to the specification sheet discussed in Chapter 1 as well as the requirements and desires listed below[4]. These requirements and desires stem from conversations with Civil Engineers at The University of Texas at Austin.

Requirements:

- *Mount inside of box-girder(s) at several locations along length of bridge.*
- *Mount on I-girder(s) at several locations along length of bridge.*

Desires:

- *Mount outside of box-girder(s) at several locations along length of bridge.*
- *Possible to mount without need of a man-lift truck.*
- *Possible to mount without stopping traffic under or over bridge.*
- *Mount with common tools and common skills.*
- *Single mounting design for all harvester designs.*

Alteration of the bridge structure is restricted in this project, which prohibits welding, drilling, cutting, gluing, and magnetic fastening. The first three methods are prohibited as they may deteriorate the structural integrity of an already weakened structure. The last two methods are restricted because secure, long-term connection cannot be fully guaranteed, and the liability of public injury from falling objects onto roadways would be an unnecessary risk. Fastening using magnets to the steel girders

[4] Mounting concentrates upon the *Interface with environment*, *Direct energy from environment, Interface with user,* and *Divert debris, theft, and vandalism* functions.

seems, at least to the author, to be an excellent choice as extremely high pull neodymium magnets may be purchased commercially which are rated to high temperatures, and installation time could be minimized.

Figures 24-23 show some of the generated fastening concepts. Clamping to the web stiffeners and cross-frames of I-girders are the easiest solution, and since several such structures exist along the spans of the bridges, harvesters may be mounted in many locations. A web stiffener is a vertical plate, 0.5-0.625” thick, extending between the top and bottom flanges of the I-girder, as shown in Figure 24b. Cross-frames are truss-structures constructed of angled steel, 0.25-0.5” thick, which span between I-girders, as shown in Figure 24a,b. For the box-girder bridge, vibration harvesters could be housed inside of the girder as shown in Figure 23b. Mounting an energy harvester between two box-girders is fairly difficult due to the trapezoidal shape of the girders, and the very small (~0.5”) flange at the bottom of the girders. Therefore a concept was generated to mount a harvester to the outside of a girder by extending threaded rods with footpads between the bottom of the deck and the top of a support column. Since this concept relies on a support column, harvesters may not be placed at many locations along the bridge span.

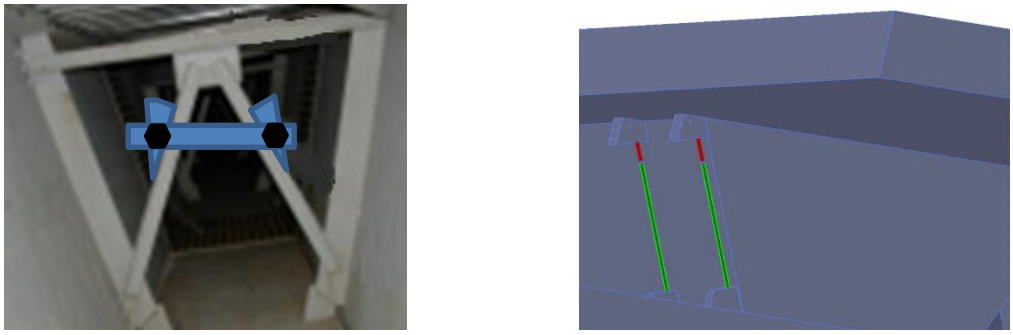

(a) (b)

Figure 23. Box-girder mounting concepts.

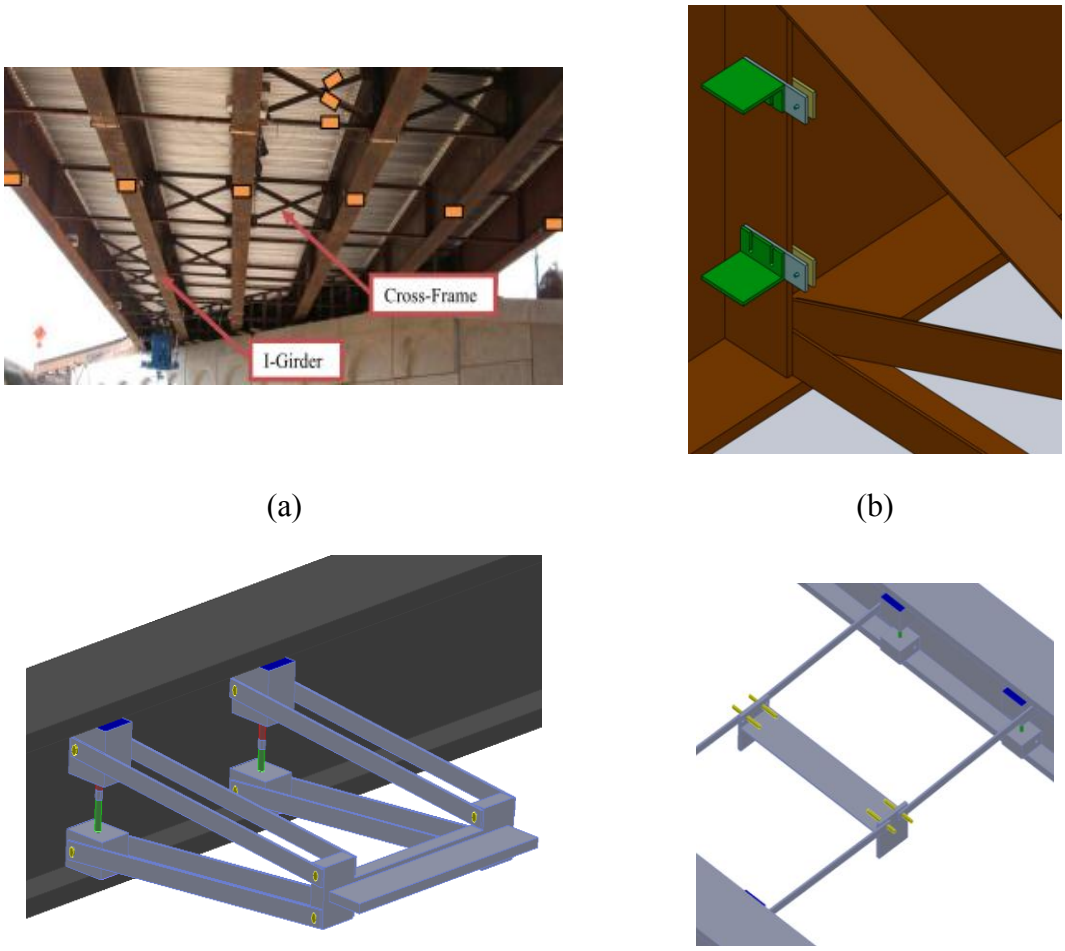

Figure 24. I-girder mounting concepts.

3.1.3: Relevant Patents

Patents expressly including energy harvesting on bridges and roadways were reviewed to understand approaches which have already been pursued. The patent search was performed following the broad concept generation in order to avoid fixation on designs similar to those in the patents. Many energy harvesting patents exist which do not focus on bridges or roadways, but the scope of this search was limited to this application. Of the patents found, a few relied upon vehicles driving over rollers, spring-loaded plates,

and spring loaded pistons to turn electric generators (Martinez, 1978; Smith, 1978; Toberman, 1975). These solutions would likely give high power but violate the constraint that no part of the harvester may be placed on top of the road surface or interfere with traffic. Another patent proposed placing piezoelectric cylinders in airport runways and roads to be compressed by the tires directly (Abramovich, Harash, Milgrom, & Amit, 2009). This patent seems to discuss only the general idea, not a detailed design. Another general idea (Retti, 2007), proposes solar or thermoelectric panels on the road surface which would capture electricity to inductively charge passing electric vehicles. Surprisingly, a patent exists proposing the harvesting of bridge expansion joints (Bradford & Pabst, 2009). The system uses a transmission to amplify the vertical displacement between two bridge sections caused by vehicles passing over the joint. The transmission drives an electric generator to convert the energy into usable form. A basic calculation presented in the patent predicts an average power of 10 W for one truck passing every nine seconds, based upon one set of measured displacement and traffic data. The design requires the harvester to be implanted in the joint during bridge construction or retrofitting, making monitoring of existing bridges very expensive. It is concluded from this patent search that the field of energy harvesters for bridge application is far from saturated.

3.2: CONCEPT SELECTION

After review, the most feasible energy harvesting sources for bridge monitoring were identified by The University of Texas Mechanical Engineering Energy Harvesting design team as:

- *Solar radiation using photovoltaic cells*
- *Wind flow from the environment and traffic*

- *Vibration of the bridge from traffic*

Solar cells are of highest power density by an order of magnitude (Weaver et al., 2010), but concerns by bridge engineers over mounting above or to the side of the bridge as well as obstruction by dirt and bird waste, damage by vehicles, hail and vandals, and theft raise some doubt. Of next highest power density is wind (Weaver et al., 2010), which inherits similar concerns unless located on the underside of the bridge which introduces obstruction to the airflow. Vibration harvesters have lower power densities but can be sealed from the environment or placed inside box-girders. Piezoelectric ceramics are naturally stiff, resulting in high natural frequencies and thus are typically used in applications where dominant frequencies are above 40 Hz (Priya & Inman, 2008). Dominant frequencies measured from local bridges are below 15 Hz and typically less than 5 Hz, increasing the difficulty of using piezoelectric harvesters. The details of this data analysis are discussed in Chapter 4. Electrostatic harvesters could work but there is a strong concern about robustness, given that the harvester would cease to produce power if the polarization voltage was ever lost. Electromagnetic harvesters are more robust because they rely upon a permanent magnetic field, and are naturally suited for low frequency vibration as the large mass of a permanent magnet works to decrease the natural frequency of the harvester. (Beeby & O'Donnell, 2008) performed a detailed study of micro vs. macro-scale generators finding that efficiency is much lower in micro systems due to the scaling of coil resistance and inductance. Piezoelectric harvesters are used most often in commercial applications because they are low in mass and may be incorporated in MEMS structures easily as laminates. As there is room for macro scale systems on a highway bridge, the focus for this design effort was on macro-scale systems. After review the energy harvesting team decided to pursue an electromagnetic vibration harvester for the author's thesis, and a piezoelectric vibration harvester and a vertical axis

wind turbine to be pursued by two other graduate students. A solar photovoltaic harvester was developed by an undergraduate research assistant with collaborative effort from each of the graduate students. In this way the energy harvesting team explored several options in parallel with possibilities to expand or consolidate as the project progresses.

3.3: FIELD MEASUREMENTS

With the decision to pursue vibration harvesting, the next step is to gain an understanding of the vibrations present in highway bridges. To assess this vibration, low frequency, high resolution Crossbow CXL02LF1Z accelerometers were placed on the box girders of the IH-35N-US-290E direct connector and the I-girders and cross-frames of the SH-71E bridge over US-183 and the IH-35N bridge over the Medina River. For the box girder bridge, accelerometers were placed longitudinally along one girder over two spans of a four-span, twin box-girder bridge to evaluate the variation of amplitude and frequency at various distances along the bridge axis. The two spans were 210 and 230 feet long, respectively, with sensors distributed evenly along the spans. Samples were recorded at 100 Hz for approximately one week.

The layout of the sensors may be seen in Figure 25 and Figure 26, along with 60 second samples in which a fuel truck, garbage truck, and moving truck passed over each sensor. The maximum and minimum accelerations, relative to gravity, measured during these samples are also included. Minimum, maximum and RMS acceleration amplitudes for each sensor over approximately one day are shown in Figure 27, following the same trend as the previous figure but with slightly larger peak amplitudes. The first span experiences its highest acceleration half way through the span and its lowest at its right, eastern end, which is expected. The relatively high acceleration at the abutment is likely due to the energy transferred from the vehicles as they traverse the expansion joint at the

beginning of the bridge. Smaller accelerations are found on the second span, likely due to the increased flexibility and damping of the straddle bent support at its furthest end. The increased damping likely caused the reduction in sharpness of the peaks corresponding to each vehicle, as compared to those on span 1.

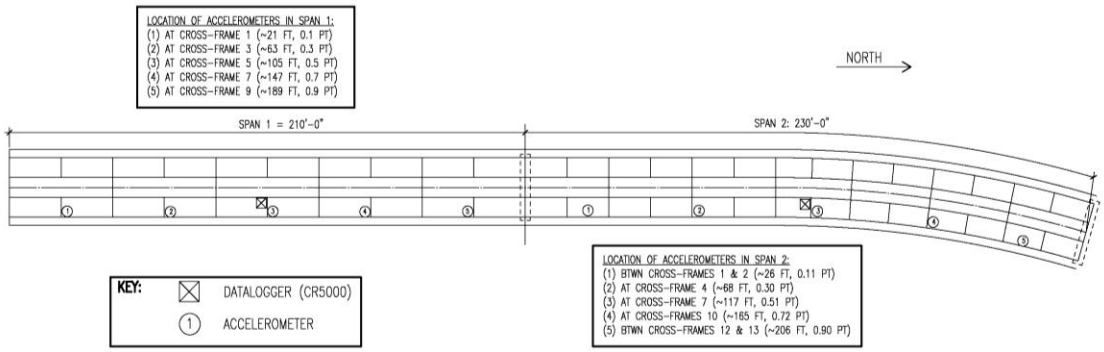

Figure 25. Accelerometer locations in first two spans of IH-35N-US-290E direct connector.

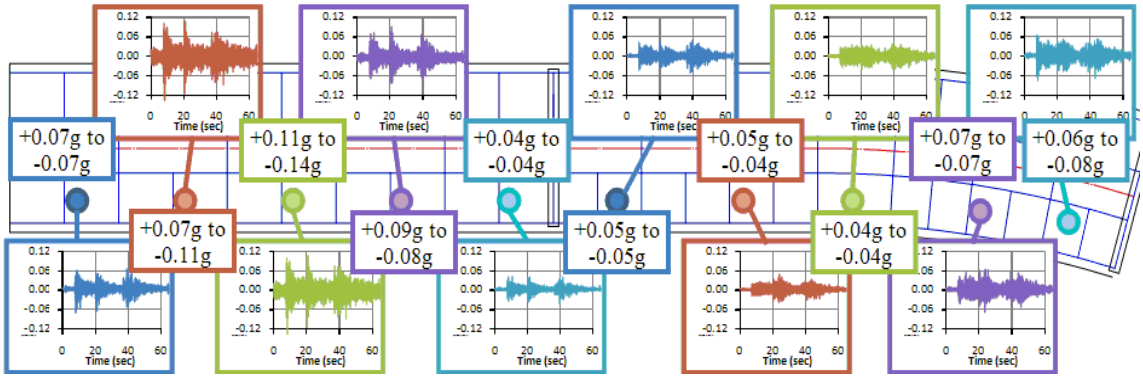

Figure 26. 60 second acceleration waveforms at each sensor location showing three passing trucks.

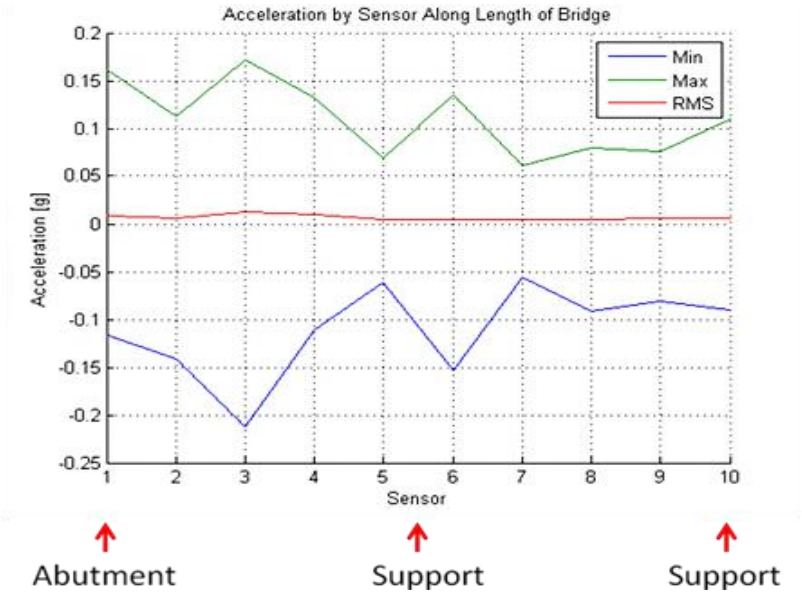

Figure 27. Minimum, maximum, and RMS acceleration by sensor location on box-girder bridge.

The frequencies also varied with sensor location along the bridge. Figure 28 shows the power spectrum of each sensor on span 1, and Figure 29 shows the same for span 2. The spectrograms are on a logarithmic vertical scale with each subplot having the same range to aid in comparison. The high wideband noise present from sensors 3 and 4 were due to defective accelerometers, as was verified in a later experiment. For both spans, the frequencies of highest power are around 1.8, 2, 4.1, and 5.3 Hz.

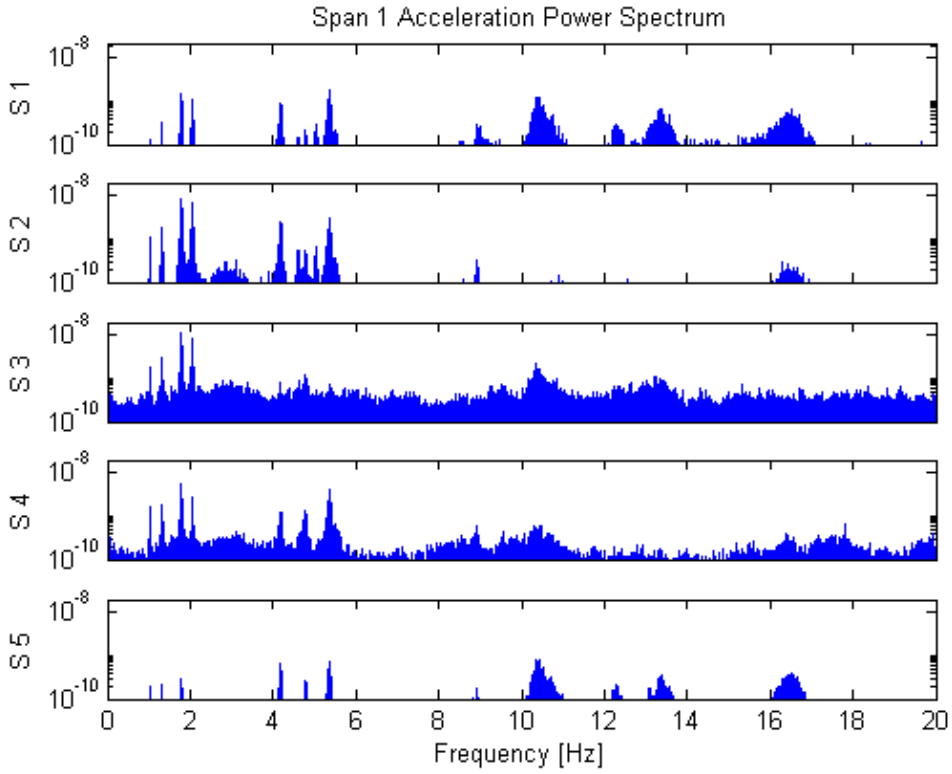

Figure 28. Acceleration power spectrum of span 1, showing variability of frequencies with sensor location.

The dependability of the frequencies of interest may be observed by a Spectrogram, which is a plot composed of a series of power spectrums over consecutive time spans. A spectrogram of approximately 4.5 hours of data from sensor 2 on span 1 is given in Figure 30 with a power spectrum of the entire time period underneath. Regions of highest power are colored in red, with lowest intensity colored in green. This spectrogram shows good stability of the frequencies of interest since the lines are vertical, at least in this time frame. A comprehensive analysis would encompass a much longer time span. The variability with the seasons of the year may be seen by combining spectrograms of each season after acquisition of additional bridge data. Also included in the spectrogram are thin horizontal lines—such as the one at 6000 seconds—representing

short excitations across all frequencies in range. These are likely the result of impacts caused by the heaviest vehicles traversing the expansion joint as they enter the bridge.

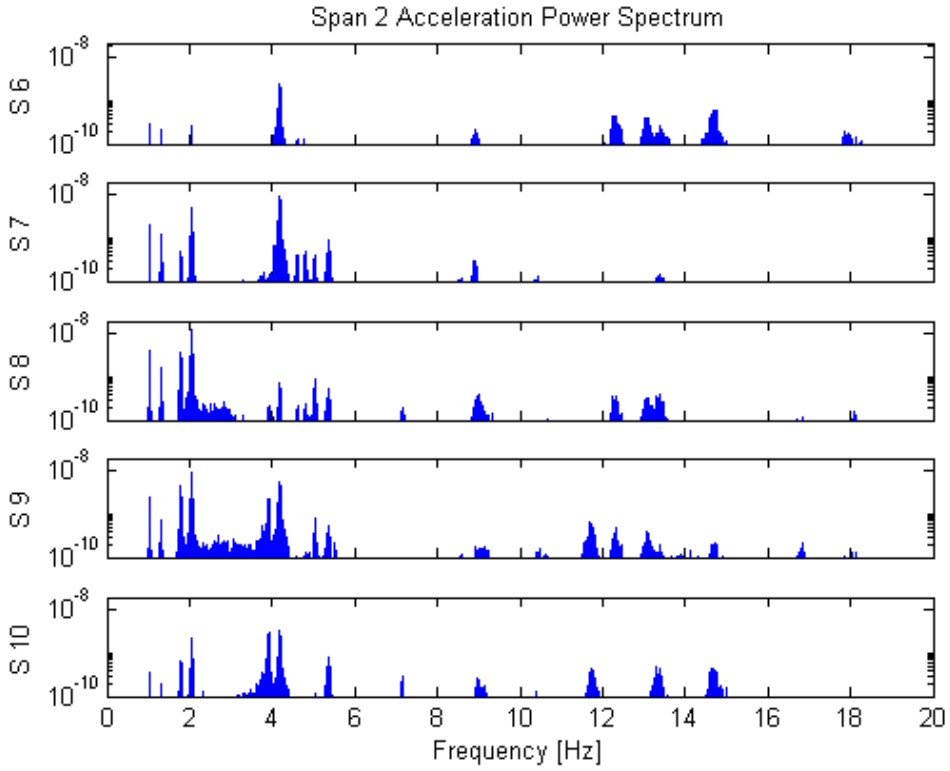

Figure 29. Acceleration power spectrum of span 2, showing variability of frequencies with sensor location.

The amplitude levels were similar for the three bridges instrumented, but each bridge was found to have a different frequency range, which was observed via a power spectrum. The stiff box-girder bridge was dominated by 1-10 Hz vibrations, while the short-span I-girder bridge occupied the 10-20 Hz range. The second I-girder bridge was a half-century older and vibrated between 5 and 25 Hz, depending upon traffic. The bridge vibration is mostly induced by heavy vehicle traffic such as trucks and buses, which indicates some dependence on the amount of traffic and speed. This dependency rapidly increases the complexity of predicting available energy for harvesting. Even so, there

exist some models of bridge vibrations excited by traffic, showing vibration patterns predominantly in the 1-15 Hz range (Cheung, Au, Zheng, & Cheng, 1999; B. T.-lo Wang, Huang, & Shahawy, 1992; Yin, Fang, Cai, & Deng, 2010). Each bridge has different geometry, supports and traffic loads, which have varying effects on the bridge response. Data were recorded at levels of both high and low traffic, where shifts in frequencies were observed, but further data analysis is needed to decouple the effects of added vehicle mass from the effects of temperature on the response of the bridge. This effort is ongoing with the significant portion of work being performed by the Civil Engineers involved in this project.

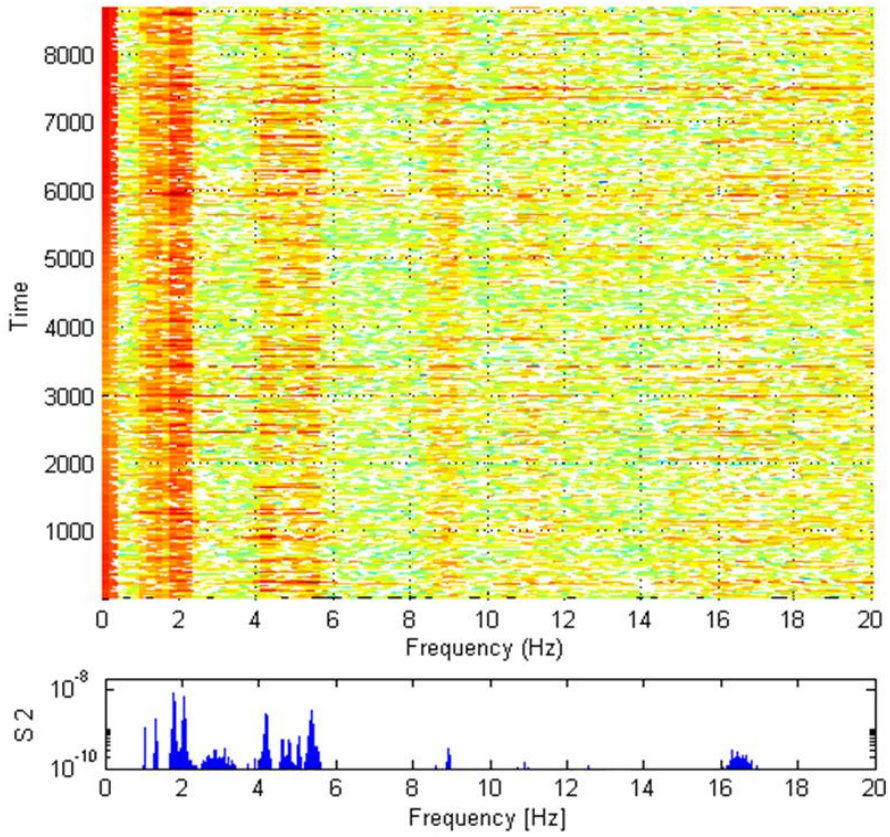

Figure 30. Spectrogram and power spectrum of accelerometer 2 of span 1, showing the stability of dominant frequencies over approximately 4.5 hours.

3.4: CHAPTER SUMMARY

The key functions a fully evolved energy harvester should perform were identified as: interface with environment, direct energy from environment, separate energy, transform energy, convert energy, store energy in short term, store electrical energy in long term, supply energy to electric load, interface with user, divert debris, theft, vandalism, and adapt to changing environment. Considering these functions, many concepts were generated and organized into a mind-map. Several of these were further developed and sketched, including road hose, wind-belt, reflected solar, expansion joint, electromagnetic vibration, and piezoelectric impact concepts. A few concepts were generated for mounting a generic harvester to the two most-common bridge types: I-girder and box-girder, with a focus on meeting the limiting design constraints set by the project. Patents relating to energy harvesting from bridges and roadways were briefly presented, with the most developed invention harvesting the motions of expansion joints from within the bridge. After review, the author selected vibration harvesting using induction for further development. Harvesting vibrations requires more sophisticated design, incurring larger risk than solar or wind harvesters, but with greater satisfaction of the project requirements and constraints if successful. To counter this, other students on the project are pursuing solar and wind harvesters in parallel efforts. To characterize the bridge vibrations, accelerations were measured at various positions and times and analyzed in the frequency and time domains. Further measurement and analysis is being performed by a Civil Engineering graduate student on the project, with a focus on temperature and traffic effects. The data presented thus-far shows stable, dominant frequencies in the 1.5-16 Hz range which may be harvested by tuned linear harvesters.

Chapter 4: Review of Electromagnetic Vibration Energy Harvesting

A literature review was performed to identify areas of opportunity, resulting in a discussion of important research work, review article, associated circuitry, and applications of electromagnetic vibration energy harvesting. Various functions and topologies utilized are discussed, emphasizing their contribution to improved energy harvesting in their environment. Two such functions are resonant frequency tuning and bandwidth widening. The review is presented by answering the following questions:

1. *What are the fundamental works in the field?*
2. *How can the harvester's resonant frequency be tuned?*
3. *How can a wide bandwidth harvester be achieved?*
4. *What circuitry is needed for high efficiency?*
5. *What works are specific to low frequency applications?*

4.1: WHAT ARE THE FUNDAMENTAL WORKS IN THE FIELD?

The seminal paper concerning harvesting vibrations is by (Williams & Yates, 1996)[5] at the University of Sheffield, U.K. The paper serves as a feasibility study where the performance of a simple mass, spring, electric and mechanical damper model, utilizing a generic electromechanical transducer is predicted analytically. Equation 4.1 shows the key governing equation of harvested power (P) in terms of mass (m), excitation frequency (ω), natural frequency (ω_n), excitation displacement amplitude (Y_o), electrical damping ratio (ξ_e), and mechanical damping ratio (ξ_m).

$$P = \frac{m\xi_e Y_0^2 \left(\frac{\omega}{\omega_n}\right)^3 \omega^3}{\left[1-\left(\frac{\omega}{\omega_n}\right)^2\right]^2 + \left[2(\xi_e+\xi_m)\frac{\omega}{\omega_n}\right]^2} \tag{4.1}$$

[5] This chapter contains many figures from the sources under review, with citations to the original source. The author of this thesis does not claim copyright on any figures or tables with a citation in the caption.

The analytical model is used to gain insight into the relation of each of these variables to increased harvested power. The first insight is the harvester's natural frequency should be designed to match the highest excitation frequency with adequate displacement amplitude, as the generated power increases with the cube of the frequency and the square of the displacement amplitude. Second, an increase in seismic mass is desired, at least much as is permitted by the design constraints. Third, it is desired to reduce total damping (electrical + mechanical) for high peak power if the excitation is of a constant frequency, or increase total damping for wider bandwidth and average power at the cost of peak power if the excitation frequency shifts or is broadband. Finally, the parasitic mechanical damping should be reduced as much as possible while the electrical damping should also be reduced but remain significantly higher than the mechanical damping. Geometric constraints place a limit on the minimum allowed electrical damping ratio, since the maximum displacement increases with total damping. Given a specified maximum displacement (Z_{max}), the maximum generated power is expressed by Equation 4.2, which assumes the harvester is operating at resonance ($\omega=\omega_n$).

$$P = m(\xi_e + \xi_m)Z_{max}^2\omega_n^3 \tag{4.2}$$

The first published concept that applies this specific theory was a MEMS generator with a magnet suspended from a diaphragm above a coil as shown in Figure 31a, one year later at the same university, (Shearwood & Yates, 1997). The first prototyped harvester powered a Digital Signal Processing chip by a spring suspended coil near a permanent magnet as shown in Figure 31b. A static magnet rather than coil necessitates flexible or sliding electrical contacts, but specific reasons for this decision were not given. It could be because the system is likely inspired by loudspeakers, which use a moving coil to achieve relatively high frequency voice representation. The

prototype was intended to harvest human walking, but quickly shifted focus to higher frequency vibration.

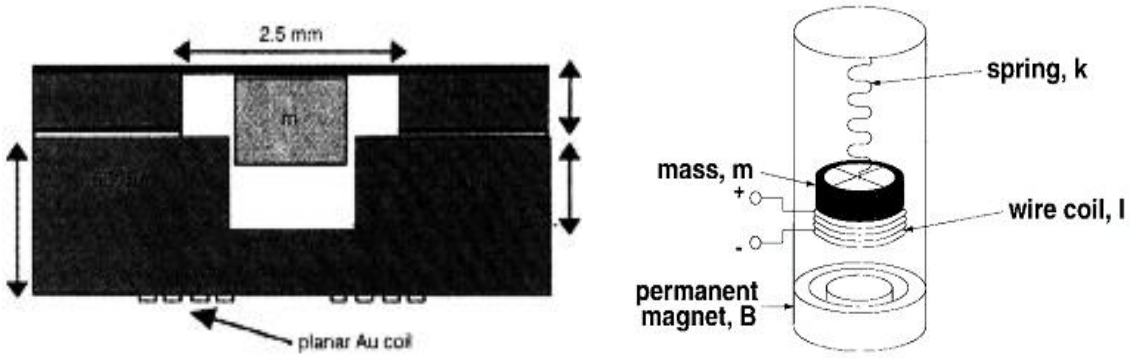

(a) (b)

Figure 31. First concept (Shearwood & Yates, 1997) (a), schematic of first prototype (Amirtharajah & Chandrakasan, 1998) (b).

(El-hami et al., 2001) and (El-hami, Glynne-Jones, N. M. White, & Beeby, 2000) at the University of Southampton, U.K. replaced the spring by a cantilevered beam, and used soft ferromagnetic iron plates to concentrate the magnetic flux density through the coil, resulting in increased power density. (Glynne-Jones, M J Tudor, Beeby, & N M White, 2004) further increased power density by using two magnetic poles rather than one, therefore increasing the magnetic flux gradient, as shown in Figure 32.

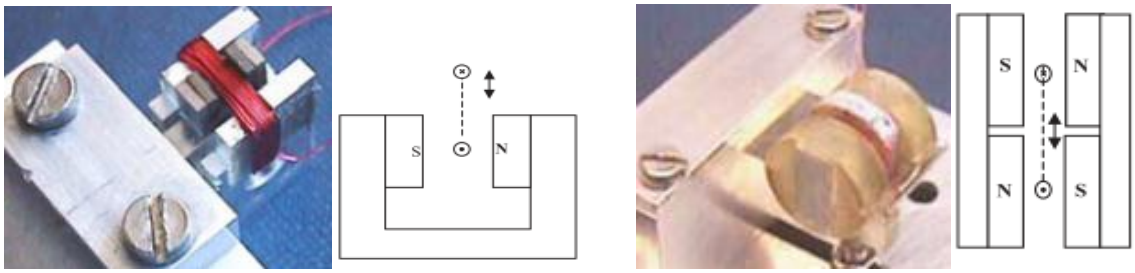

(a) (b)

Figure 32. Increasing magnetic flux gradient by utilizing two sets of magnets rather than one (Glynne-Jones et al., 2004).

(Stephen, 2006) introduced the concept of tuning resonant frequency to the excitation frequency to maximize generated power. He proved analytically that for maximum generated power, harvesting of a variable excitation frequency should begin at the lowest excitation frequency with adequate power. The harvester should then be tuned as the excitation frequency increases. He also presented an expression for optimal power transfer from a harvester to its load by impedance matching, shown by Equation 4.3. This equation relates the electrical load impedance (left side) to the total (electrical + mechanical) harvester impedance (right side).

$$R_l = R_c + \frac{K^2}{c_m} \tag{4.3}$$

where R_l is the load resistance, R_c is the resistance of the coil, K is the electromechanical conversion coefficient relating the coil electromotive force (EMF) to magnet velocity (or conversely the coil current to the force imposed on the magnet), and c_m is the mechanical viscous damping coefficient.

Four papers found during this literature review provide a fairly comprehensive review of work done in electromagnetic vibration harvesters: (Beeby & O'Donnell, 2008), (Beeby et al., 2006), (Arnold, 2007), and(Zhu et al., 2010). (Beeby & O'Donnell, 2008) tabulated many electromagnetic vibration harvesters giving author, location, date, maximum output power *P*, center vibration frequency *F*, peak vibration amplitude *A*, volume, normalized power *NP* (normalized at A=1m/s^2) and normalized power density *NPD* (normalized by volume). Additional works were added to this table resulting in Table 5.

Most vibration energy harvesters are second order systems with a resonant peak at the natural frequency and attenuation at either high or low frequencies depending upon system parameters. The total damping dictates how sharp (high Q-factor) the resonant peak is. A harvester with little damping has a sharp resonant peak which covers a very

narrow frequency band (Williams & Yates, 1996). Deviations of the excitation frequency from the harvester's resonant frequency will result in significant loss of harvested power, especially if the harvester's damping is low. Damping may be increased to make the harvester more robust to a dynamic excitation source, but at the loss of peak harvested power (Williams & Yates, 1996). An ideal vibration harvester would be implemented on several bridges of each type, regardless of the bridge's vibration characteristics. For this to be possible the harvester should be capable of tuning its resonant frequency and/or have a wide bandwidth. Methods for achieving both, with examples, are investigated by the next two questions.

Table 5. Electromagnetic harvester properties (Beeby & O'Donnell, 2008).

Reference	Year	$P(\mu W)$	F (Hz)	A (ms-2)	Volume (cm3)	NP	NPD
Shearwood 1997, Sheffield University (UK)	1997	0.3	4400	382	0.025	2 x 10-6	8 x 10-5
Amarithajah 1998, MIT (US)	1998	400	94	-	-	-	-
Li, Hong Kong University (China)	2000	10	64	16.16	1	0.04	0.04
El-hami, University of Southampton (UK)	2001	530	322	102	0.24	0.05	0.21
Ching, Hong Kong University (China)	2002	830	110	95.5	1	0.09	0.09
Mizuno, Warwick University (UK)	2003	0.0004	700	12.4	2.1*	3 x 10-6	1 x 10-6
Huang, Tsing Hua University (Taiwan)	2003	1.4	100	19.7	0.03*	0.004	0.12
Glynne-Jones (2001), University of Southampton (UK)	2004	2800	106	13	3.66	16.6	4.5
Kulah, Michigan University (US)	2004	0.004	25	-	2	-	-
Perez-Rodrfguez, Univerity of Barcelona (Spain)	2005	1.44	400	63	0.25	4 x 10-4	1 x 10-3
Beeby, University of Southampton (UK)	2005	0.021	9500	1.92	0.3	5 x 10-3	0.02
Scherrer, Boise State University (US)	2005	7000**	35	-	9	-	-
Beeby, University of Southampton (UK)	2007	58	52	0.59	0.15	166	1110
Wang, Shanghai Jiao Tong University	2007	-	121	14.7	0.1*	-	-
Hadas, Brno University of Technology (Czech Republic)	2007	3500	34.5	3.1	45	364	8.1
Sari, Middle East Technical University (Turkey)	2007	0.5	3300-3600	-	1.4	-	-
Serrer, University of Barcelona (Spain)	2008	55	380	29	0.8*	0.07	0.08
Perpetuum PMG-17, UK company	2008	1000	100	0.25	135	16000	118
Ferro Solutions VEH-360, US Company	2008	430	60	0.25	250	6880	28
Lumedyne Technologies, US Company	2008	1000	53	1	27	1000	37

*Estimated value from literature

**Simulated value

4.2: How can the harvester's resonant frequency be tuned?

A harvester's resonant frequency can be tuned mechanically or electrically. Most EM harvesters utilize mechanical methods, as the dominant electrical method is through the use of piezoelectric ceramics. In electrical tuning, an applied voltage or capacitance is used to control the stiffness of a piezoelectric material, effectively changing the resonant frequency. The capacitance is changed by switching in/out capacitors connected in parallel to the piezoelectric ceramic (Charnegie, 2007). This method is not as efficient as some mechanical methods, but is straight-forward to implement *in situ* to adapt to rapidly changing excitations. The method could be adapted to an inductive system by adding piezoelectric material to a cantilever beam then increasing or decreasing that beam's stiffness.

Mechanical tuning methods are generally more efficient but typically add more mass and volume than electrical methods, reducing power density. Mechanical systems cannot tune as fast as electrical methods, making them less suitable for *in situ* tuning (although it is still possible). Common mechanical methods include changing stiffness through geometry or magnetic fields, altering axial preloading, or shifting the center of gravity.

The most commonly changed dimension is the length of a cantilevered beam. This method is applied manually by (Beeby et al., 2007) who uses a simple clamp, and actively in a patent by (Gieras, Oh, Huzmezan, & Sane, 2005) which uses a linear actuator to adjust the clamping position as shown in Figure 33a. Higher frequency sensitivity is achieved by decreasing beam length rather than increasing, especially if reduced more than 60%, Figure 33b. This method does not introduce extra damping so long as the clamp is tight, but is relatively difficult to implement in an energy efficient manner.

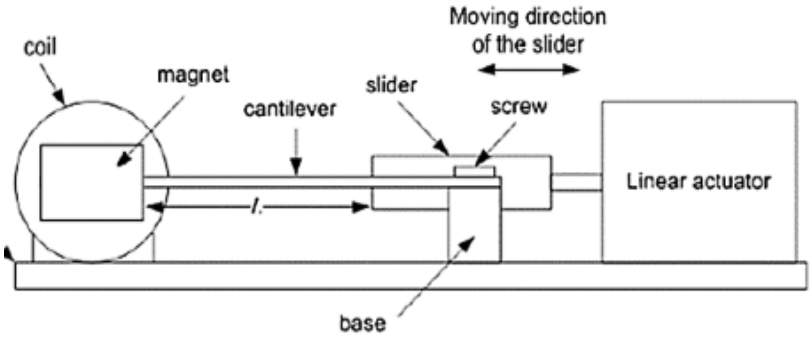

(a)

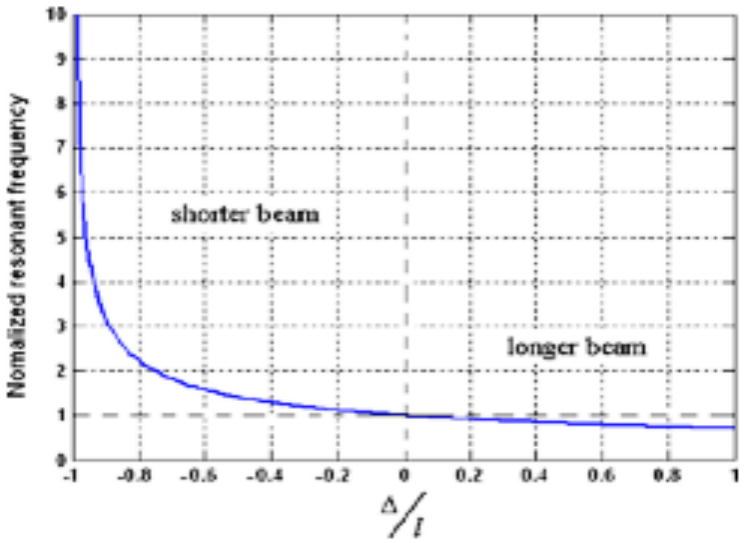

(b)

Figure 33. Patented tuning by changing clamped length via actuator (Gieras et al., 2005) (a), and variation of resonant frequency with change in beam length (Zhu et al., 2010) (b).

The method of changing the center of gravity (CG) also introduces no damping and has been successfully used in one prototype where a bolt was threaded in/out through a proof mass at the free end of a cantilever (Wu et al., 2008). The variation of resonant frequency with change in center of gravity is shown in Figure 34a, with highest

sensitivity when the CG is close to the beam's base. This method is fairly difficult to perform *in situ* as the mass to be shifted is vibrating with the beam, although it would be possible to automate.

The utilization of compressive and tensile axial loading has also been successfully implemented with cantilevers. Compressive loading is more common as it has greater sensitivity than tensile loading (Figure 34b), but at the cost of additional mechanical damping (Zhu, Roberts, Michael J Tudor, & Beeby, 2008). One concept actively changes the tensile preload of a cantilever using magnetic attraction to prevent the addition of damping, as shown in Figure 35. One magnet is fixed to the free end of the cantilever and the other to a linear actuator. To maintain a constant tensile force and prevent introduction of other magnetic forces, concave and convex magnets are used to maintain the gap distance constant throughout the full range of travel. Implementation of the axial loading method is relatively straight-forward and *in situ* adjustment may be performed, but energy consumption would be high due to large forces.

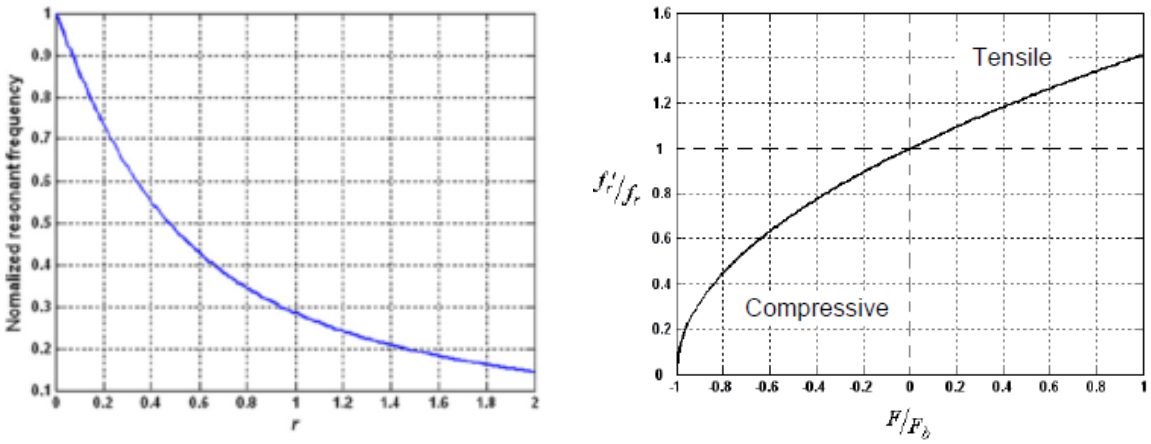

(a) (b)

Figure 34. Change in normalized resonant frequency with normalized center of gravity (a), and axial preload (b), (Zhu et al., 2008).

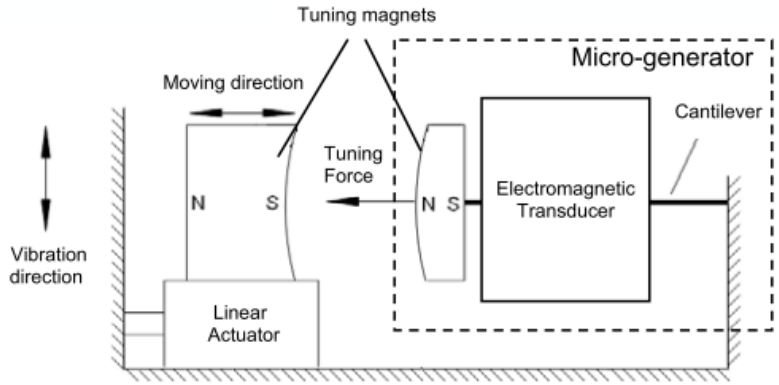

Figure 35. Concept to add tensile preload using magnets (Zhu et al., 2008).

Magnetic forces have also been used to alter the compliance of a harvester. Figure 36a shows a piezoelectric cantilever whose frequency is tuned by translating the beam vertically with a power screw to change the initial spacing between magnets on the housing and tip of the beam. The effective stiffness is reduced when the beam is closer to the top attracting magnet, and increased when closer to the bottom repulsive magnet. A disadvantage to this tuning method is the introduction of damping at all but the untuned natural frequency (Challa, Prasad, Shi, & Fisher, 2008). Adjustment of the prototype is performed manually, but the authors suggest adding an actuator to automate tuning. The two other concepts shown in Figure 36 rely completely upon magnets as the compliant member rather than a spring or cantilever. This approach allows easy tuning by threading the spring magnets relative to the translating magnet. Both methods were prototyped with tuning performed manually although *in situ* adjustment would likely be easier than other mechanical methods. The use of magnetic compliance in this manner does not introduce damping unless the force is larger than the inertial force of the moving mass, inhibiting its motion (Zhu et al., 2008).

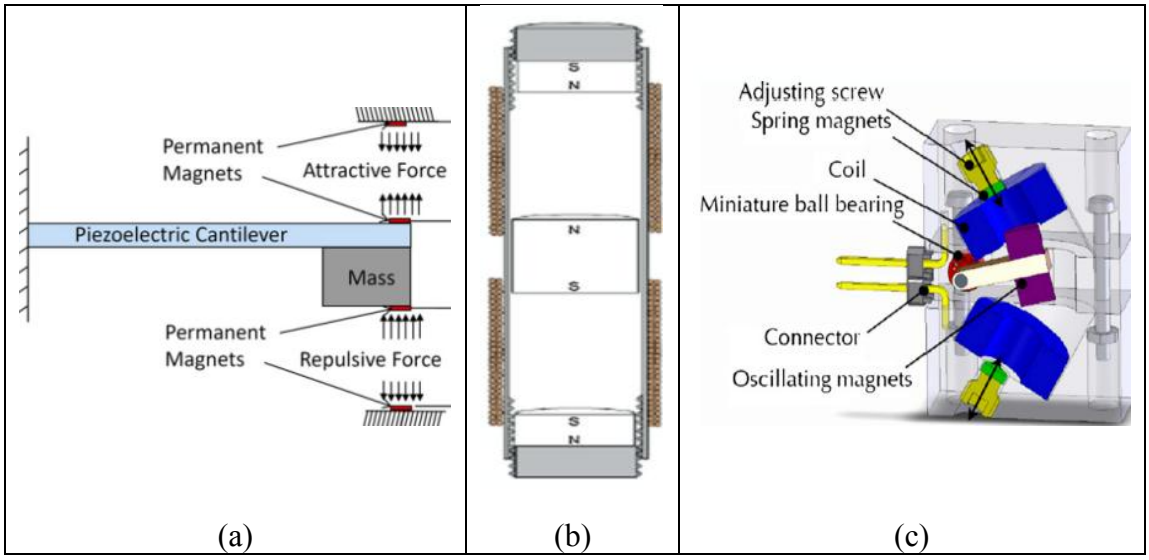

Figure 36. Adjustment of compliance through magnetic forces for (a) piezoelectric cantilever with magnetic tip mass, (b) permanent magnet linear generator, and (c) permanent magnet generator, (Challa et al., 2008), (Mann & Sims, 2009), (Spreeman, Folkmer, Maurath, & Manoli, 2006).

A breadth of tuning methods exist including electrical, mechanical, passive, active, intermittent, and continuous, each with advantages and disadvantages. The advantages and disadvantages of electrical and each type of mechanical have been presented in context. Active tuning, either intermittent or continuous, comes at the cost of energy as the actuators require power to tune the harvester, but with potential to net more energy capture. Calculations must be performed to validate the required energy usage and potential gain particular to the harvester, actuator, and excitation. Excitations which shift quickly would benefit most from continuous tuning, but the required energy would be too great for most other applications. Bridge vibration harvesting is an application which could use passive tuning to set the frequency to a specific location on a specific bridge, but a return trip to alter the tuning at a later time would likely not be worthwhile. It is possible that an intermittent, active tuning system could be successfully designed for the bridge application, but a more robust solution would be to increase the bandwidth of the

harvester to cover all frequencies it will experience throughout its use. For other applications tuning will likely grow in popularity as the harvesters evolve into smart structures in order to maximize energy harvesting from sources characterized by fewer simultaneous frequencies.

4.3: How can a wide bandwidth harvester be achieved?

Wide bandwidth harvesters are capable of capturing energy from multiple frequencies simultaneously over a large range. Many harvesters employ a bandwidth widening technique to increase the robustness for non-stationary and/or aperiodic excitations, where tuning becomes complex. Wide bandwidth systems can harvest from rapidly changing frequencies as they do not require time to adapt like tunable harvesters. Common methods include the use of arrays of harvesters, coupled harvesters, high damping, and nonlinearities such as mechanical stops, bistable structures, magnetic fields, and nonlinear compliance.

The most basic method to widen bandwidth is to increase damping (either mechanical or electrical). This method reduces peak power output but increases average power output across its bandwidth. This method therefore works best when ample acceleration is available but at unpredictable frequencies (Beeby et al., 2006). The resistance of the electric load could be changed to alter the electric damping to widen the bandwidth intermittently, although an example of this being used in vibration harvesting has not been found.

If ample volume is available and the harvesters are not too expensive, using an array of harvesters tuned to different frequencies is a viable option that is not as complex as many others. With an array, peak power is not diminished by the widening technique and additional damping is not introduced. (Xue, Hu, & Q.-M. Wang, 2008) demonstrated

how bandwidth is widened by increasing the number of piezoelectric cantilevers in series and how the bandwidth may be shifted by changing the number in parallel. The use of arrays is not as common since much vibration harvesting applications require small packages. The bridge application has room for an array, so the cost of each harvester and the total number required become the driving factors.

Another method utilizing nonlinearity is to add a mechanical stop along the length of a cantilever beam. This method effectively changes the beam length upon impact, increasing the frequency of oscillation of the portion between the stop and beam end. The nonlinearity is not seen until high amplitude vibration is caused by adequate energy in the excitation, such as an impact. The disadvantages of this approach are the introduction of fatigue and the reduction of peak output power.

Bandwidth has also been widened by mechanically coupling multiple harvesters. Two examples are given in Figure 37, the first of which uses two masses (magnets) connected in series with springs. Each coil is mounted to the housing to harvest the total motion of both masses rather than the relative motion between the masses. Additional masses could be used to increase the bandwidth further. The second example uses multiple masses (magnets) distributed along a supported beam. The beam is designed to harvest the beam's first three modes of vibration, which may be designed by changing the beam geometry and mass locations. Mechanically coupled harvesters are simple to design and build, but produce reduced peak output power, a common disadvantage.

Another strategy is to include nonlinear compliance such as nonlinear springs or repelling/attracting magnets. The frequency response of the harvester is identical to a linear system when excited at low amplitudes, and then becomes increasingly nonlinear as excitation amplitudes increase, as shown in Figure 38a. The nonlinear system delivers higher power output at frequencies higher than its equivalent linear resonant frequency,

so long as sufficient excitation is present to maintain the large oscillations. When this is no longer true, the oscillation transfers to a lower amplitude state. This is shown in Figure 38a as the solid line to the right of the dashed line. The load resistance may be tuned to maintain high amplitude oscillation for higher power levels (Mann & Sims, 2009). An inherent trait is the hysteresis between response to increasing and decreasing frequencies, as shown in Figure 38b. When the harvester is exposed to decreasing frequencies, it remains in a low-amplitude oscillation state, whereas increasing frequencies allow a high-amplitude state. Further work needs to be carried out to evaluate the performance of nonlinear harvesting of sources with many frequencies, like that of a highway bridge. The three harvesters previously discussed and shown in Figure 36 utilize nonlinear magnetic compliance to widen bandwidth as well as provide a tuning mechanism.

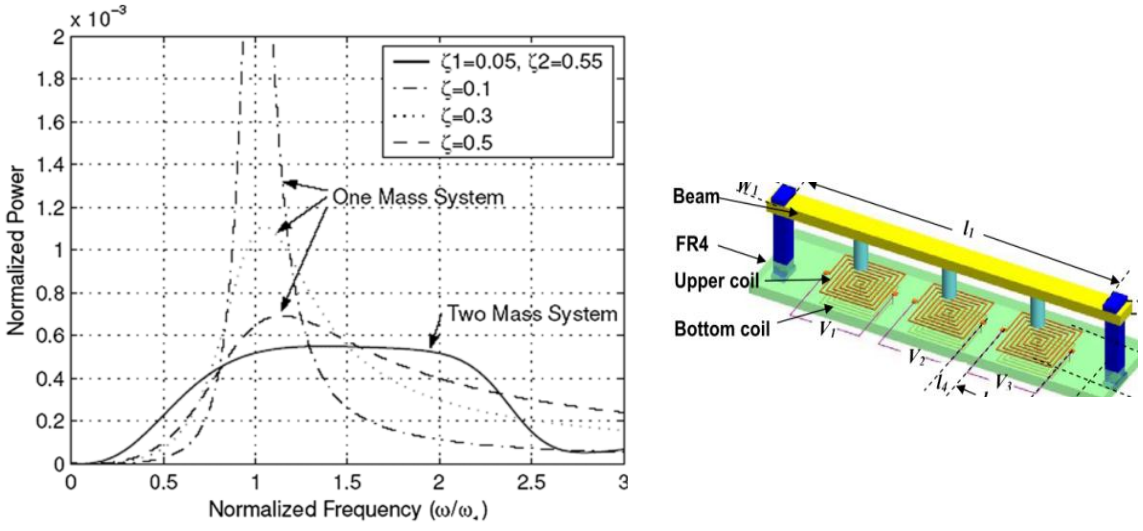

(a) (b)

Figure 37. Power from a coupled two-mass system and equivalent one-mass system (a) (Zhu et al., 2010), and coupled harvester utilizing the first three modes of a beam (b) (B. Yang et al., 2009).

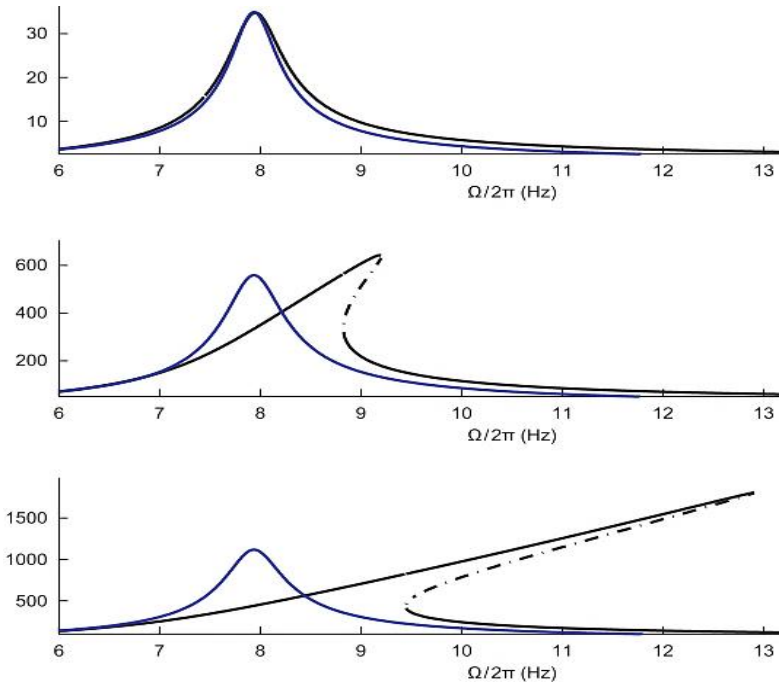

(a)

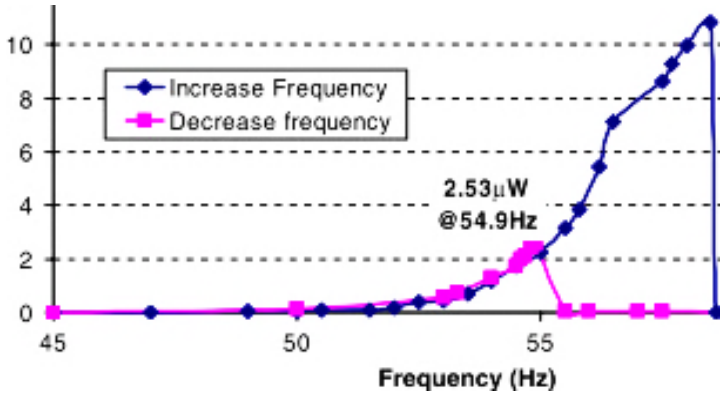

(b)

Figure 38. Increasing nonlinear response with increasing excitation amplitude (from top to bottom) (a), and hysteresis for a typical nonlinear harvester (b) (Mann & Sims, 2009) (Beeby et al., 2007).

One interesting patented harvester design by (Dick, Fralick, Jazo, Kerber, Brewer, et al., 2009)combines coupled harvesters with nonlinear compliance for harvesting of

wideband ambient vibrations. In this device, a magnet is suspended from an extension spring above a coil, with an opposing magnet resting on a compression spring below the coil, as shown in Figure 39. The magnets repel each other, thus making them magnetically coupled. As the magnets move close to each other, the field intensifies through the coil generating a voltage. The nonlinear compliance results in wide bandwidth and provides tunability by switching the springs for others with higher or lower spring rates.

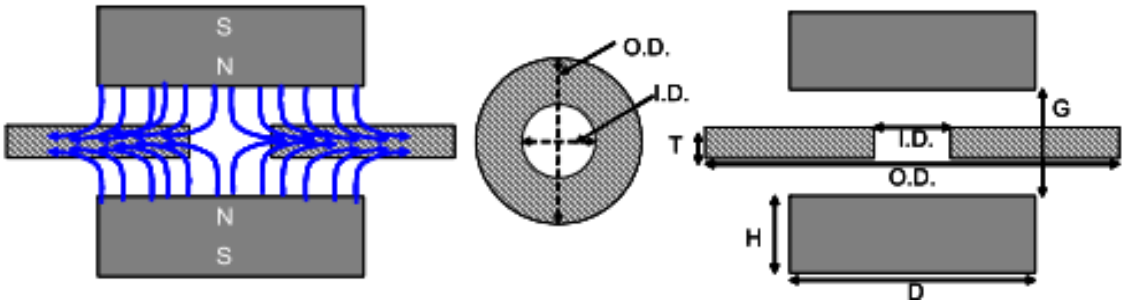

Figure 39. Coupled harvester with magnetic compliance to achieve wide bandwidth (Dick, Fralick, Jazo, Kerber, Brewer, et al., 2009).

It is also possible to exploit bistable behavior to widen bandwidth. Bistable structures are characterized by two regions of low potential energy separated by a region of higher potential energy. This "double well" potential as it is often called is exemplified by Figure 40a, which shows varying degrees of potential wells resulting from different parameter values. These systems perform better than linear harvesters at excitation frequencies significantly lower than the resonant frequency (Zhu et al., 2010), provided the excitation contains enough energy to transition the system between low potential states. (Cottone, Vocca, & Gammaitoni, 2009) designed and tested a bistable piezoelectric cantilever which used axially repelling magnets at the tip to achieve

approximately 600% increase in power compared to the harvester without bistability. The degree of bistability was controlled by the distance between the repelling magnets, with increasing bistability as the gap was reduced (see Figure 40a). An interesting bistable EM vibration harvester was developed by (Xing et al., 2009) which used magnetic attraction between a highly permeable cantilever and static magnets located at the limits of deflection, as illustrated in Figure 40b. The iron-based high permeability material allows the cantilever to be easily magnetized and attracted to the magnets, giving "wells" of low potential energy at the limits. The elasticity of the cantilever acts to restore the beam to its neutral position which is of higher potential than either limit. Since the magnets are oppositely polarized, the coil sees a moving magnetic field of varying intensity, resulting in higher induced voltage than just a moving field of constant intensity.

Several bandwidth widening methods were found with examples, advantages, and disadvantages of each. The bridge monitoring application seems to favor a wideband harvester over a tunable harvester, given the wideband excitation. The application is not constrained by the volume required by a harvester array or mechanically coupled system, making them worthy of further pursuit. The potential for nonlinear, amplitude limited, and bistable methods is dependent upon adequate excitation to maintain the high energy state, so more investigation is required to evaluate the feasibility of successful implementation of these methods to the bridge application.

4.4: WHAT CIRCUITRY IS NEEDED FOR HIGH EFFICIENCY?

To power the project's wireless system as it is designed, a vibration harvester must store the harvested energy between uses, as the power density is too small for direct power usage. The power generated by a vibration harvester is AC which must be rectified before it can be stored in a capacitor, ultracapacitor, or battery. For an efficient system

the impedance of the load must match the harvester (Stephen, 2006), leading to the use of voltage regulators between rectification and storage circuits. For these reasons the typical system is composed of subcomponents to perform the functions of rectify, regulate, store, and deliver upon need.

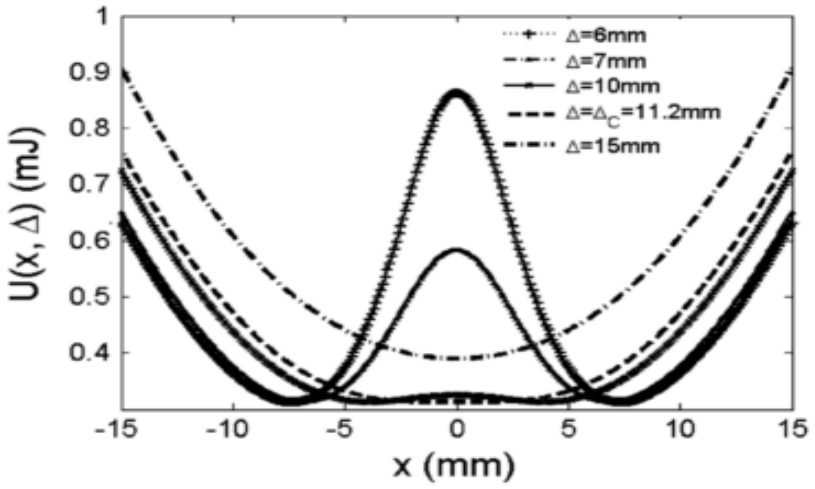

(a)

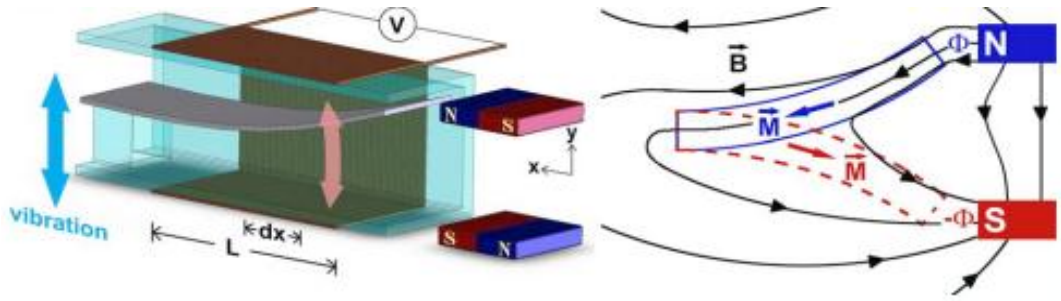

(b)

Figure 40. Bistable potential field (a), and bistable EM harvester (b) (Cottone et al., 2009) (Xing et al., 2009).

A basic system for these functions is composed of a full-wave rectifier with smoothing capacitor, DC-DC voltage regulator (buck-converter if decreasing voltage,

boost-converter if increasing voltage and buck-boost converter both are desired), storage capacitor or lithium-ion battery with charge controller, and switching circuitry to deliver the stored energy to the load (Priya & Inman, 2008). An impedance matching circuit could also be added between the storage and load. The most important property of the storage device is leakage, or self-discharge, which is minimized in tantalum and ceramic capacitors as well as solid-state lithium-ion batteries (Dick, Fralick, Jazo, Kerber, Brewer, et al., 2009), (Infinitie Power Solutions, 2010). The downside of using lithium batteries is the additional power needed to monitor an over/under voltage protection circuit.

Research to increase the efficiency of rectifiers has led to three solutions: passive, low forward threshold voltage diodes, switching converters, and a switching inductor in parallel with the rectifier. Standard diodes have a threshold voltage of 0.7 V, blocking current until the voltage rises above the threshold. Schottky diodes may be used to boost efficiency as they have low leakage, low on-resistance, and low forward threshold voltage of 0.375 V (Dick, Fralick, Jazo, Kerber, Brewer, et al., 2009).

Much work has been developed in the piezoelectric domain, as this domain is by far the most prominent in vibration harvesting. A common method is Synchronized Switch Harvesting on Inductor (SSHI), which uses a switch and inductor in parallel with the rectifier to change the voltage shape into a square-wave synchronized with the strain-rate of the piezoelectric. The result is drastically increased efficiency, but the method only works for transducers with low electromechanical coupling like piezoelectrics, so EM harvesters require an alternative. The frequency and output voltage from an EM harvester is usually lower than a piezoelectric or electrostatic harvester and the circuitry must accommodate. (Rincon-Mora, 2009) discusses methods which may be used with EM harvesters, including switching AC-DC converters (rectifiers) and switching DC-DC

converters. In these methods, triggered MOSFETs are used to conduct when the voltage is above 0 V and block when negative to give a very low effective threshold voltage. Some commercial devices are available from Advanced Linear Devices (Advanced Linear Devices, 2011). In addition, the triggering may be used to match impedance to further boost efficiency.

(Curry, 2008) developed a system with four times the efficiency of a basic passive system which is now offered commercially as the Ambiosystems Ambiomote™ (AmbioSystems, 2011). The circuit, designed for a low frequency EM harvester, uses a full-wave rectifier and actively triggered DC-DC buck converter composed of BJT MOSFETs, operating in Discontinuous Conduction Mode. The converter requires a timing signal which is supplied by an embedded microcontroller's pulse-width modulation function which is software-timed (allowing for adaptation of timing to different bridges). The Texas Instruments MSP 430™ is an excellent low power microcontroller for this purpose. The harvester first charges a small capacitor which enables the microcontroller to power on, allowing efficient charging of a larger capacitor for storage. A general block diagram of the system is presented in Figure 41a. The system enables the WSN node to record a measurement and transmit whenever enough energy is stored in the large capacitor, following the state diagram shown in Figure 41b. Similar but more general and less advanced circuits and transmitters are offered by Texas Instruments, Crossbow, MEMSIC, and Microstrain (Dick, Fralick, Jazo, Kerber, & Waters, 2009). Many of the components for these devices may be purchased from Linear Technology (Linear Technology, 2011).

There is much more to be reviewed in the field of vibration energy harvesting circuitry, but the scope of this thesis is set upon the electromechanical design and detailed circuitry will follow after successful implementation. For now, knowledge of the

existence of a specialized, high-efficiency EM harvesting circuit available commercially suffices.

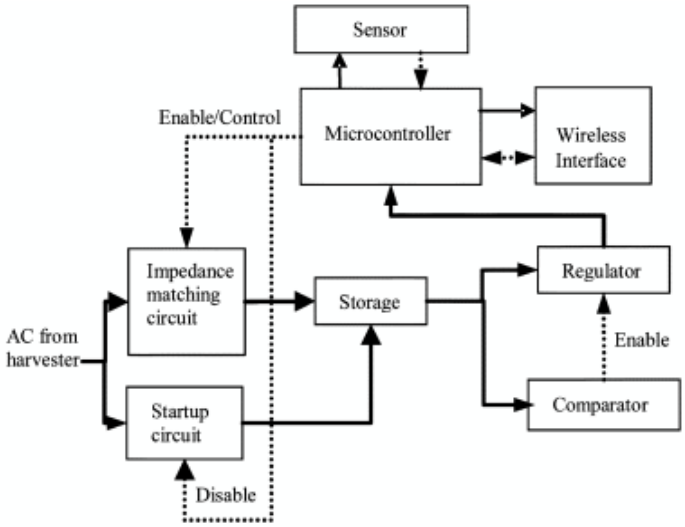

(a)

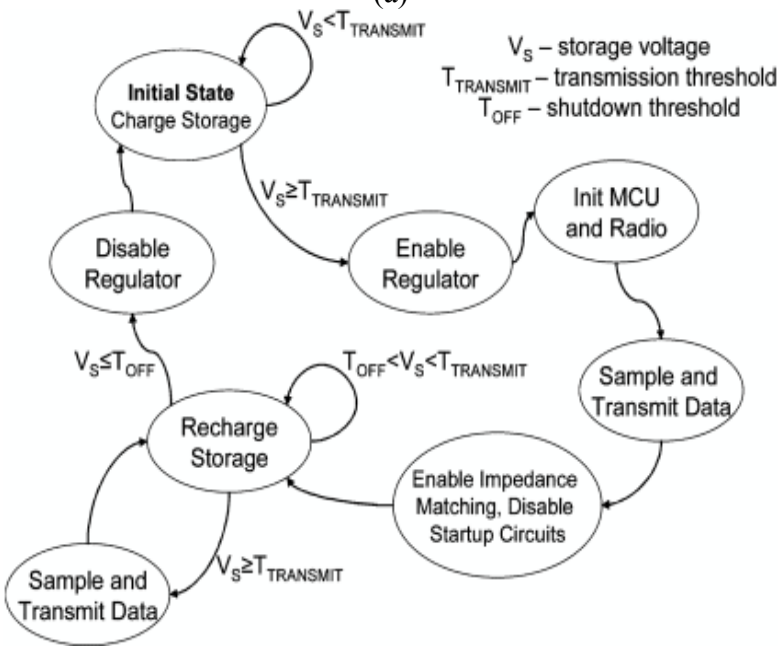

(b)

Figure 41. System block diagram (a) and state diagram (b) (Sazonov et al., 2009).

4.5: WHAT WORKS ARE SPECIFIC TO LOW FREQUENCY APPLICATIONS?

It is interesting to note that the majority of published research does not discuss why a specific topology or method was selected, as more effort is spent on the development of the specific system. Each harvester topology, tuning method, and bandwidth widening method has advantages and disadvantages promoting their use in one application over another. An exploration of EM harvesters for low frequency excitations is presented here.

Clarkson University used EM vibration harvesters to power a wireless sensor on a highway bridge in 2008 as a proof of concept. The three harvesters are shown in Figure 42, and were designed to 10, 10, and 3 Hz, respectively (Li, 2008; Li & Pragasen Pillay, 2008; Sazonov et al., 2009). The specific reasons for each harvester choice are not given, so it is likely a result of exploration. The first is similar to (El-hami et al., 2000), discussed in section 4.1, where an iron "mover" was used to connect two magnets to increase the field intensity. The second design utilized iron "teeth" to concentrate the field on the coil windings, which introduced "ripple" or "cogging" forces. These forces result from magnetic attraction between the moving magnets and teeth, and required additional design and extensive finite element analysis to refine. The third design used iron disks, called pole pieces, between opposing magnets to concentrate the magnetic field over the coil. This topology required less iron than the first and second designs, and generated a three-phase voltage in an attempt to boost circuitry efficiency by delivering a more constant voltage.

In a similar application, tidal waves were harvested using a linear generator on the sea floor connected to a buoy by a rope (Danielsson, 2003), as shown in Figure 43. The topology is very similar to the second design by Clarkson University, but places the magnets in the interior and the coils on the exterior. Similar flux concentrating teeth are

used, but the resulting cogging force is not as significant to this harvester as much higher energy is contained in the waves than in bridge vibration.

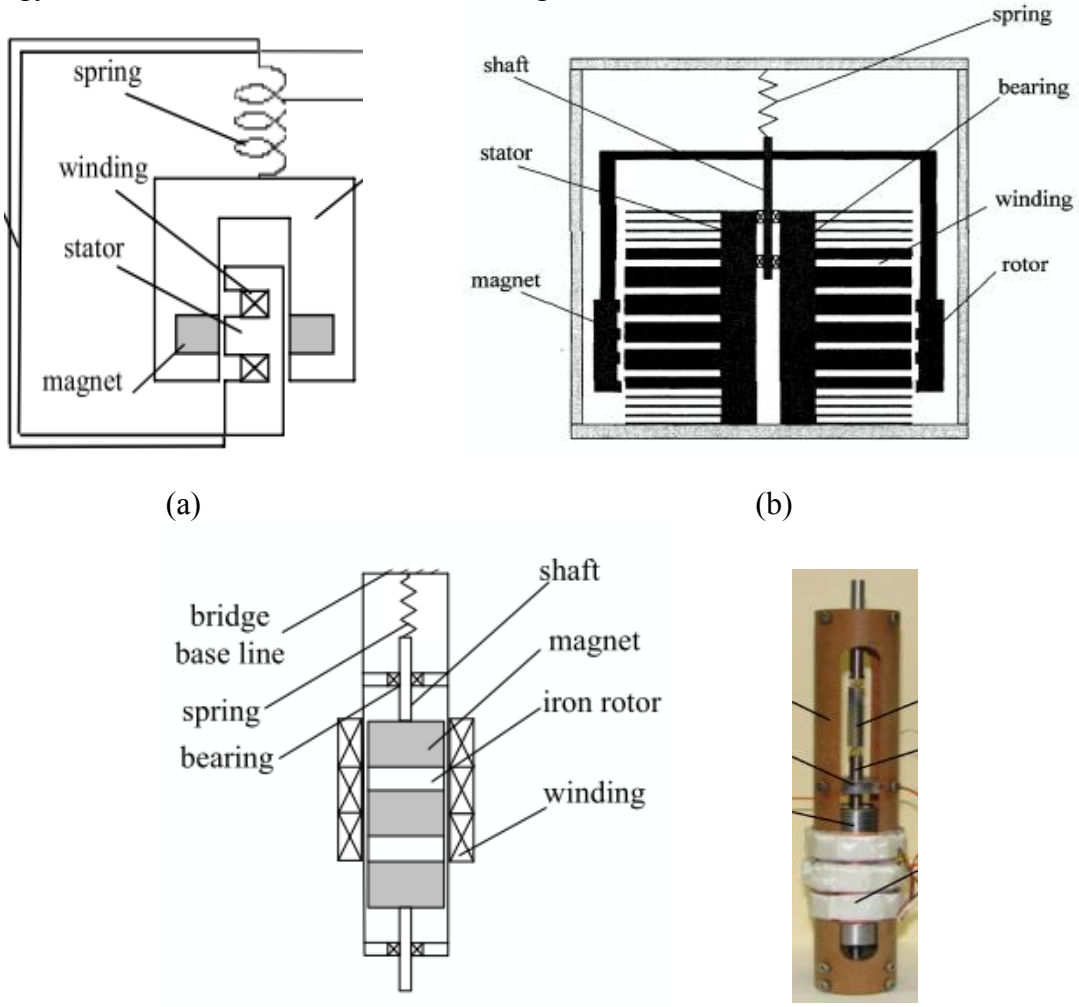

Figure 42. Clarkson University's bridge-specific harvesters: single phase horizontal axis coil, flux concentrating teeth, and three phase vertical axis coils (Li & Pragasen Pillay, 2007), (Li, 2008), (Li & Pragasen Pillay, 2008)

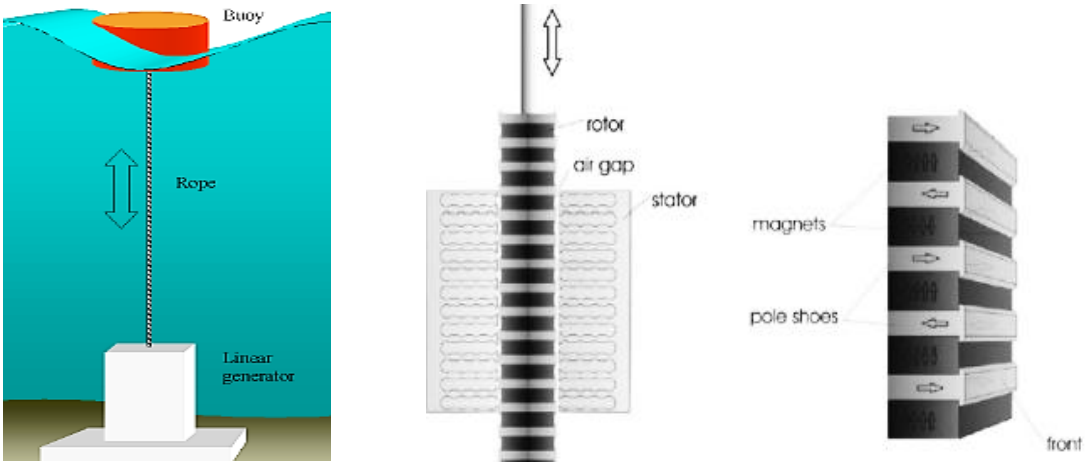

(a) (b)

Figure 43. System schematic (left), rotor topology (middle), and coil topology (right) (Danielsson, 2003).

A prototype of a human-powered lock for a safe was developed by (Jewell & Howe, 2002), as seen in Figure 44. The user pushes the shaft inward, generating a voltage from the changing reluctance of the shaft. The shaft is referred to as a salient-pole armature, similar to salient-pole electric motors which also use changing reluctance to induce a voltage. This type of harvester is acceptable at very low frequencies, but performs poorly at high frequencies where eddy current losses become significant in systems using changing reluctance. Using this topology for a bridge harvester could introduce additional losses compared to others.

The final harvester to be discussed was designed to be worn by a user and was built to power motion capture accelerometers in movie production, where the design focuses on capturing energy at an excitation frequency of 2 Hz and amplitude of up to 0.5g (von Büren & Tröster, 2007). The harvester, shown in Figure 45, used a magnetic structure identical to that of Clarkson's third design. An aluminum four-bar mechanism with living hinges was used as the compliant member for longevity, as the author states.

The four-bar mechanism allows the translator to move vertically only over a short distance before contact with the coils, so the harvester is not ideal for large displacements. Of most importance is the author's parametric optimization of the magnet, coil, and pole piece geometry for maximum average power output. The optimization results are given in terms of ratios of magnet radius/coil outer radius, magnet height/coil height, and magnet assembly height/coil outer radius, such that scaling to a larger harvester is possible.

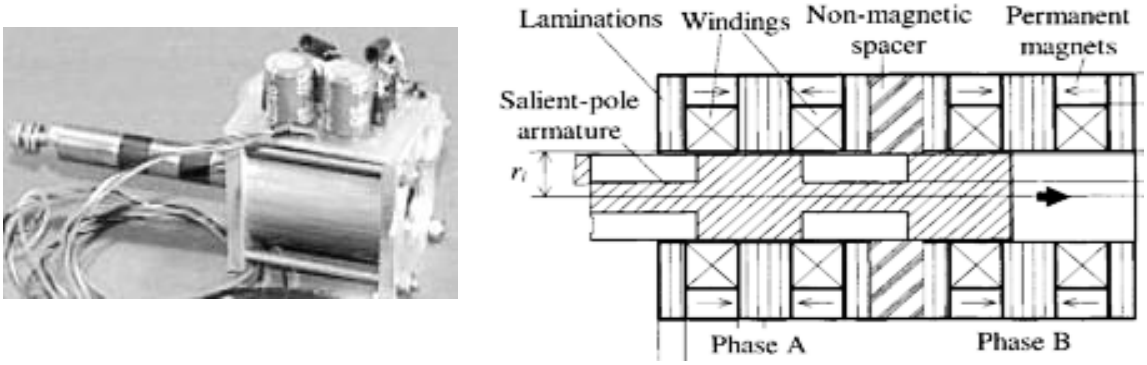

(a) (b)

Figure 44. Prototype and cross-section schematic of salient pole harvester (Jewell & Howe, 2002).

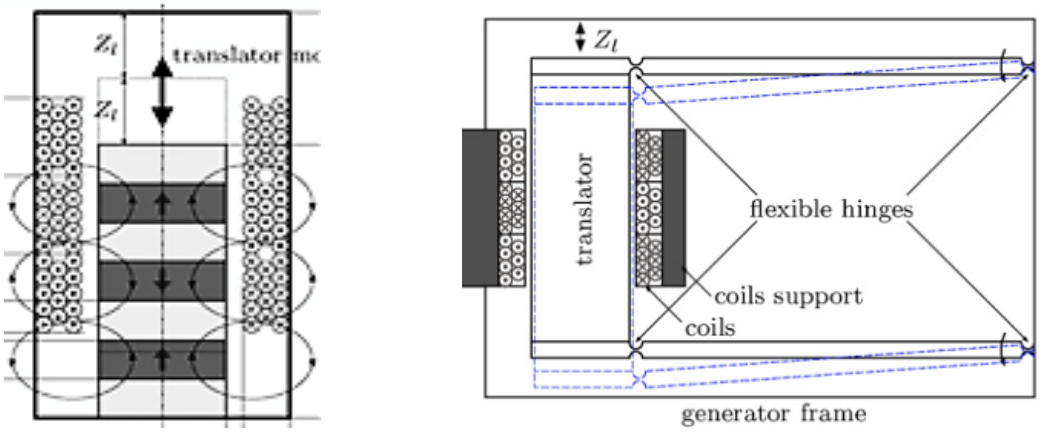

(a) (b)

Figure 45. Wearable flexible hinge harvester (von Büren & Tröster, 2007).

From this review it seems that cogging forces and variable reluctance should be avoided to minimize parasitic losses and maximize translator displacement from small bridge excitations. Also, the use of pole pieces between opposing magnets seems to be a topology worthy of further investigation as it is used in two low frequency applications (one at 2 Hz and the other at 3 Hz).

4.6: CHAPTER SUMMARY

The harvesters found thus far utilized a breadth of compliant members such as helical springs, cantilevered beams, supported beams, and flexible hinges on rigid beams. Others use soft ferromagnetic material such as iron to concentrate the magnetic flux in the region of the coils to give higher induced voltages. A common trend amongst almost all published research in the field is a lack of discussion or justification for the concept selection. Regardless, the key findings of this literature review are:

(1) For high peak power output:

- *a. High seismic mass is desired.*
- *b. Target high acceleration amplitudes.*
- *c. Target high frequencies with sufficient acceleration amplitudes.*
- *d. Match harvester and load impedance.*
- *e. Use Schottky diodes if reverse breakdown voltage is acceptable.*
- *f. Use a tantalum or ceramic-type capacitor for storage.*
- *g. If significant benefit, use a switching AC-DC or switching DC-DC converter.*
    - *i. Use a commercially available system.*
- *h. Omit cogging/ripple forces and variable reluctance to reduce losses.*

(2) For high average power output (robustness):

- *a. Desire wide bandwidth for simultaneous harvesting of multiple frequencies*

i. *Mechanically coupled, nonlinear, arrays, or bistable harvesters seem good for ambient vibration.*
    1. *Individual harvesters in an array should be rectified independently to avoid destructive interference.*

b. *Desire passively tunable bandwidth to match specific bridge during installation.*
    i. *Tune without introduction of damping by changing length, center of gravity, or tensile axial loading.*
    ii. *Design for lowest frequency with capability of tuning to higher frequencies.*

In the end, the vibration source's characteristics, the risk vs. reward preferences and budget of the project heavily influence the type of harvester and circuitry which should be used.

Chapter 5: Focused Conceptual and Embodiment Design

Conclusions from the literature review of works on electromagnetic energy harvesting, resonant frequency tuning methods, bandwidth widening methods, and associated circuitry were used to drive the focused generation of electromagnetic vibration energy harvester concepts. One concept was then selected and embodied in the form of two designs: an alpha design for the sole purpose of lab testing and verification with predicted performance, with no emphasis on end user-interaction (presented in this chapter), and a beta design which includes this emphasis (presented in Chapter 7).

5.1: Focused Concept Generation

The first generated concept is inspired by the harvester presented by (Zhu et al., 2008) which uses tensile axial preload to tune without the addition of damping. The concept in Figure 46 uses a two-pole magnet topology developed by (Glynne-Jones et al., 2004) for the electromagnetic transducer not disclosed by Zhu. The concept replaces the linear actuator for tuning with a manually adjusted bolt as a simplified, less-expensive alternative.

The concept shown in Figure 46 was expanded into a bistable harvester to achieve wide bandwidth as inspired by the design developed by (Cottone et al., 2009), mentioned previously[6]. Figure 47 shows this concept, which uses an EM transducer rather than the piezoelectric bimorph of the original. Two more coils were added in addition to the center coil to harvest the oscillations when the magnets are in the two potential "wells", with the center coil harvesting the transitions between these wells. A higher number of coils of potentially varying design may also be included, allowing the damping as a

[6] Bistable harvesters are particularly useful for random vibrations and make use of the function *Adapt to changing environment* with minimal user interaction.

function of displacement to be designed as desired. For instance, the coils in the potential wells may have low electrical damping to allow larger oscillations in this region, while the coil(s) in the potential barrier may have high electrical damping to extract more energy as the beam "snaps through" to the lower potential well. The bistability is created by repelling magnets – one at the beam's free end and the other attached to the housing – just as by (Cottone et al., 2009), but the magnets are convex to provide a gradual force on the beam as it nears the center position. The force experienced is proportional to the spatial derivative of magnetic field being traversed, which is high for sharp-cornered magnets like those used by (Cottone et al., 2009). Making the fields more gradual will reduce this force as well as potentially increase the probability of travel between wells. Simulation of this concept would have to be performed to fully evaluate how the barrier's sharpness affects the power output.

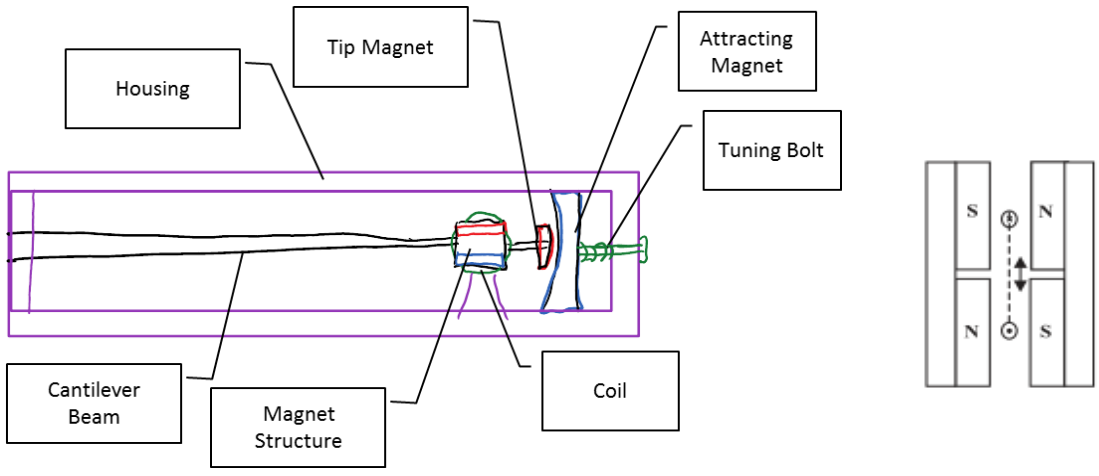

Figure 46. Focused concept A: Tensile axial load tuning (a), using two-pole magnet and coil topology (b).

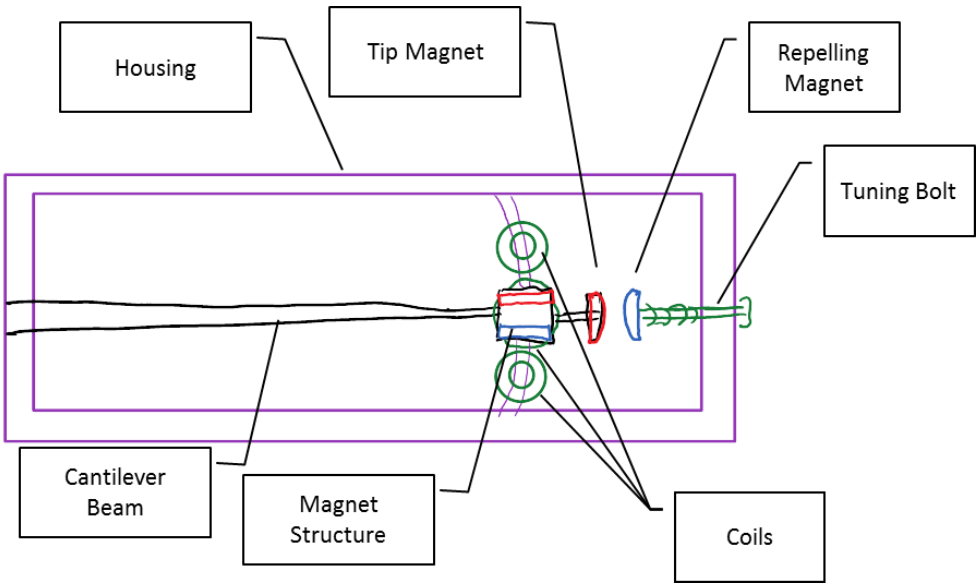

Figure 47. Focused concept B: Tunable bistable cantilever.

The third concept utilizes magnetic levitation instead of springs to achieve a nonlinear response which may be tuned by adjusting the distance between the tuning and translating magnets, as illustrated in Figure 48a. The basic concept was inspired by (Mann & Sims, 2009), presented in Figure 36. One addition is flux concentration with the use of high permeability pole pieces in the translating magnet structure to achieve higher induced voltage in the coils. Another is the *optional* placement of coils in the region between the tuning and translating magnets, similar to the harvester of (Dick, Fralick, Jazo, Kerber, Brewer, et al., 2009) presented in Figure 39. In this case the coils between these magnets have the same orientation as the other coils, as a design around the patent. The major advancement of this concept is its optional modularity for use in a harvester array, as the harvester *may* be joined to adjacent harvesters, as suggested in Figure 48b. Each harvester could be tuned to a specific frequency range, and then connected into an array. The bandwidth of the array may then be shifted by adjusting the tuning bolts at

either end of the array, which would alter each harvester's frequency by the same amount. The frequency of each harvester could be adjusted by threading the top tuning magnet relative to the connecting member. With this harvester array, the bandwidth may be shifted to match the specific bridge fairly easily. Newer, stiffer bridges could require the array to operate at higher frequencies, while older fatigued bridges could require lower frequencies. If a given bridge contains significant power at both high and low frequencies the individual harvesters may be adjusted to match during installation.

The final concept is composed of two magnetically coupled harvesters in a topology inspired by (Dick, Fralick, Jazo, Kerber, Brewer, et al., 2009), but with the use of flux concentrating structures to increase power output, Figure 49. Additional magnets repel each other to magnetically couple the two harvesters, while also concentrating the magnetic flux in the coil regions. Wave springs are also used to reduce system volume. The resonant frequency is tunable by threading the top and bottom portions relative to each other to change the magnet spacing.

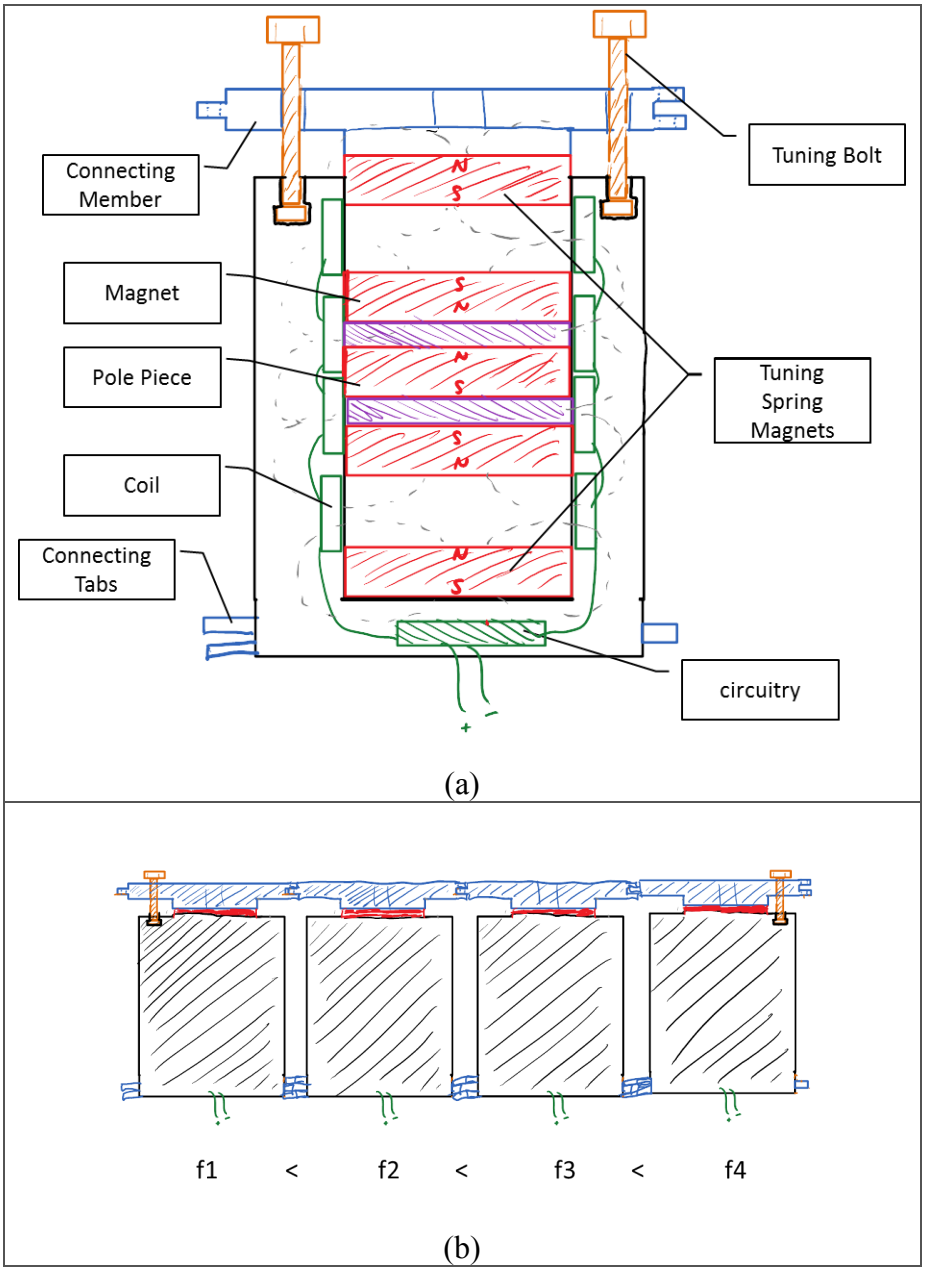

Figure 48. Focused concept C: Modular array with magnetic levitation tunability.

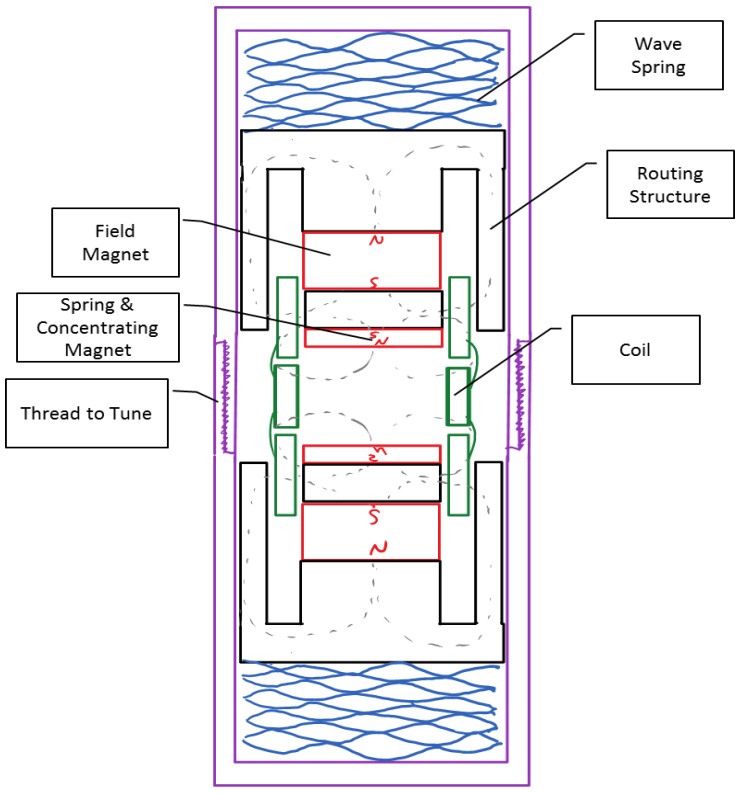

Figure 49. Focused concept D: Magnetically coupled with flux concentration and tunability.

5.2: Focused Concept Selection

Concept C, *Modular array with magnetic levitation tunability*, was selected for embodiment, prototyping, and testing for several reasons. First, the relatively large dimensions needed for cantilever beam harvesters, such as in concepts A and B, operating at low frequencies (1-15 Hz) are a concern for large-scale implementation across many bridges. Concept A, *Tensile axial load tuning using two-pole magnet and coil topology* uses attracting magnets to tune the resonant frequency with tensile force along the beam's axis. This method is desirable for tuning as it does not introduce damping, but the method also does not add bistability to the system and therefore remains linear. This design results in a narrow bandwidth linear harvester which must be tuned to

resonate at a specific bridge frequency. This response is acceptable as long as the bridge the harvester is mounted on contains stable dominant frequencies. This particular design would benefit most from an active tuning system capable of measuring and adapting to any changing bridge frequencies. At the early stage of this project, efforts are being concentrated on exploring systems which do not require active control. Designs which exploit active control will not be ruled out, though, and are suggested to be revisited at a later stage in the project. For these same reasons, the actively tuned vibration harvester concept detailed in Section 3.1, Figure 22 is left for future consideration.

Concerning Concept B—which exploits bistability through axially repelling magnets—early experiments by fellow graduate student Jason Weaver suggest that increasing the bistability of the system by decreasing the distance between the repelling magnets adds considerable damping, significantly reducing the ability of the beams to "snap through" the potential barrier. More detailed investigation into this bandwidth widening method is needed for a final conclusion, though, so the design is also left for future consideration if the selected concept is not successful.

Concept D is a fairly complex design for a first generation prototype in this project, although the author feels it is worth further investigation. A more basic version of this design is being used by the British vibration harvesting company Perpetuum, but only at frequencies above 20 Hz, which raises some concern (Arnold, 2007; Beeby et al., 2007; Field, Energy, Begins, & Ripen, n d; Perpetuum, 2011). This concept provides high magnetic flux in a similar fashion as the common loudspeaker. This configuration provides higher flux per unit magnet mass than Concept C, but uses more core iron to guide the magnetic field. Concept C uses magnetic components on the inside of the coil only, allowing larger displacements without colliding with the coil.

Concept C provides the *option* of a modular harvester which is tunable and of wider bandwidth than an equivalent linear harvester, and easily formed into an array of adjustable bandwidth. The design exploits recommendations 1b and 1c listed in Section 4.6: *Target high acceleration amplitudes*, and *Target high frequencies with significant acceleration amplitudes*, respectively. The nonlinear stiffening compliance created by the repelling magnets harvests the most energy from high acceleration amplitudes and frequencies, while occupying a relatively small volume compared to concepts A and B. This concept is not without risk, though, as no literature has been found which tests such a harvester with random vibrations. Exciting this design with replicated bridge vibration will certainly fill a gap in the research literature, and could find potential benefits.

5.3: Analytical Model

The first step to develop the selected concept is to understand its physics through first principles. The following sections present an analytical model of the design separated into its electromagnetic and mechanical components, followed by the combined system equations. These equations then serve in the construction of a numerical model of the harvester to parametrically design its components and predict performance.

5.3.1: Electromagnetic Components

Electromagnetic vibration energy harvesters use induction to convert kinetic energy into electrical energy. Faraday's law of induction, Equation 5.1, states that the electromotive force (*EMF)* is equal to the time derivative of total magnetic flux (Φ) experienced by the coil, with opposite polarity so to induce a current which will produce a magnetic force to oppose the change in magnetic flux (Lenz' Law). The EMF is the potential difference, or voltage, across the ends of the open-circuited coil. The total magnetic flux is equal to the product of the total number of coil turns (N) and the average

flux through each turn (φ), Equation 5.2, where φ is calculated as the area surface integral of magnetic flux density (B) over the coil area (A). The EMF may therefore be represented by the product of the flux gradient and the velocity as in Equation 5.3. The average flux gradient of each turn is calculated as the product of the average flux density (B_{avg}) and the length of the wire in the coil (l_{wire}) to form Equation 5.4, where this product is termed the average electromechanical coupling coefficient (K).

$$EMF = -\frac{d\Phi}{dt} \tag{5.1}$$

$$\Phi = N\varphi = \sum_{i=1}^{N} \int_{A_i} B \cdot dA \tag{5.2}$$

$$EMF = -N \frac{d\varphi}{dz} \frac{dz}{dt} \tag{5.3}$$

$$EMF = -NB_{avg} l_{wire} \dot{z} = -K\dot{z} \tag{5.4}$$

The EMF induces a current (i) in the coil and electric load given by Equation 5.6 which was obtained using Kirchhoff's Voltage Law, Equation 5.5, where R_c, L_c, and R_l are coil resistance, coil inductance, and load resistance, respectively (see Figure 50). The magnetic force this current creates, Equation 5.7, acts to oppose the motion of the translating magnets through the coil. This force may be represented mechanically as a velocity-dependent damping force with electric damping coefficient (c_e), whose value is given by Equation 5.8. The total electrical power (P_e) in the coil and load is driven by this damping action, Equation 5.9, where the portion delivered to the load may be represented by the load electric damping coefficient ($c_{e,load}$), Equation 5.10, and the remaining portion being lost as heat by $c_{e,loss}$, Equation 5.11. The model of Figure 50,

and the simulations discussed later, use the average electromechanical conversion factor (K) in place of the electrical damping coefficient (c_e), but either may be used if desired.

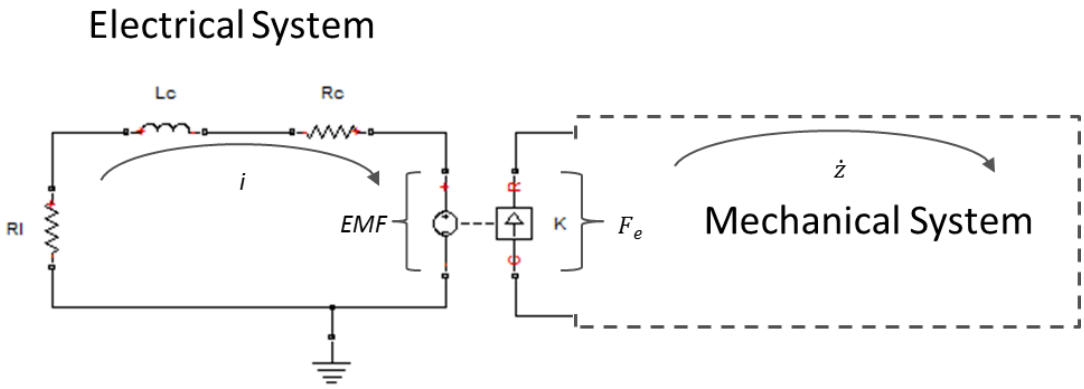

Figure 50. Equivalent circuit model of electrical system.

$$-K\dot{z} + i * (R_l + R_c + j\omega L_c) = 0 \tag{5.5}$$

$$i = \frac{K\dot{z}}{R_l + R_c + j\omega L_c} \tag{5.6}$$

$$F_e = Ki = c_e\dot{z} \tag{5.7}$$

$$c_e = \frac{K^2}{R_l + R_c + j\omega L_c} \tag{5.8}$$

$$P_e = \frac{EMF^2}{R_l + R_c + j\omega L_c} = c_e\dot{z}^2 \tag{5.9}$$

$$P_{e,load} = \frac{R_l}{R_l + R_c + j\omega L_c} P_e = c_{e,load}\dot{z}^2 \tag{5.10}$$

$$P_{e,loss} = \frac{R_c}{R_l + R_c + j\omega L_c} P_e = c_{e,loss}\dot{z}^2 \tag{5.11}$$

Maximum power is transferred from the energy harvester to its load when the impedances of each are equal. From (Stephen, 2006), the load resistance for optimum impedance matching is found by equating the electrical load impedance to the total (electrical + mechanical) harvester impedance as shown in Equation 5.12, where c_m is the mechanical viscous damping coefficient. The inductance of the coil itself, with magnets removed from its center, may be calculated using Equation 5.13, where L_c is the coil inductance (in μH), r_m is the mean coil radius (in cm), h is the total coil height (in cm), and t is the coil thickness (in cm) (American Radio Relay League, 2011). As the impedance from the inductor is low at low frequencies, L_c is often omitted unless $j\omega L_c$ is of the same order of magnitude as R_c. This omission may also apply to Equations 5.5-5.11.

$$R_l = R_c + j\omega L_c + \frac{K^2}{c_m} \tag{5.12}$$

$$L_c = \frac{0.8 r_m^2 N^2}{6r_m + 9h + 10t} \tag{5.13}$$

5.3.2: Mechanical Components

If a linear spring is used, the vibration harvester may be modeled as a second order system of translating mass (m), total damping coefficient (c_t), and spring stiffness (k), Equation 5.14. The total damping and spring forces are driven by the relative motion (z=x-y) between the mass (x) and harvester housing, which moves with the bridge (y) (see Figure 51).

$$m\ddot{x} + c_t * (\dot{z}) + k * (z) = m\ddot{y} \tag{5.14}$$

where c_t is the sum of the mechanical and electrical damping coefficients

$$c_t = c_m + c_e \tag{5.15}$$

The equation may be placed in standard form as:

$$\ddot{x} + 2\xi_t \omega_{n,linear} * (\dot{z}) + {\omega_{n,linear}}^2 * (\dot{z}) = \ddot{y} \tag{5.16}$$

where the natural frequency and total damping ratio are defined as:

$$\omega_{n,linear} = \sqrt{\frac{k}{m}} \text{ and } \xi_t = \frac{c_t}{2\sqrt{km}} = \xi_m + \xi_e \tag{5.17a,b}$$

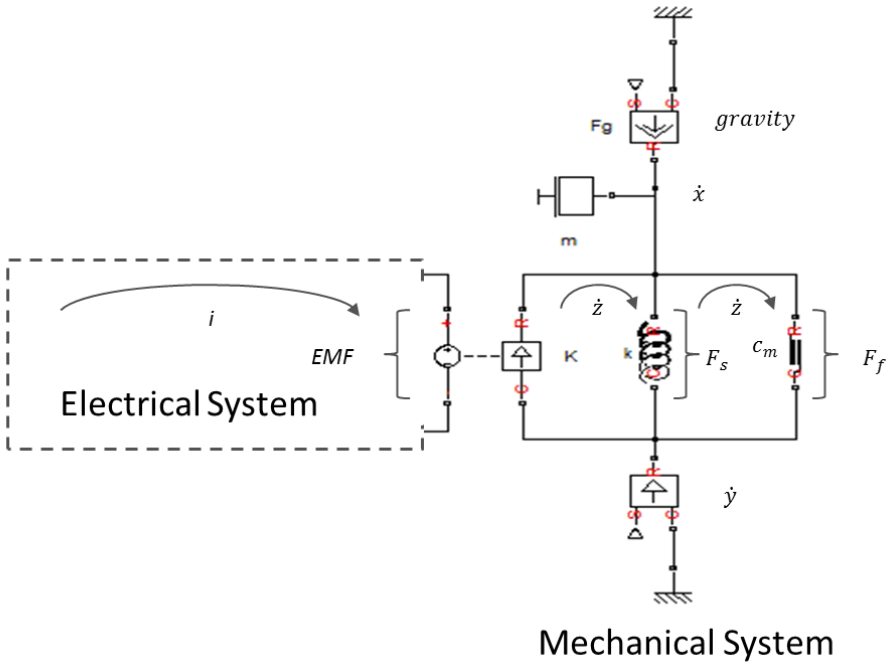

Figure 51. Equivalent circuit model of mechanical system.

If magnets are used instead of a linear spring, an additional stiffness term must be included to model the nonlinear magnetic stiffness. One quadrant of the force-displacement relationship between repelling magnets may be represented by a 3rd order polynomial, Equations 5.18a and b, with dependence upon the initial distance between the translating magnet and top and bottom spring magnets (d_t) and (d_b) (see Figure 52). Following the procedure presented by (Mann & Sims, 2009), Equation 5.19 presents a relationship governing the force ($F(z)$) on the translating magnet by the top and bottom

spring magnets ($F_{s,b}(z),\ F_{s,t}(z)$) which may be obtained in terms of the relative position between the translating magnet and harvester housing (z) and four stiffness coefficients, Equations 5.20a-d.

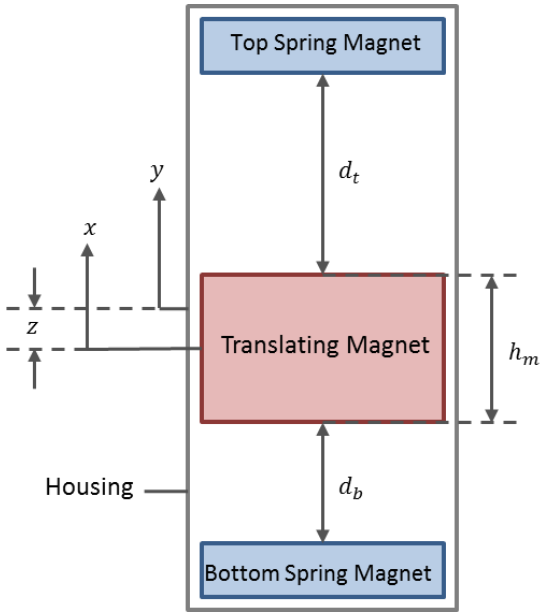

Figure 52. Schematic of mechanical components.

$$F_{s,b}(z) = \sum_{n=0}^{3} a_n * (z + d_b)^n \tag{5.18a}$$

$$F_{s,t}(z) = \sum_{n=0}^{3} a_n * (d_t - z)^n \tag{5.18b}$$

$$F_s(z) = F_{s,b}(z) - F_{s,t}(z) = k_0 + k_1 z + k_2 z^2 + k_3 z^3 \tag{5.19}$$

$$k_0 = a_3 * ({d_b}^3 - {d_t}^3) + a_2 * ({d_b}^2 - {d_t}^2) + a_1 * (d_b - d_t) \tag{5.20a}$$

$$k_1 = 3a_3 * ({d_b}^2 - {d_t}^2) + 2a_2 * (d_b - d_t) + 2a_1 \tag{5.20b}$$

$$k_2 = 3a_3 * (d_b - d_t) \tag{5.20c}$$

$$k_3 = 3a_3 \tag{5.20d}$$

If the top and bottom repulsive magnets are of equal initial distance from the translating magnet, k_0 and k_2 become zero, simplifying the model. Assuming the initial distances are equal, the mechanical system equation becomes

$$m\ddot{x} + c_t * \dot{z} + k_1 * z + k_3 * z^3 = m\ddot{y} \tag{5.21}$$

or in standard form:

$$\ddot{x} + 2\xi_t\omega_n * \dot{z} + {\omega_{n,linear}}^2 * \dot{z} + \alpha^2 * \dot{z}^3 = \ddot{y} \tag{5.22a}$$

where

$$\alpha = \sqrt{\frac{k_3}{m}} \tag{5.22b}$$

Following (Mann & Sims, 2009), the natural frequency for this nonlinear system may be calculated as

$$\omega_{n,nonlinear} = \sqrt{\frac{1}{m} * \left(k_1 + 3k_3 z_{eq}^3\right)} \tag{5.23}$$

where z_{eq} is the position of the mass in static equilibrium under the influence of gravity, which may be calculated by solving for the real root of the force-balance equation between gravity and the spring force. The tunability of the natural frequency is made possible by adjusting the magnet spacing which alters k, but not k_3, as it remains independent of d_t and d_b. This results in a linear relationship between separation distance and natural frequency, allowing straight-forward tuning.

As the energy harvester is being designed to harvest the vibrations of highway bridges which are small in amplitude, as shown in Chapter 3, minimizing friction and especially static friction will be very important in maximizing the energy captured. In what has been discussed so far, friction is represented by the mechanical damping

coefficient (c_m). This only captures the viscous component of friction which is proportional to the relative velocity between the sliding components, regardless of that velocity. In reality the friction may contain viscous, Coulomb, and Stribeck components if sliding contact of any kind exists. Figure 53 shows the friction force as a function of relative velocity, with breakaway force ($F_{f,brk}$), Coulomb force ($F_{f,c}$), Stribeck force ($F_{f,s}$), and viscous force ($F_{f,v}$). If only the viscous component was considered and the other friction components are significant, then the predicted power harvested will be larger than that produced by the physical system. This is because the breakaway force must be overcome before the magnets begin to translate, so any vibration that is insufficient will not contribute to power generation. The equations describing this friction force are given in Equation 5.24 (Armstrong & Wit, 1995).

$$F_f = \left(F_{f,c} + \left(F_{f,brk} - F_{f,c}\right)\exp(-c_{ta}|\dot{z}|)\right)sign(\dot{z}) + c_{vf} \tag{5.24}$$

where c_{ta} is the transition approximation coefficient which determines how rapidly the exponential term decays, and c_{vf} is the viscous friction coefficient which was previously termed the mechanical damping coefficient (c_m). To avoid a singularity from the discontinuity at zero velocity, a slight slope is used between the positive and negative breakaway forces (The MathWorks, 2011).

5.3.3: System

The electromagnetic and mechanical component models may be combined to form a system model represented by the schematic of Figure 54. The equivalent circuit model is excited by a velocity source ($V_{bridge} = \dot{y}$) which represents the bridge motion which is undiminished by the harvester's small energy extraction from the bridge, as well

as the constant force of gravity (F_g). This motion is imparted on the harvester's housing which is directly connected to the coil and indirectly connected to the translating magnet mass (m) through compliance (k) and friction (f). The translating mass' inertia causes relative motion between it and the housing. This relative velocity determines the frictional, compliant, and electromagnetic forces applied to the translating mass. The electromechanical conversion is represented by a gyrator which prescribes an EMF in the coil which is proportional to the relative velocity, and a magnetic force on the mass proportional to the current flowing through the coil and load.

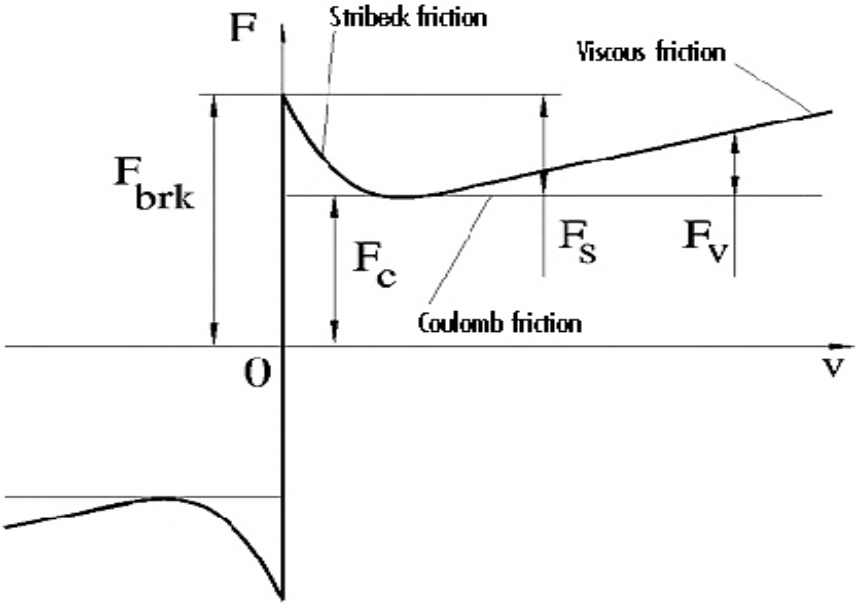

Figure 53. Detailed friction model (The MathWorks, 2011).

Performing a force balance and a sum of loop voltages results in the system equations, Equations 5.25 and 5.26, where $F_s(z)$ is the spring force as a function of relative displacement (z)—from either a linear spring or repulsive magnets—and $F_f(\dot{z})$ is the friction force as a function of relative velocity ($\dot{z}$). The friction force may be

composed of only viscous or all friction components based upon measured response and the physical layout (bearings, bushings, sufficient lubrication, etc.). These equations are of the most general form to include all effects but may be placed in various simplified forms using the equations listed previously in this chapter, such electrical and mechanical damping coefficients, for example.

$$m\ddot{x} + F_f(\dot{z}) + F_s(z) + Ki = m\ddot{y} \tag{5.25}$$

$$-K\dot{z} + i * (R_l + R_c + j\omega L_c) = 0 \tag{5.26}$$

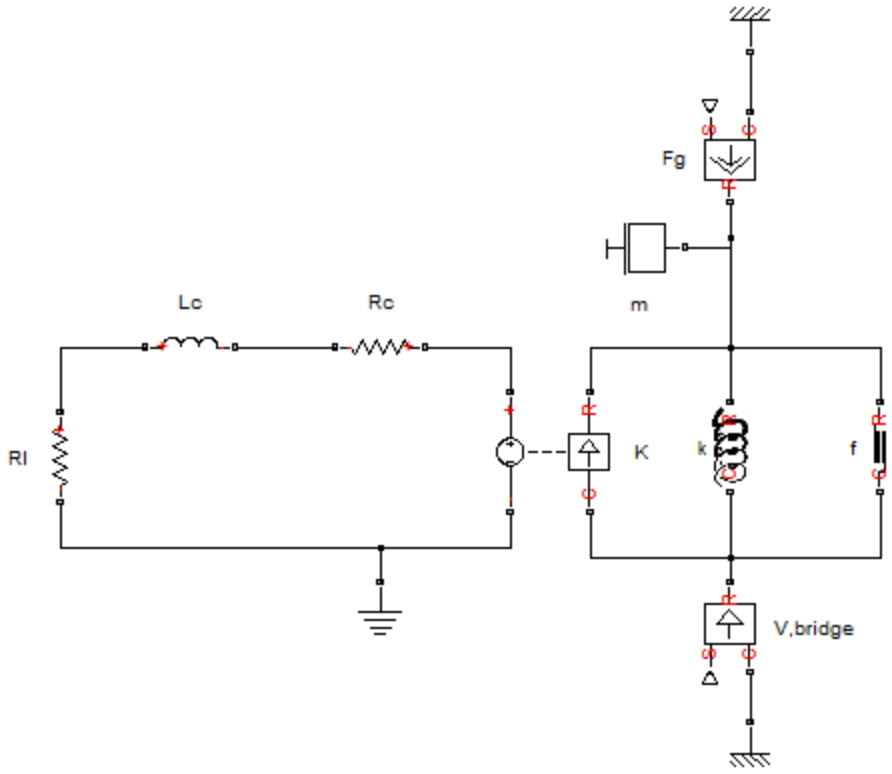

Figure 54. Equivalent circuit model of the electromechanical system.

5.4: NUMERICAL MODEL

The analytical model was transformed into a numerical model using MATLAB, Simulink, and the plugin SimScape to help size components and simulate performance. SimScape allows icon-based, acausal[7] physical modeling of multi-domain dynamic systems, allowing straight-forward visualization and debugging, as well as eases model refinement to include more detail as the research evolves. The Simulink/SimScape block diagram is shown in Figure 55, which is an expanded version of the model shown in Figure 54 that includes excitation by sine wave, swept sine wave, and measured bridge acceleration, as well as processing. To perform a simulation, a MATLAB .m file is executed, which calculates the system parameters from user-supplied inputs. These inputs include:

1. Excitation acceleration of sine wave, swept sine wave, or measured bridge acceleration (with 3 available bridge datasets).
2. Selection to use linear spring or nonlinear magnetic spring.
3. Dimensions and properties of magnets, coils, spring, etc.
4. Damping coefficients.
5. Selection to perform load resistance parameter sweep on any of the excitations.
6. Selection to perform initial magnet separation parameter sweep on any of the excitations.
7. Selection to perform resonant frequency parameter sweep for sine wave or measured bridge acceleration excitation.

[7] Acausal physical modeling refers to the simultaneous solution of systems of differential algebraic equations, without need to prescribe inputs and outputs needed by causal physical modeling.

8. Selection to use inferred parameters of the harvesters from (von Büren & Tröster, 2007) and (Li, 2008).

The Simulink/SimScape block diagram is called from within the .m file and the parameters are loaded into the diagram and simulated. The excitation acceleration is integrated to velocity, and then prescribed as the harvester housing velocity (illustrated in blue in Figure 55). Sensor blocks (illustrated in red in Figure 55) measure absolute and relative position and velocity, open circuit or load voltage, and current, sending the measurements to a processing block (illustrated in green in Figure 55) which calculates power and energy. The processing block then returns the measurements to the .m file where they may be post-processed and plotted.

Before meaningful simulations could be performed, more details about the harvester are needed in order to quantify the parameters. The following section describes this process.

5.5: Component Layout and Parameter Selection

As discussed in the focused concept selection, the translating magnet structure consists of opposing magnets squeezed together with iron alloy disks between them to concentrate the magnetic flux outward across the coil, as shown in Figure 56. As a first approximation, the dimensions were selected following the recommendations of (von Büren & Tröster, 2007). This work provided nondimensionalized geometry ratios for the magnets, disks, and coils from detailed optimization of an FEA coupled lumped parameter model. Their model was developed for a significantly smaller energy harvester, so extrapolation to larger geometries is assumed but not guaranteed to be correct. Future refinement of these dimensions should consider modeling through the use of an electromagnetic FEA software package. Optimizing the magnet assembly and coil

is very important to achieve the most power, which is exemplified by (Dick, Fralick, Jazo, Kerber, Brewer, et al., 2009) who showed over *five-fold* increase in peak output power by optimizing the coil inner and outer diameters for their type of harvester.

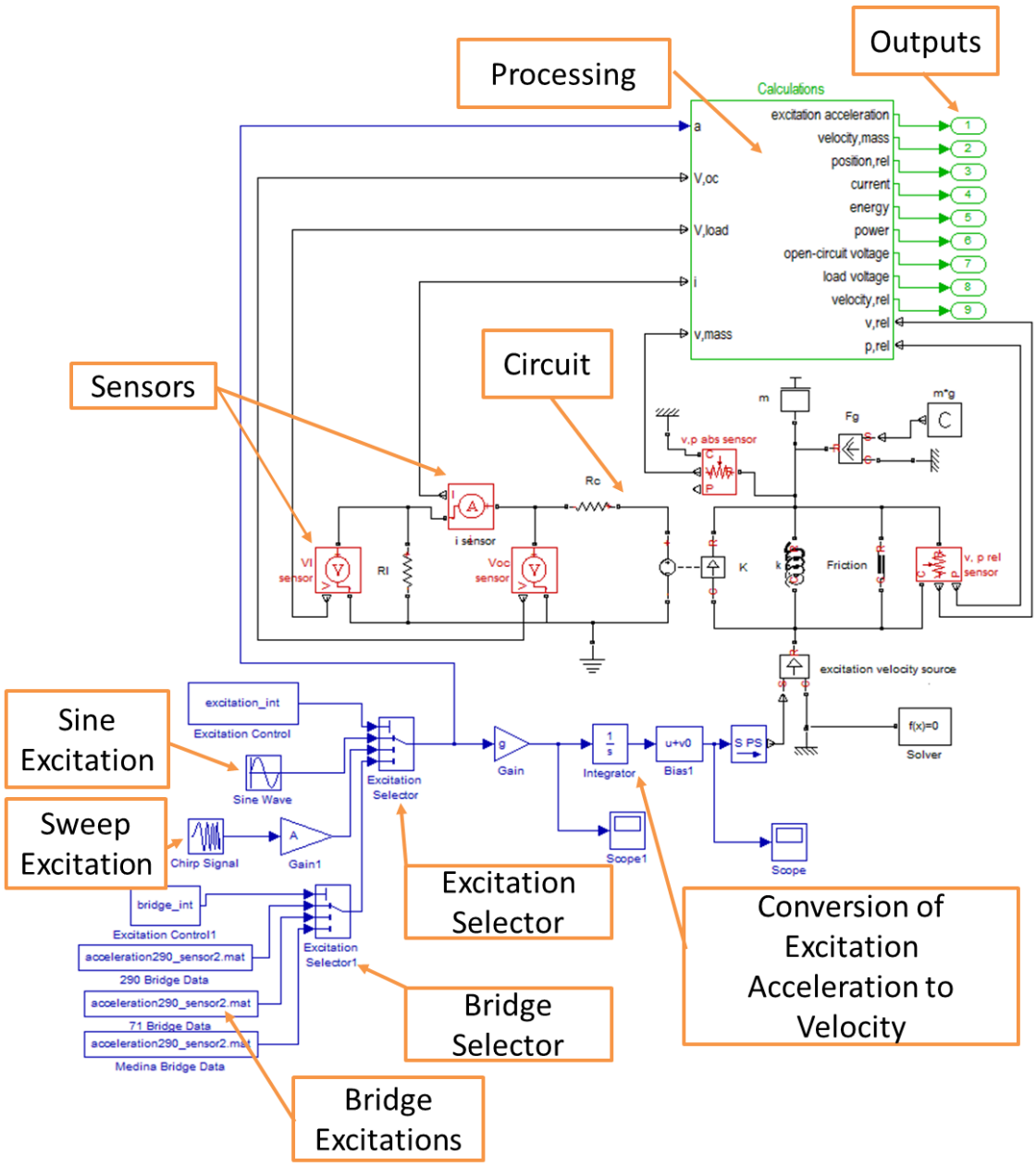

Figure 55. Diagram of the Simulink and SimScape portion of the numerical model.

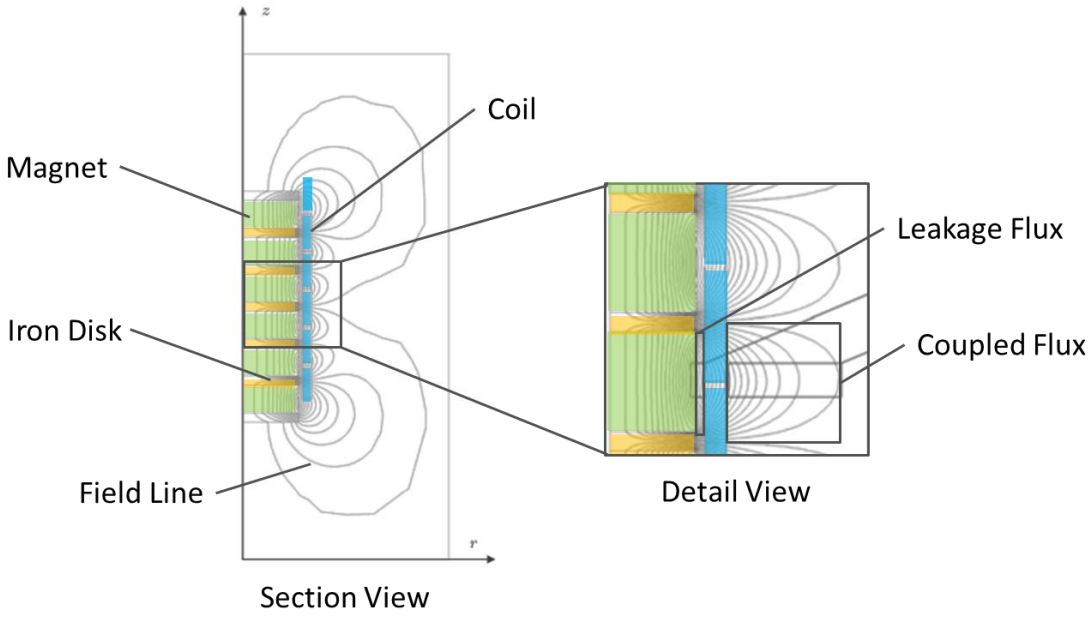

Figure 56. FEA model of magnetic assembly and coil (von Büren & Tröster, 2007).

The parameters used to size the system were based on the fourth topology von Büren optimized, as this topology provided the greatest mean electrical damping over the stroke length while still maintaining a high peak value. These values are presented in Table 6. In this table, pole height is the combined height of one magnet and one iron disk, which is equal to the height of one coil for maximum power. The coils are connected electrically in series and positioned such that the center of each coil is directly over an iron disk, where the flux density is highest. In this way, the gap between coils is in the area with lowest density to minimize the energy that is not captured. As there are an equal number of coils and magnets, and the coils are centered over the disks which lie between magnets, the magnet assembly must be offset vertically from the coils by one half pole height, as may be seen in Figure 56.

Table 6. Optimized geometry relations from (von Büren & Tröster, 2007).

Parameter	Value
Magnet outer radius / Coil outer radius	0.73
Single magnet height / single pole height	0.86
Magnet assembly height / Coil outer radius	7.35
Number of magnets	6
Number of coils	6

5.5.1: Translating Magnet Assembly and Linear Spring

The parameters of Table 6 were used to calculate the magnet height to radius ratio to be 1.4169. This calculation included dividing the assembly height to coil radius ratio by the magnet radius to coil radius ratio, then dividing by the number magnets and compensating for one more iron disk. Magnets with a diameter of 37mm and height of 12mm were selected for use, where two magnets would be stacked in order to satisfy the height to radius ratio. The fields of the two stacked magnets add constructively to act as one magnet, but likely with slightly less strength as a single, congruent magnet of the final dimensions. The mass of the translating magnet assembly was calculated using the density and geometry of the magnets and iron disks. This value was used to calculate the necessary spring stiffness of a linear helical extension spring so that the harvester resonates at 1.8 Hz, which is the measured dominant frequency of the instrumented box-girder bridge (see Figure 28 in Section 3.3). The required spring stiffness was found to be 184.05 N/m for a mass of 1.439 kg. This stiffness value is low but may be purchased from a number of suppliers. Checking this value was important to verify that the harvester was capable of linear and nonlinear resonance for comparison. Spring fatigue calculations were used to assure the spring would last 10 years without failure. A MATLAB optimization resulted in the conclusion that wide diameter springs will provide low spring constants with minimal height. This property is exploited by the wave spring

which is recommended in a future version. A summary of the parameters set thus far is presented in Table 7.

Table 7. Desired mechanical parameters.

Parameter	Value
Translating Magnet Assembly Mass	1.439 kg
Desired Linear Natural Frequency	1.8 Hz
Linear Spring Stiffness	184.05 N/m
Number of Iron Disks	5
Height of Iron Disk	3.9 mm
Magnet Diameter	37 mm
Height of Magnet Pair	24 mm

5.5.2: Spring Magnets

To predict the performance of the nonlinear harvester and determine the position of the spring magnets for tuning, it is essential to know the effective magnetic stiffness between the translating and spring magnets. In this measurement two sizes of spring magnet were used, with parameters stated in Table 8. A set of N38 Neodymium magnets were acquired with the dimensions of Table 7 to serve as the translating magnets. The experimental set-up was composed of a digital scale, nonmagnetic ruler, adjustable slide-mount, translating magnets, and spring magnet held in place with a plastic housing surrounding a shaft for guidance. The force from the scale was recorded for a range of measured distances between the magnets, providing force to distance relationship, as shown in Figure 57. This information was used to fit the magnetic stiffness polynomial described in Equations 5.19-20, with coefficients given in Table 9.

Table 8. Spring magnet properties.

Name	Vendor	OD	ID	Thickness	Grade	Pull	Surface Finish
Large	K&J Magnetics	1.5"	0.75"	0.75"	N42	?	Nickel Plated
Small	McMaster-Carr	1.181"	0.63	0.394"	?	4 lbf	None

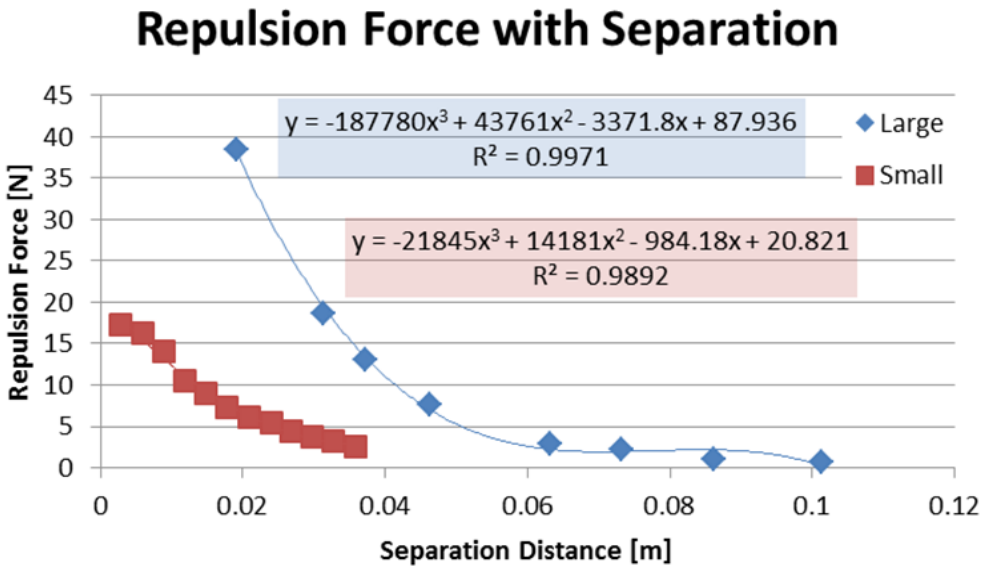

Figure 57. Magnetic repulsion force measurement results with corresponding 3rd order polynomial fits.

Table 9. Magnetic stiffness polynomial fit coefficients, used in Equation 5.20 to calculate the magnetic stiffness for the given initial magnet separation.

	Large Spring Magnet	Small Spring Magnet
a0	87.936	20.821
a1	-3371.776	-984.18
a2	43761.002	14181
a3	-187780.044	-2185

5.5.3: Coil

When the translating magnet dimensions were prescribed in Section 5.5.1, the outer radius of the coil was defined, as the two are related by the ratios of Table 6. The inner radius should be as close to the magnets as possible to minimize the leaked flux, as shown in Figure 56. With the inner and outer coil radii set, the optimal wire gage may be found. Selecting a small wire gage (diameter) will allow more turns in the coil which will

in turn produce a larger EMF (see Equation 5.4). At the same time more turns requires a longer wire length and smaller area which result in higher coil resistance. There is an optimal gage in which the highest EMF is achieved with lowest possible coil resistance, while staying under the gage's maximum permissible current.

As a first approximation, the optimal wire gage was extracted from the information supplied by von Büren's optimization. The first step was to find which packing factor was used to verify the legitimacy of the parameters. The packing factor is dependent upon the winding type and tightness of winding, and is the ratio of area available in one coil to the area that is filled with insulated wire. The packing factor was found to be 90%, which is the value used for orthocyclic winding in which the wire lies in the valley created by two previous windings (Beeby & O'Donnell, 2008). This value assumes perfect orthocyclic winding, which may be obtained with care but to be safe a slightly lower value should be used. Next, a relationship between the insulated wire diameter and coil outer radius was determined, using other parameters stated in the paper. This resulted in the suggested insulated wire diameter of 330 μm, which lies between the diameters for AWG 29 and 28 magnet wire (MWS Industries, 2011). For a slightly more conservative winding, a smaller wire diameter (AWG 30) with single-build insulation was selected, with the number of turns kept the same. The insulation build is a measure of the insulation thickness, with single-build being the most common. The result was a coil with the parameters shown in Table 10. Future refinement should consider the use of an electromagnetic FEA software package.

Table 10. Desired coil parameters.

Parameter	Value
Wire gage	AWG 30
Wire diameter with insulation	277 µm
Wire diameter without insulation	254 µm
Single Coil Height	2.79 cm
Number of coils	6
Total number of turns	9618
Outer Diameter	5.07 cm
Inner Diameter	4.3 cm
Resistance	476 Ω
Inductance	954.6 mH

5.6: PREDICTED PERFORMANCE

The parameters were loaded into the numerical model to allow simulation. As the prototype was not yet constructed and electromagnetic FEA tools were unavailable, damping values were borrowed from harvesters with similar construction (von Büren & Tröster, 2007) and (Li, 2008), with these values presented in Table 11.

Table 11. Damping values used to predict harvester performance[8].

Parameter	Value	Unit
Load Resistance Rl	10500*	Ω
Mechanical Damping Coeff cm	0.006**	Nm/s
Electrical Damping Coeff ce	0.2*	Nm/s
Total Damping Coeff ct	0.206	Nm/s
EM Conversion Coefficient K	25.6125*	Vs/m

5.6.1: Linear Case

The first step was to evaluate the predicted harvested power of the linear harvester with varying load resistance for a sine wave compared to a sample bridge excitation.

[8] * Values from by (von Büren & Tröster, 2007). ** Values from by (Li, 2008).

Figures 58-59 show the bridge excitation benefits from an increased load resistance as the acceleration levels of the bridge are less than that of the sine wave, on average. In the final application, the load will change impedance dynamically to harvest the most energy possible. For the rest of the tests, the load value from the sine test at 0.01g was used, which is 2.9kΩ.

Following this, the predicted harvested power for a range of acceleration amplitudes was evaluated under sinusoidal excitation. Figure 60 presents the result, plotted with a logarithmic vertical axis to allow visualization of the power at low amplitude levels. To gain an understanding of the frequency response of the linear harvester, a swept sine excitation was applied, resulting in Figure 61. A wider bandwidth may be achieved at the compromise of peak power by increasing the load resistance. The linear harvester was then excited by a 50 second sample IH-35N-US-290E direct connector (a box-girder bridge) acceleration for the linear case, as presented in Figure 62.

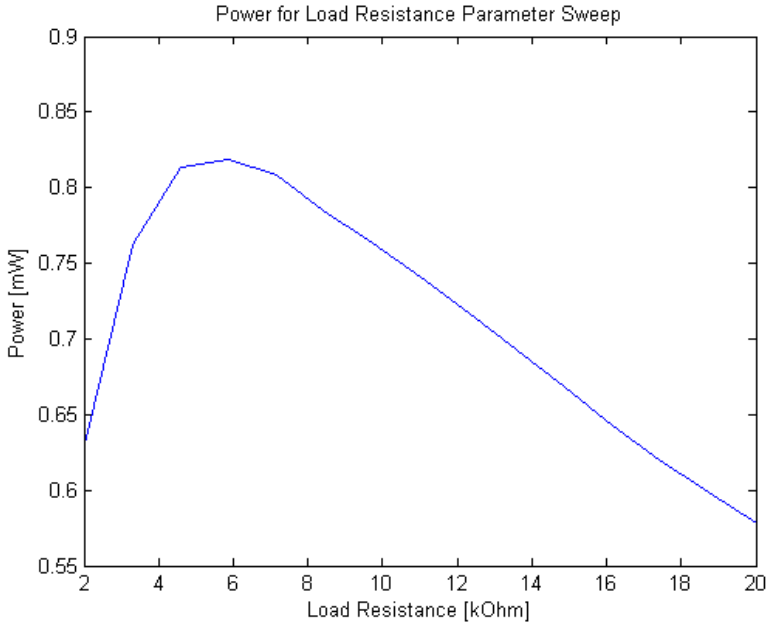

Figure 58. Peak harvested power for load resistance sweep under 50 seconds of replicated IH-35N-US-290E direct connector acceleration for the linear case.

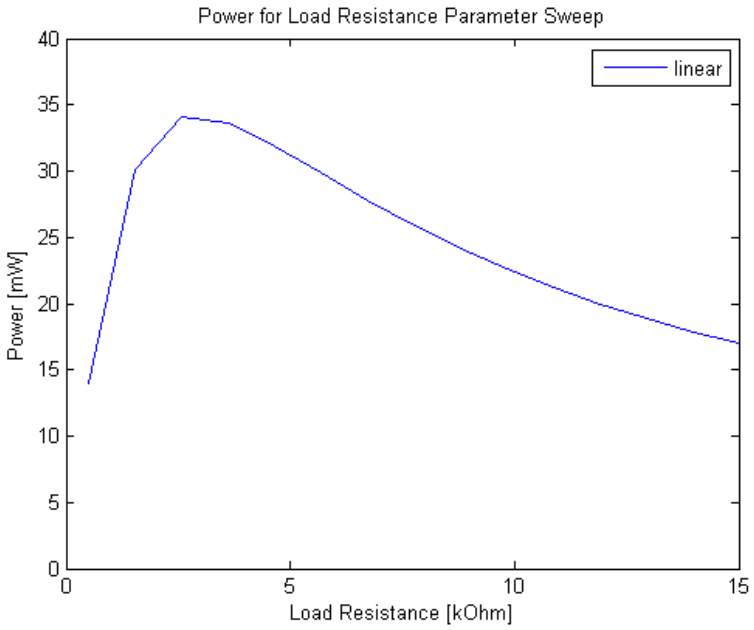

Figure 59. Peak harvested power for load resistance sweep with sine wave excitation of 0.01g and 2.2Hz for the linear case.

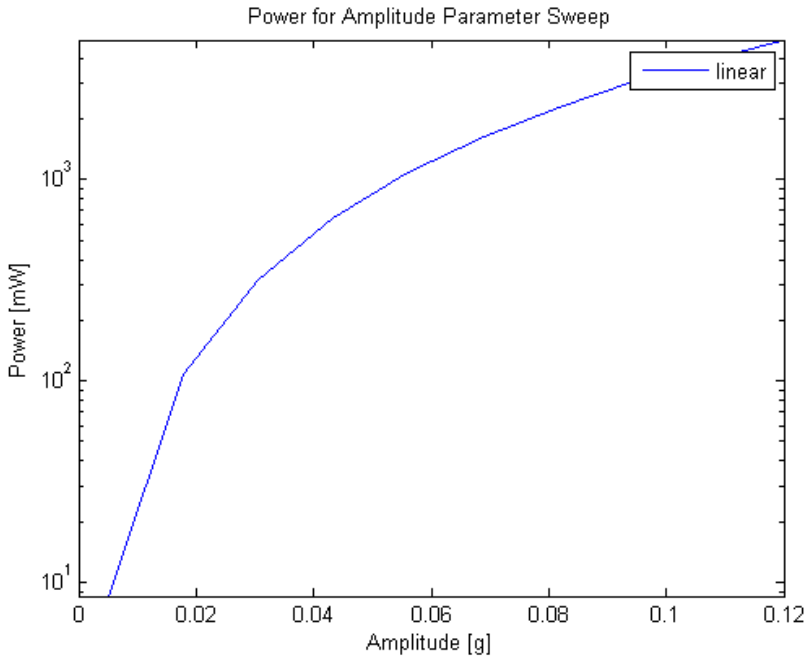

Figure 60. Peak harvested power for an excitation acceleration sweep for the linear case under sinusoidal excitation at 2.2Hz and a load of 2.9kΩ.

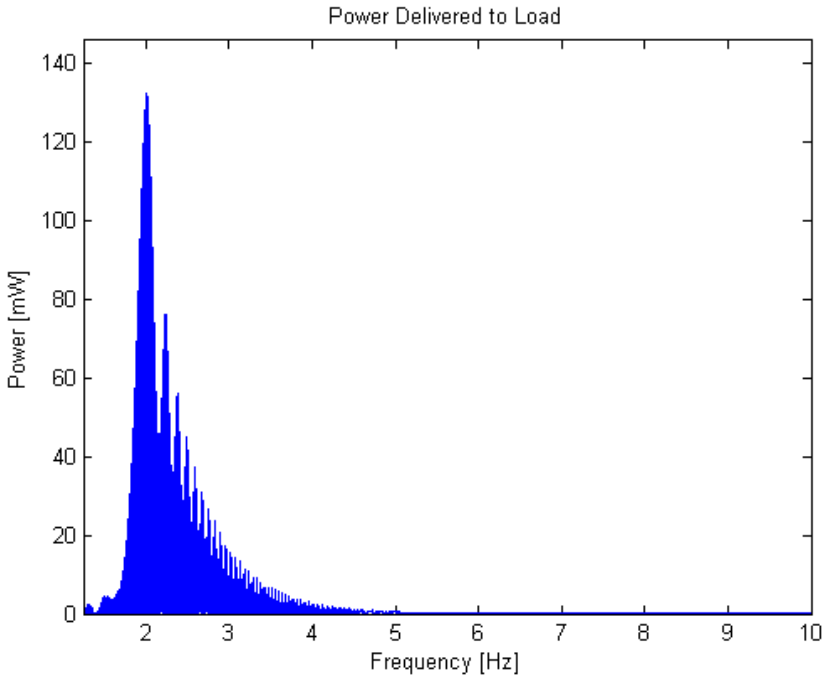

Figure 61. Peak harvested power under increasing swept sine wave over 120 seconds at amplitude of 0.05g and load of 2.9kΩ.

5.6.2: Nonlinear Case

To evaluate the predicted resonant frequency tuning range, a simulation was performed in which the separation distance between the translating and small spring magnets was varied, with result shown in Figure 63. This gives a relatively large linear tuning range in the field.

A frequency sweep was performed for comparison of bandwidth with the linear case. As with the linear case, the load resistance has a large effect on bandwidth, with a larger value resulting in larger bandwidth but lower peak power. The two following figures demonstrate this, with loads of 2.9 and 14kΩ, respectively.

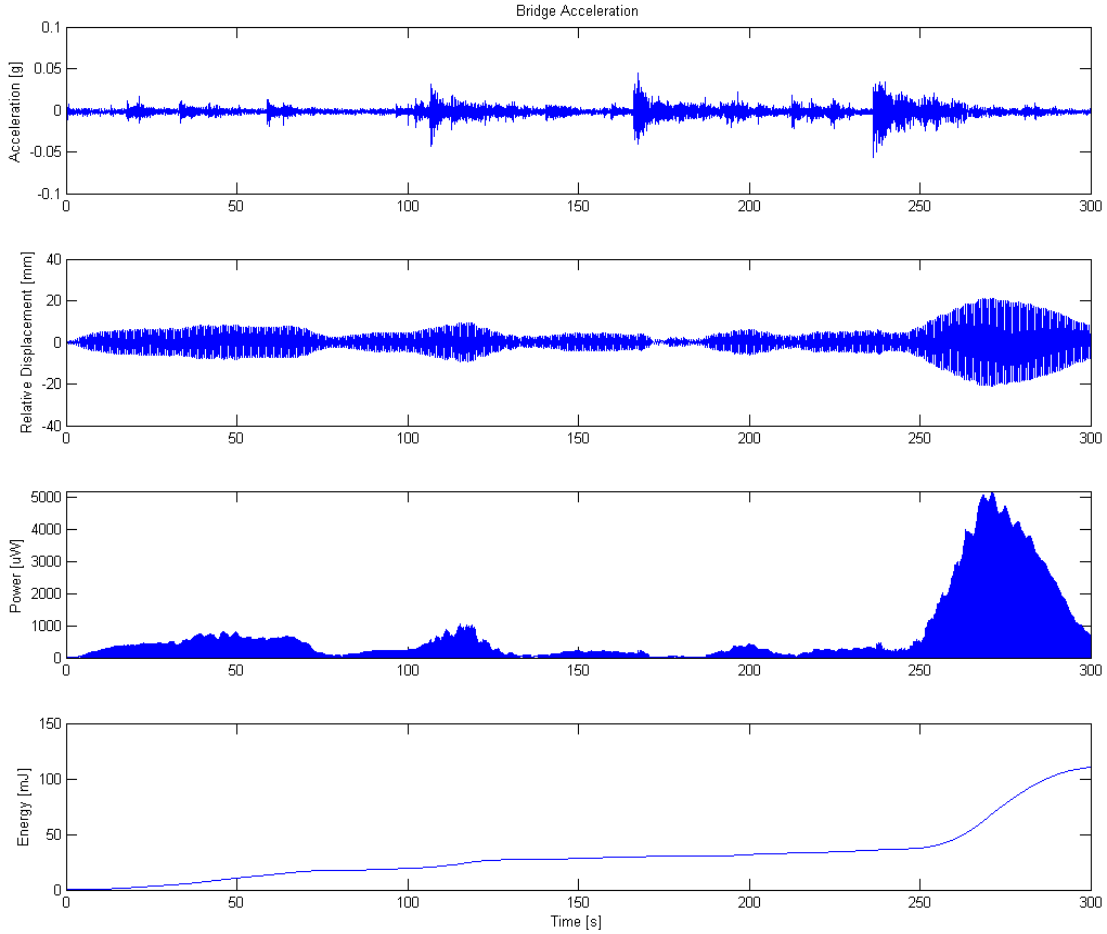

Figure 62. Bridge acceleration, relative displacement (between magnet and coil), peak harvested power, and harvested energy for 300 seconds of IH-35N-US-290E direct connector acceleration for the linear case.

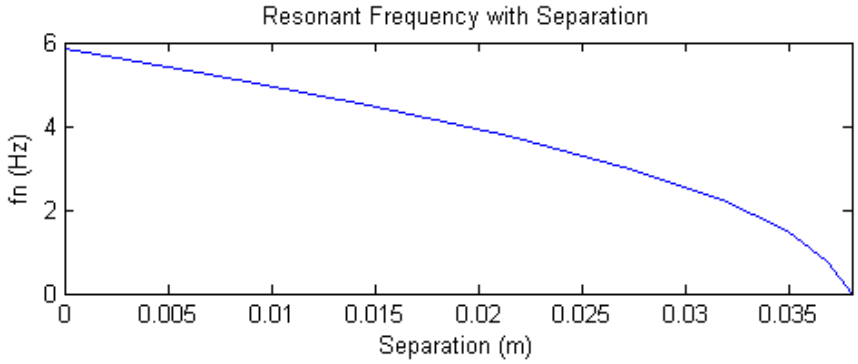

Figure 63. Tunable frequency range of nonlinear harvester using the small magnets.

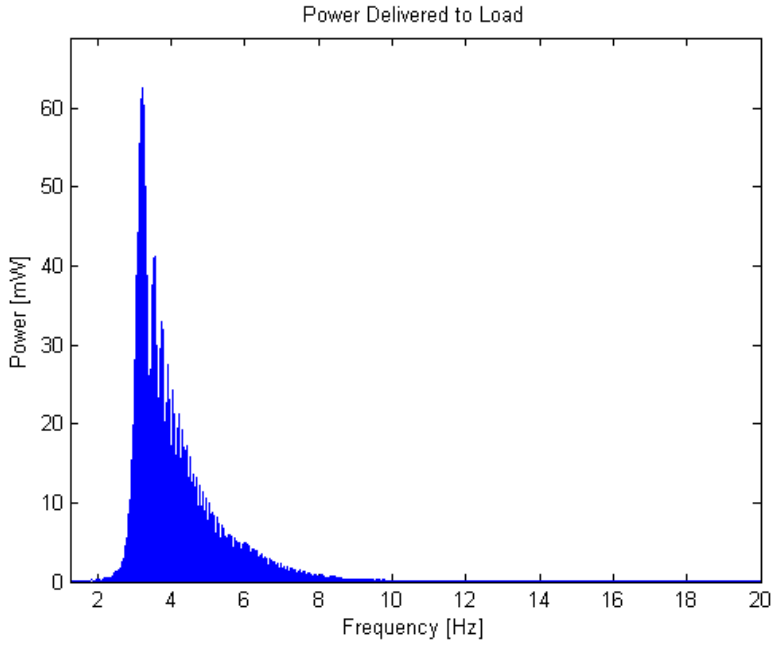

Figure 64. Peak harvested power under increasing swept sine wave over 120 seconds at amplitude of 0.05g and load of 2.9kΩ, for the nonlinear case.

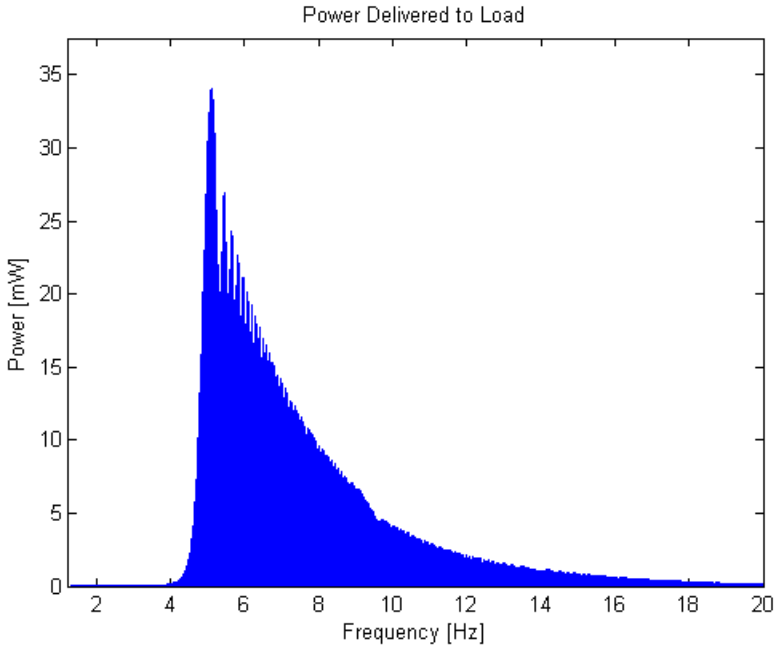

Figure 65. Peak harvested power under increasing swept sine wave over 120 seconds at amplitude of 0.05g and load of 14kΩ, for the nonlinear case.

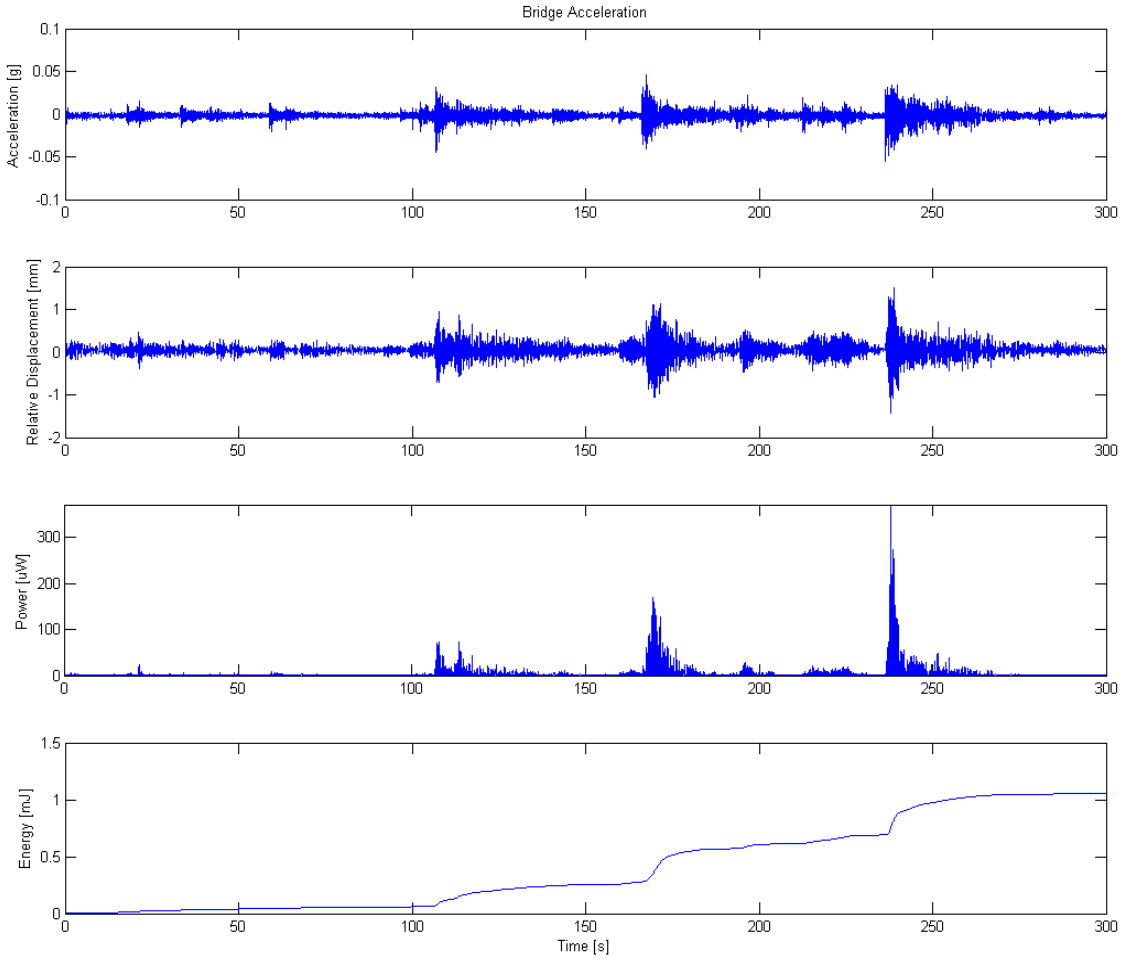

Figure 66. Bridge acceleration, relative displacement (between magnet and coil), peak harvested power, and harvested energy for 300 seconds of IH-35N-US-290E direct connector acceleration for the nonlinear case.

Simulation results suggest that the linear case will significantly outperform the nonlinear case for bridge vibration harvesting by a factor of 100 for this specific test. This is because the bridge vibration is fairly random and intermittent, and the nonlinear harvester excels with consistent excitation. This is a major find in this thesis as much literature favors this type of nonlinear harvester for other applications. Research papers which support nonlinear harvesters over linear harvesters always evaluate the two with a

sinusoidal frequency sweep. The nonlinear harvester performs better for this excitation, but when it comes to random vibrations which are intermittent, the linear case is preferred.

5.7: EMBODIMENT

An alpha prototype of concept C (first presented in Figure 48) was designed with convenient experimental testing in mind. This harvester is sized to be convenient to manipulate and include a removable linear helical extension spring for comparison of the nonlinear and linear response of the harvester. The spring magnets may be removed for linear testing, and are adjustable to evaluate the tunability of the device, as illustrated in the solid models of Figure 67. The translating magnet structure is guided by a precision ground shaft with linear ball bearings to maintain alignment within the coil. This was chosen over relying on the coil bobbin for this function because a smooth surface would be difficult to attain with the magnet structure's layered surface and difficult-to-machine magnets. This decision was reinvestigated for a final design, though. A cylindrical housing is well suited to align and mount the internal components in a vertical, top-down construction. The outer shell of this prototype consists of a polycarbonate tube such that the internal components can be viewed in demonstration. Vertical slots in the housing allow the spring magnets, bearings, and linear spring to be adjusted vertically for adaptability in testing and tuning.

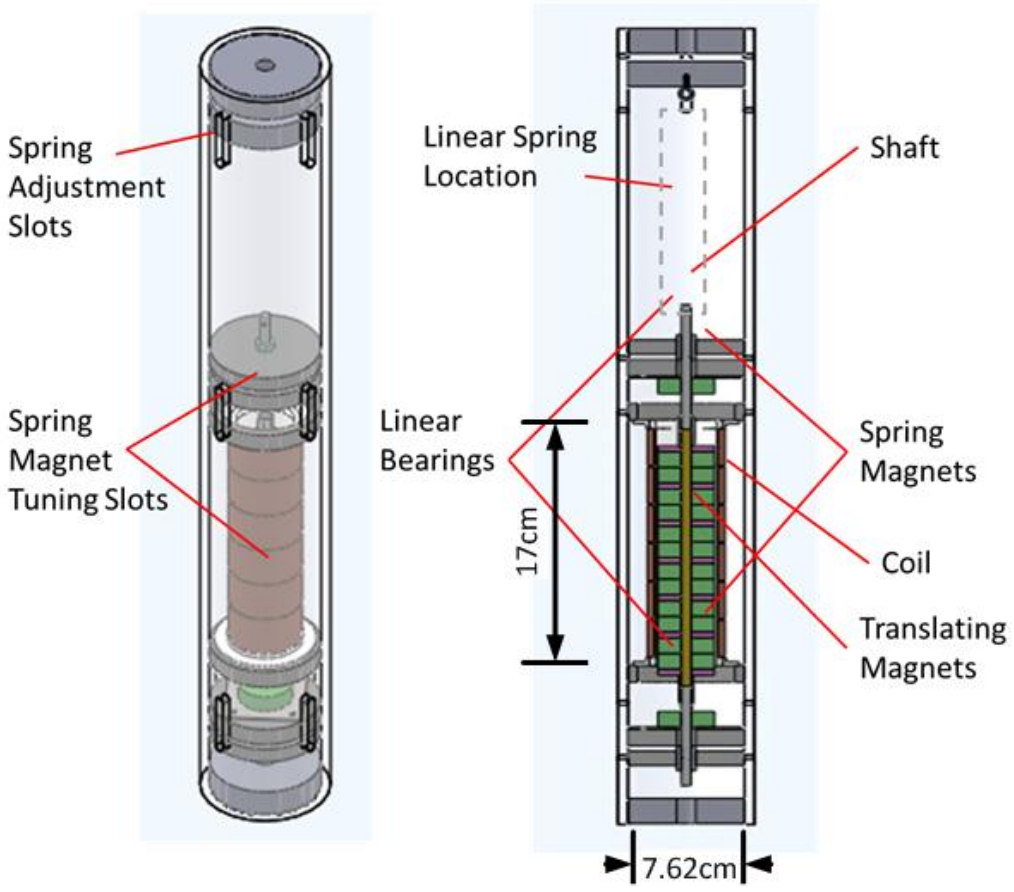

Figure 67. Solid model of test prototype.

Cylindrical ring magnets were selected to allow a central 316 Stainless Steel threaded rod to squeeze the opposing magnets to the iron disks, with 316 Stainless Steel nuts on each end to secure them in place. 316 Stainless Steel was used for the rod and nuts instead of ferromagnetic material to avoid guiding a portion of the magnetic field away from the coil and reducing the power output. Vim Var Core Iron alloy from Ed Fagan, Inc. was selected as the iron disk material (Ed Fagan Inc., 2011). This material has very high saturation induction[9] (2.15 T) as well as high relative magnetic permeability[10]

[9] Saturation induction is the maximum magnetic flux density permissible in a given material.
[10] Magnetic permeability is analogous to electrical conductivity for a magnetic flux.

(10,000), allowing a high magnetic flux density to exist in the material easily. To create the magnetic field, high strength N38 Neodymium magnets were used, with a diameter of 37mm and height of 24mm in order to satisfy the suggested ratios of Table 6.

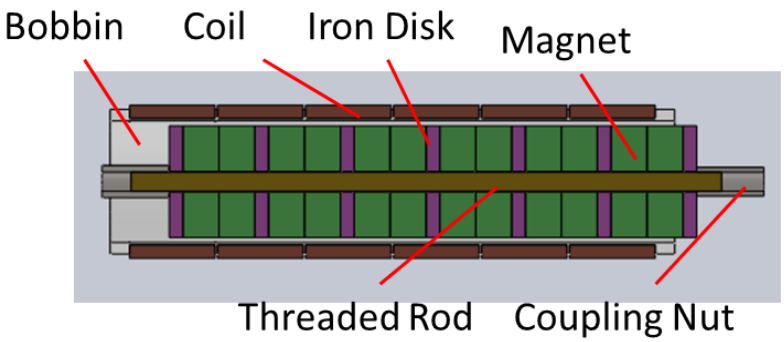

Figure 68. Magnet assembly and coil sectional view, rotated horizontally. The iron disks at each end must be removed if repelling magnets are to be used in place of a spring, as the iron disks would attract the repelling magnets.

5.8: CHAPTER SUMMARY

Four electromagnetic vibration energy harvester concepts were generated which include resonant frequency tuning and bandwidth widening methods. The concept including stiffening magnetic stiffness was selected, modeled analytically and numerically, and then designed parametrically. Simulations were performed to predict the performance of the harvester using the numerical model. More work is needed to expand the capabilities of the numerical model, but preliminary results favor the linear case for bridge vibration as it has better performance under random vibrations. The harvester was then embodied for construction and testing to follow in the next chapter.

Chapter 6: Prototype Fabrication and Experimentation

6.1: Prototype Fabrication

The test prototype was constructed by the author beginning with the translating magnet assembly, followed by the coil, then the housing and supporting components. The iron disks were turned on a lathe from a solid cylinder of Vim Var Core Iron, and then squeezed between the opposing magnets on a brass threaded rod, using nuts at each end to hold the assembly together. Coupling nuts were used which allowed the shafts to be attached to the assembly. These shafts translate with the assembly, supported by self-aligning linear ball bearings which are lubricated with oil. The shafts are nonmagnetic 316 Stainless Steel for strength and diamagnetism. The coil bobbin was turned on a lathe from a PVC pipe and then taken to an electric motor repair shop to be wound with AWG 30 magnet wire. The coil parameters differed from ideal because the PVC pipe used for the bobbin had a larger inner diameter. The top-most coil was damaged during construction so this portion of wire was removed, leaving a 5 section coil rather than 6. These differences resulted in the coil parameters of Table 12.

Table 12. Actual coil parameters[11].

Parameter	Value
Wire gage	AWG 30
Wire diameter with insulation	277 μm
Wire diameter without insulation	254 μm
Single Coil Height	2.59 cm
Number of coils	5
Total number of turns	7192*
Outer Diameter	4.83 cm
Inner Diameter	4.18 cm
Resistance	465 Ω
Inductance	1.62 H*

[11] *Calculated from measured values

A 3” ID, 0.25” thick polycarbonate tube was used as the housing and the disks needed to support the bobbin, spring, spring magnets, and bearings to the housing were turned on a lathe from High Density Polyethylene (HDPE). The completed prototype and some internal components are shown in Figure 69. This prototype can accommodate different spring magnets. The parameters of the two magnets sizes used in testing were given in Table 8 of Section 5.5.

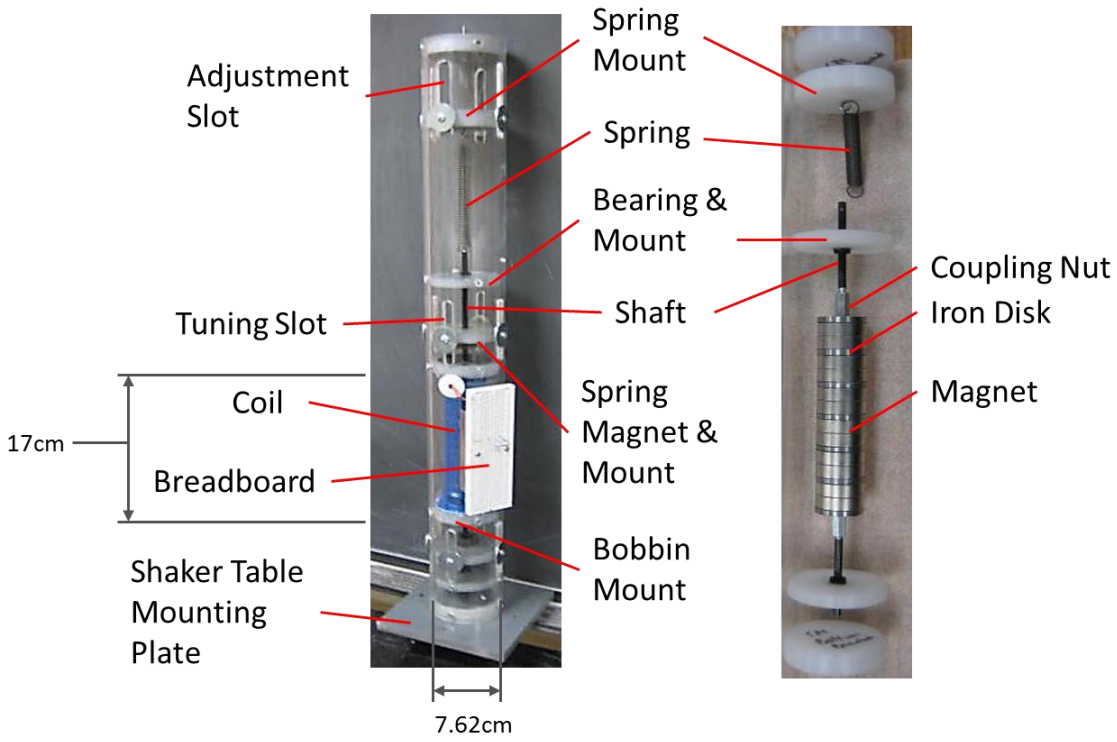

Figure 69. Completed prototype (left), magnet, shaft, spring, and mounts (right).

(a) (b)

Figure 70. Coil bobbin before windings are added (a), and small spring magnet with mount (b).

6.2: EXPERIMENTATION

6.2.1: Laboratory Setup

A test setup was constructed to excite the harvesters via a shaker table and measure performance, as outlined in Figure 71. A laptop computer running NI LabVIEW sent the desired excitation signal to a NI CompactDAQ, which output the appropriate voltage through a NI 9269 Voltage Output Module. A Crown DC 300A amplifier was used as a pre-amplifier to boost the current of the signal[12], which was then sent to a Labworks CP-123 Amplifier Control Panel and Labworks PA-123-500 Power Amplifier (Crown Audio, 2011; Labworks, 2011). The regulated signal then drove the Labworks ET-127 Electromagnetic Shaker Table, exciting the attached harvester with acceleration proportional to the current flowing through the shaker's armature coil and velocity proportional to the voltage sent to the table. To ensure the harvester was excited at the proper acceleration, a Crossbow CXL04GP1Z low frequency, single axis accelerometer was mounted to the base of the harvester, sending measurements to the computer via a NI 9219 Sensor Input Module connected to the CompactDAQ (Moog Crossbow, 2011). The gain settings of the LabVIEW Virtual Instrument (VI), pre-amplifier, shaker table

[12] Without this pre-amplifier, the 9269's voltage output is diminished from the desired value.

amplifier, and control panel were adjusted to match the measured acceleration to that prescribed by the user. For proper signal replication, the desired acceleration signal was integrated to velocity within the VI. The harvester's load voltage and current were recorded through two channels of the 9219 module, with the current measured in series with the load through the module's internal shunt resistor[13].

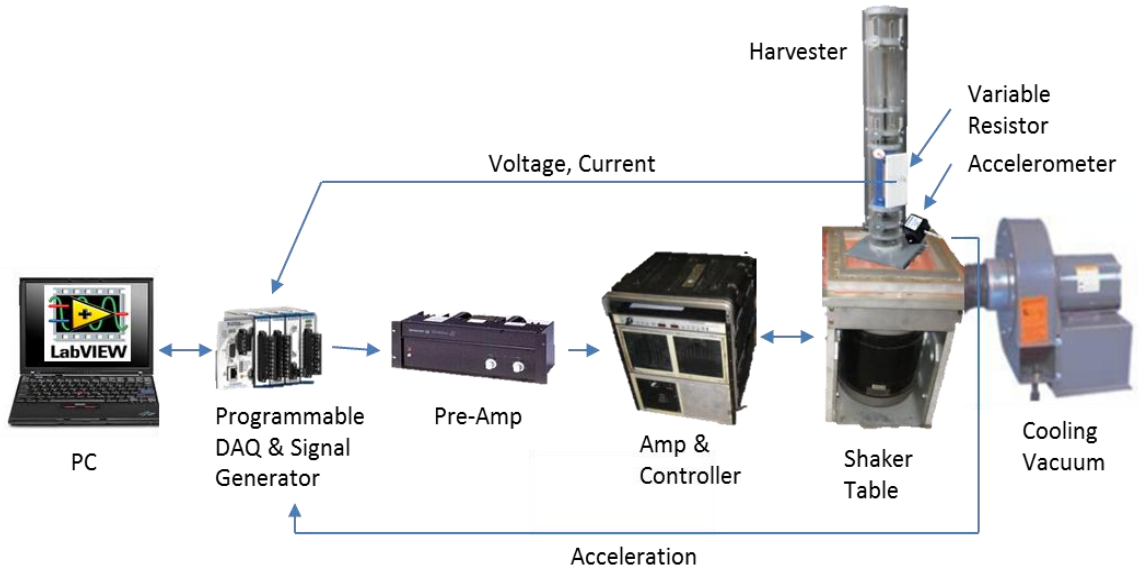

Figure 71. Laboratory test setup for measurement of harvester performance.

This setup in conjunction with the LabVIEW VI provided the following testing capabilities:

- *Excite harvester with:*
  - *Sine wave(s) with customizable frequency and amplitude.*
  - *Swept sine wave with customizable starting/stopping frequencies/times and amplitude. Sweep frequencies may be increasing, decreasing, or a*

[13] This configuration is accurate for currents up to +/- 25 mA. The minimum current necessary for accurate measurement depends upon the measurement range set by the user in software.

combination. Maintain constant acceleration amplitude throughout sweep (within 5%) via software compensation (in the VI) for hardware drift

  - *Measured bridge acceleration waveform.*

- *Measure:*
  - *Acceleration of harvester housing.*
  - *Peak open and closed circuit voltage, and current under different loads.*
- *Calculate from measured data:*
  - *Power spectrum.*
  - *Spectrogram.*
  - *RMS and average power and energy.*
  - *Frequency of accelerometer and voltage signals.*
- *Filter out measured signal noise (mostly from shaker table field coil) and monitor all signals between all hardware components.*
- *Save, view, and post-process recorded data.*

The setup would ideally include a two laser vibrometer to measure the position of the translating magnet and the position of the harvester's housing throughout excitation. This would boost accuracy of the following measurements greatly. One laser position sensor was purchased after this realization and will be used in future work. If the sensor is adequate, a second will be purchased to complete accurate measurements. Additionally, a closed-loop control system would ensure the harvester is excited with the desired waveform, further increasing accuracy and eliminating the tedious adjustments necessary to account for the shaker table's nonlinearity at low frequency and high displacement. A NI CompactRIO™ was purchased following this realization, and is being used to control the shaker in real-time for future tests.

6.2.2: Parameter Measurement

Before testing the completed prototype, its key parameters were measured to complete the numerical model and allow comparison of simulation to testing. The mechanical and electrical damping ratios and damping coefficients were measured first. The mechanical damping ratio (ξ_m) may be compared with other published research to determine how well the energy harvester is constructed in terms of losses, such as friction. The electrical damping ratio (ξ_e) may be used to calculate the average electromagnetic coupling coefficient (K) of the magnet/coil system, and may be compared with other published values to determine the relative magnetic field strength. The mechanical damping coefficient (c_m), present in the system ODEs, was measured first by recording the induced coil voltage, Figure 72. Mechanical damping was measured with no electrical load, i.e., an open-circuit. The amplitudes of two peaks were used in conjunction with the Logarithmic Decrement Method to measure the damping ratio, Equations 6.1 and 6.2 (Silva, 2000). The mechanical damping coefficient was then calculated using Equation 6.3. The measured values are given in . There is a great deal of variation in the damping ratio and coefficient, depending upon which portion of the recorded data is used in the calculation (up to a 300% difference). This greatly reduces the author's confidence in the Logarithmic Decrement Method, yet the method is commonly used for calculation of these parameters.

To complete the calculation of the mechanical damping coefficient, the natural frequency and mass were needed. The mass was weighed on a digital scale, and the natural frequency was calculated using this mass value and the spring stiffness. The spring stiffness was measured by placing various weights on the end of the mass, which was suspended from the spring and measuring the deflection. The data points were averaged, resulting in the value included in Table 13.

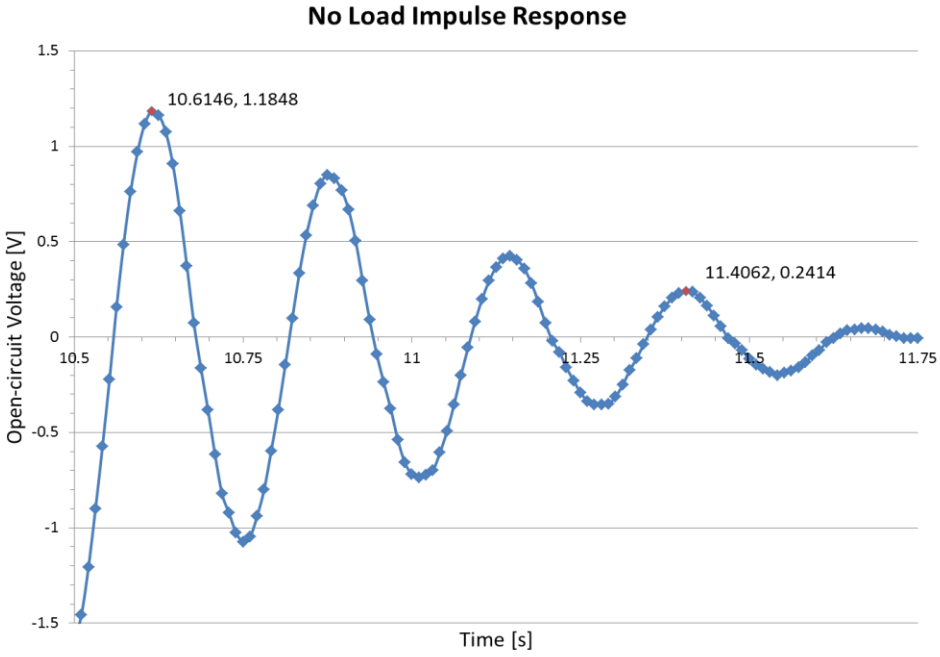

Figure 72. Transient response of open-circuit voltage to an impulse response for the measurement of mechanical damping.

$$\xi = \frac{\delta}{\sqrt{4\pi^2+\delta^2}} \tag{6.1}$$

$$\delta = \frac{1}{n}\ln\left(\frac{x(t)}{x(t+nT)}\right) \tag{6.2}$$

$$c = 2\xi\omega_n m \tag{6.3}$$

The damping measurement process was repeated with a resistive load to measure the total damping ratio (mechanical + electrical), Figure 73. The electrical damping ratio was then calculated by taking the difference between the total and mechanical damping ratios. The measured values are given in Table 13. Like the mechanical damping measurements, there is a great deal of variation in the damping ratio and coefficient depending upon the portion of data that is used in the calculation. There is even greater

variation in the electrical damping, compared to mechanical damping, which results from the dependence of electrical damping with respect to the position of the translating magnet assembly within the coil. At one position more magnetic flux is linked by the coil than at another, resulting in a different measured damping value. Without the use of electromagnetic FEA, the exact damping profile cannot be known with a great deal of accuracy. One work-around to this is to use a two-laser vibrometer to help measure electrical damping at numerous magnet positions, and then construct a profile over the full range of motion. This work is left until the proper equipment is available.

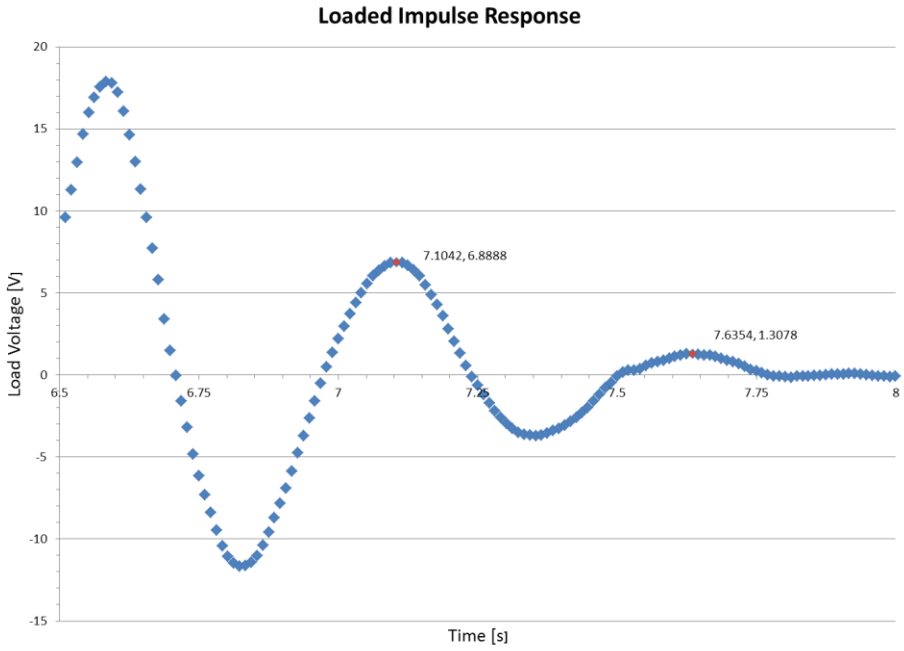

Figure 73. Transient response of closed-circuit voltage to an impulse response for the measurement of total damping.

The *average*[14] electromechanical conversion factor (K) was calculated from the measured electrical damping coefficient (c_e) by rearranging Equation 5.8 to obtain Equation 6.5.

[14] The averaging in the measurement of electrical damping is transferred to this calculation.

$$K = \sqrt{c_e(R_l + R_c + j\omega L_c)} \tag{6.5}$$

Table 13. Results of damping measurement.

Parameter	Value	Unit
Mechanical Damping Ratio ξm	0.0841	-
Electrical Damping Ratio ξe	0.2216	-
Total Damping Ratio ξt	0.3057	-
Load Resistance Rl	13995	Ω
Coil Resistance Rc	465	Ω
Mechanical Damping Coeff cm	3.064	Nm/s
Electrical Damping Coeff ce	8.072	Nm/s
Total Damping Coeff ct	11.135	Nm/s
EM Conversion Coefficient K	341.69	Vs/m
Damped Natural Frequency fd	2.05	Hz
Natural Frequency fn	2.07	Hz
Translating Mass m	1.4	kg
Linear Spring Stiffness k	236.9	N/m

6.2.3: Linear Case

The lab setup was used to perform the following tests for the linear helical extension spring and nonlinear repelling magnet cases[15]:

1. *Measure power as function of load at fixed acceleration and frequency, to find the optimum load resistance for maximum power transfer.*
2. *Measure power as function of acceleration amplitude at fixed frequency, with matching load, to predict performance with amplitude and to measure the breakaway friction force.*

15 Tests 1-3 adhere to the standard suggested by the First Draft of a Standard for Vibration Energy Harvesting, presented in Appendix A of (Priya & Inman, 2008).

3. *Measure power as function of increasing and decreasing vibration frequency, at fixed acceleration amplitude, with matching load, to predict performance with frequency and to measure bandwidth and resonant frequency.*
4. *Measure load voltage, current, and power for bridge acceleration excitation.*

The first test was performed by varying the load resistance with a potentiometer then exciting the harvester with a sinusoidal excitation of peak (half of peak-to-peak) acceleration amplitude of 0.01g and frequency of 2.2 Hz. This frequency was used for this test as it was close to the resonant frequency. The peak harvested power was recorded at 1.32 mW for the optimal load resistance of 14 kΩ, Figure 74. The load resistance was set to the optimal value for the remaining tests.

The second test was performed by varying the peak acceleration amplitude in the VI then exciting the harvester with a sinusoidal excitation at a frequency of 2.2 Hz. This was repeated for increasing amplitude, resulting in Figure 75.

The third test was performed by continuously increasing the excitation frequency linearly with time, while continuously decreasing the software amplitude gain to maintain constant excitation amplitude. This was necessary to remove a bias towards high frequencies, as the acceleration increases with the square of frequency (when measured in m/s^2 and rad/s, respectively). The algorithm used maintains constant amplitude across a 1-20 Hz sweep to within 5%. Figure 76 shows the results of this test, in which increasing and decreasing sweeps were performed. The shaker table was not physically capable of operating below 1.25 Hz for the acceleration level desired, so the sweeps are constrained to this lower limit. Both have a bandwidth of around 0.8 Hz for this load resistance (which was set for highest power rather than highest bandwidth).

The fourth test excited the harvester under replicated bridge acceleration from the middle span of the IH-35N bridge over the Medina River for a period of 50 seconds. The average power over this time was measured to be 80μW, which is around 6 times less than desired to power one WSN node (with an average power consumption of 0.5 mW under the current node design).

Table 14. Summary of linear harvester test results.

Parameter	Value	Units
Load Resistance for Peak Power	14	kΩ
Acceleration Amplitude for this Load	0.01	g
Damped Natural Frequency for this Load	2.055	Hz
Peak Power for this Load, Amplitude, and Frequency	1.38	mW
Bandwidth for this Load, Amplitude, and Frequency	0.52	Hz
Average Peak Power for Typical I-girder Bridge	80	μW

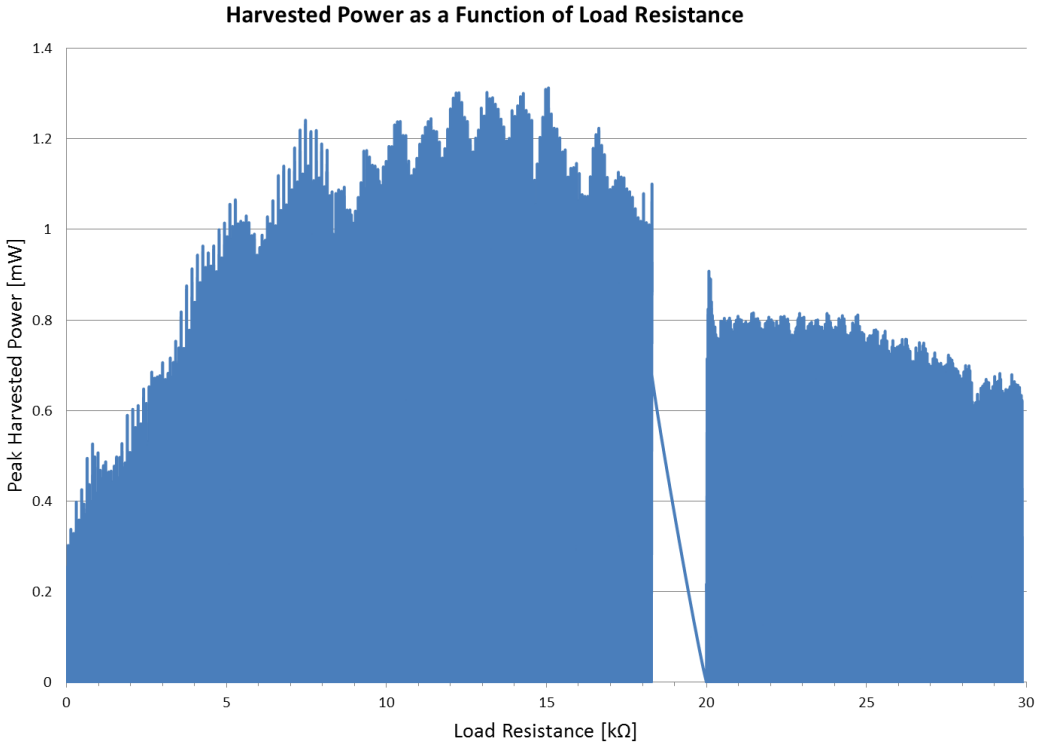

Figure 74. Peak harvested power as a function of load resistance for the linear case under sinusoidal excitation with peak acceleration amplitude of 0.01 g and frequency of 2.2 Hz.

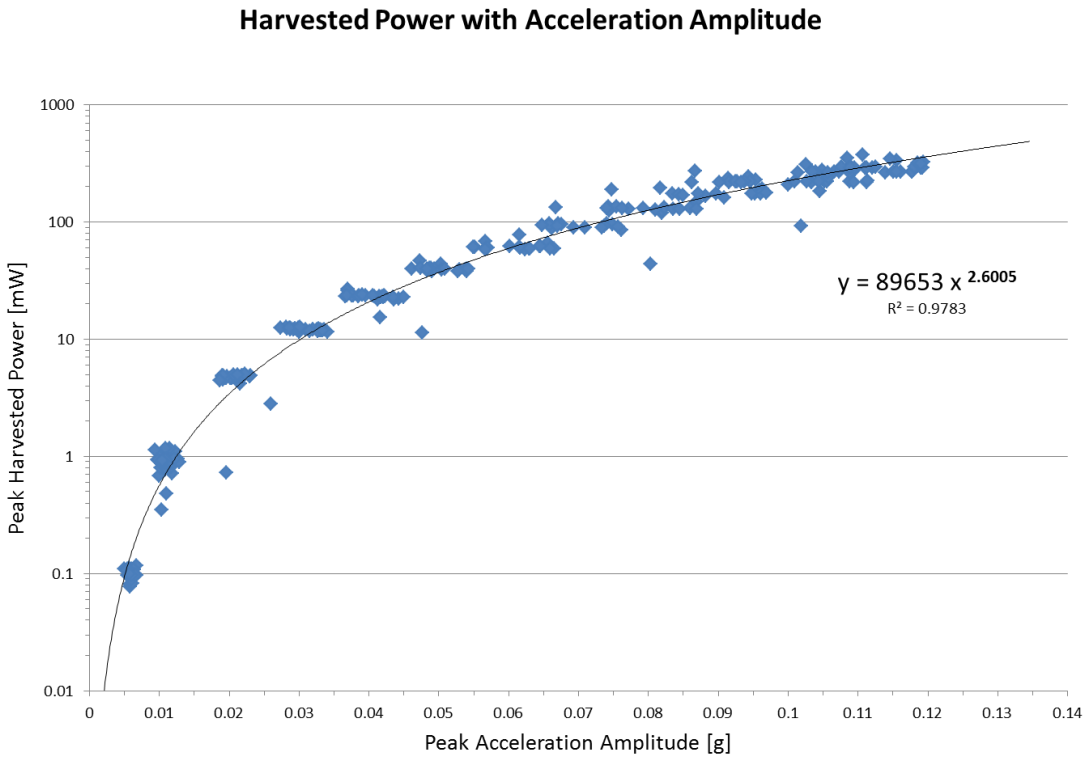

Figure 75. Peak harvested power as a function of peak acceleration amplitude for the linear case under sinusoidal excitation with frequency of 2.2 Hz and load resistance of 14kΩ.

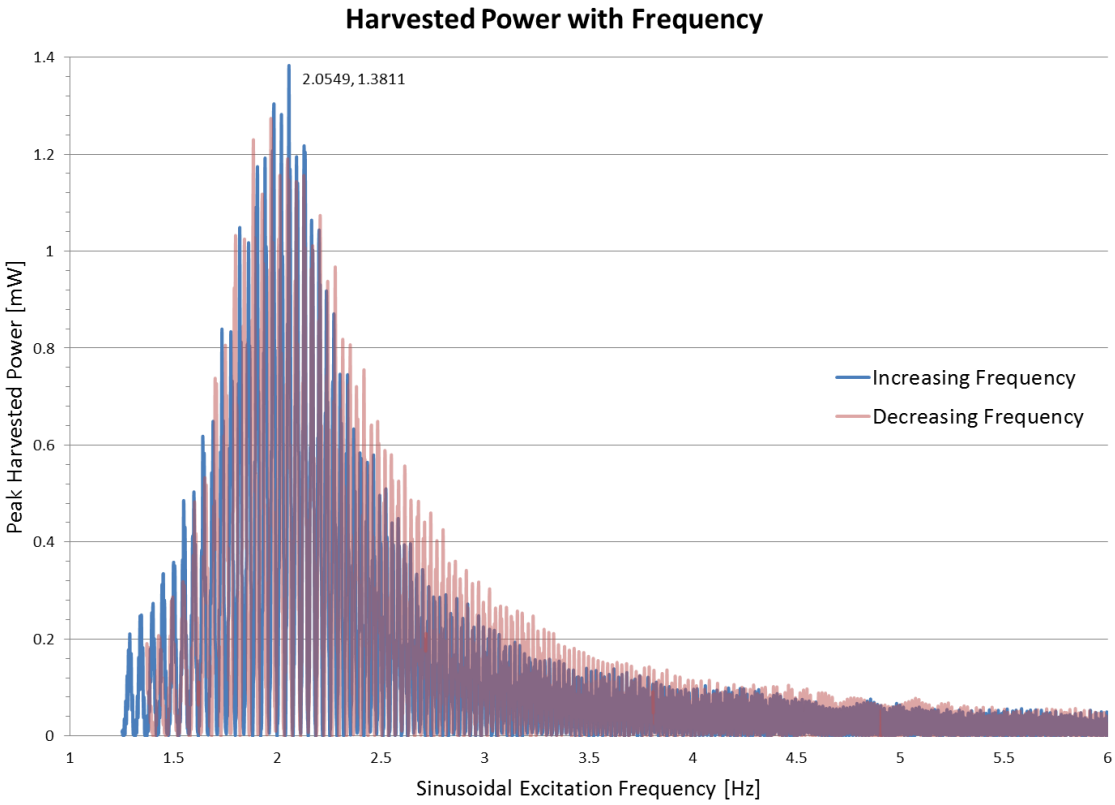

Figure 76. Peak harvested power as a function of excitation frequency for the linear case with increasing and decreasing sinusoidal frequencies, acceleration amplitude of 0.01 g, and load resistance of 14 kΩ.

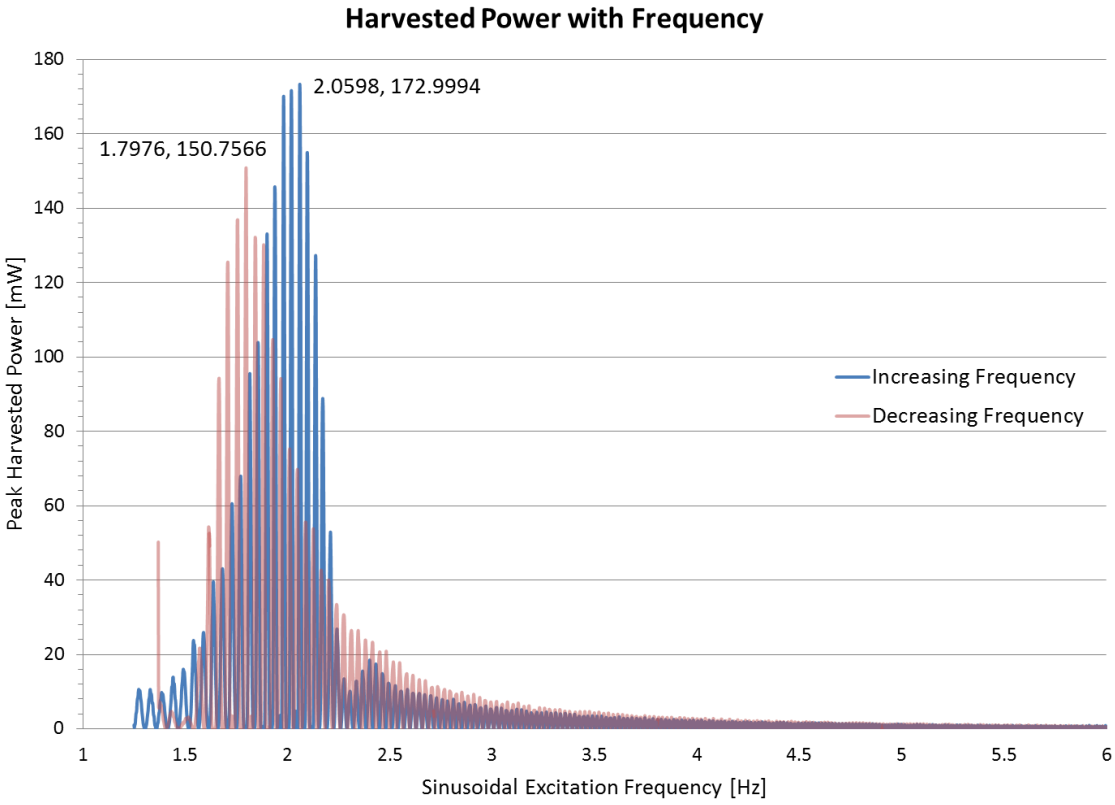

Figure 77. Peak harvested power as a function of excitation frequency for the linear case with increasing and decreasing sinusoidal frequencies, acceleration amplitude of 0.05 g, and load resistance of 14 kΩ.

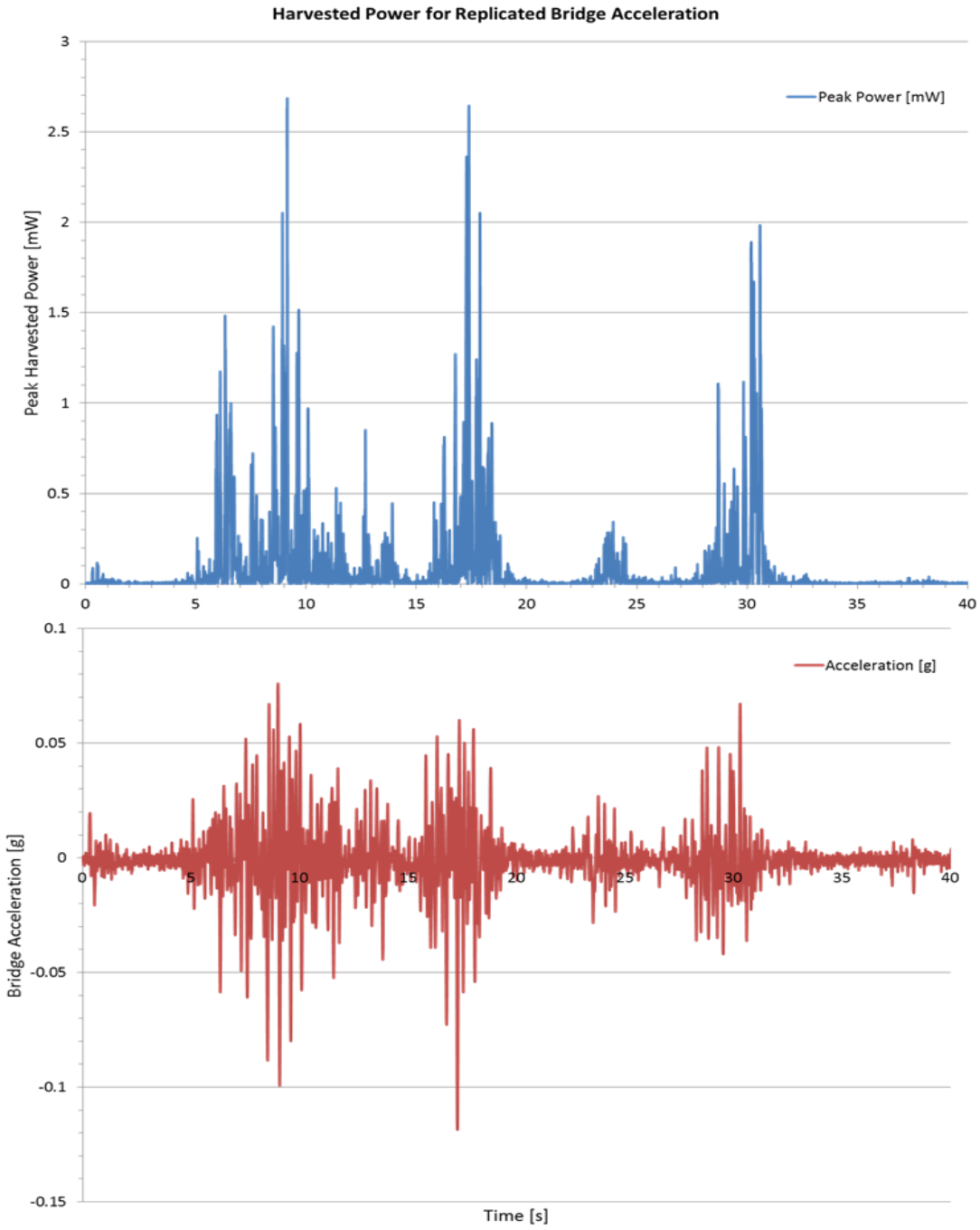

Figure 78. Peak harvested power as excited by a replicated IH-35N over Medina River acceleration profile, for the linear case with load resistance of 14 kΩ.

6.2.4: Nonlinear Case

The same series of tests were performed for the nonlinear case as were for the linear case entailed in the previous section. Unfortunately, some of the results were lost to a catastrophic failure of the hard drive in the laboratory computer. Only a portion of the data had been backed up, so the results are not fully exhaustive. The increasing frequency sweep and replicated bridge excitation are presented in the following figures, using the same load resistance as was found in the linear case.

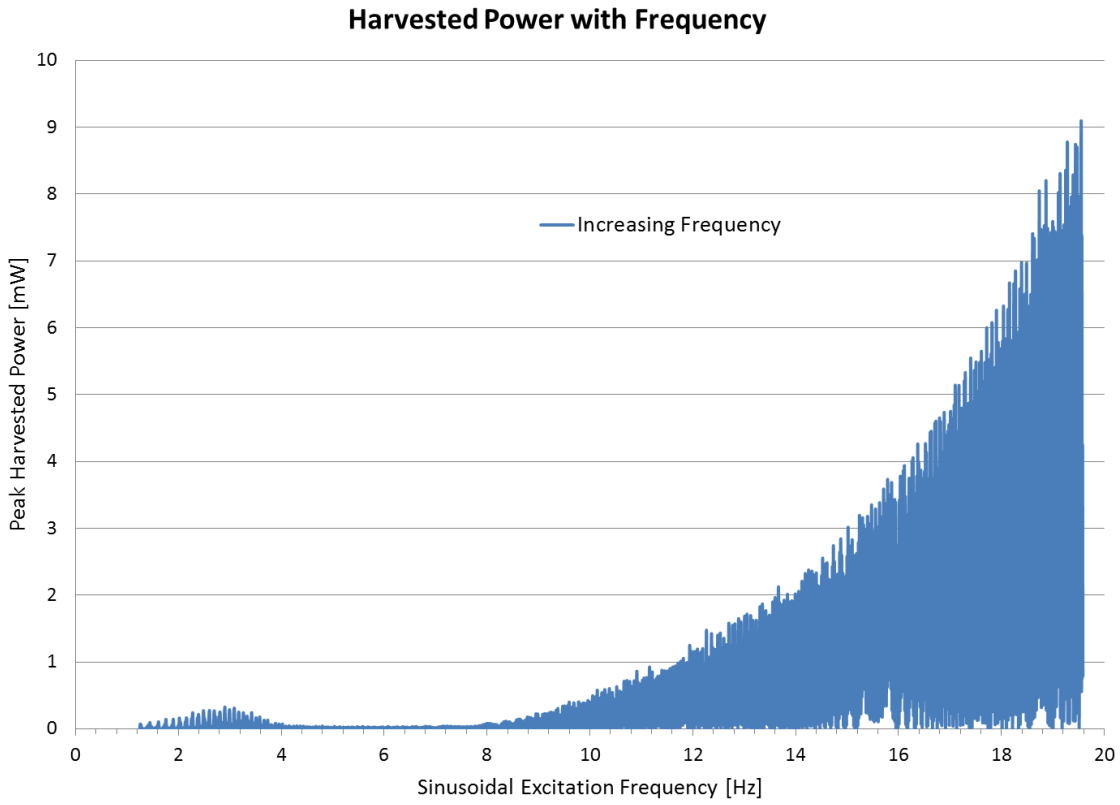

Figure 79. Peak harvested power as a function of excitation frequency for the nonlinear case with increasing sinusoidal frequency, acceleration amplitude of 0.05 g, and load resistance of 14 kΩ.

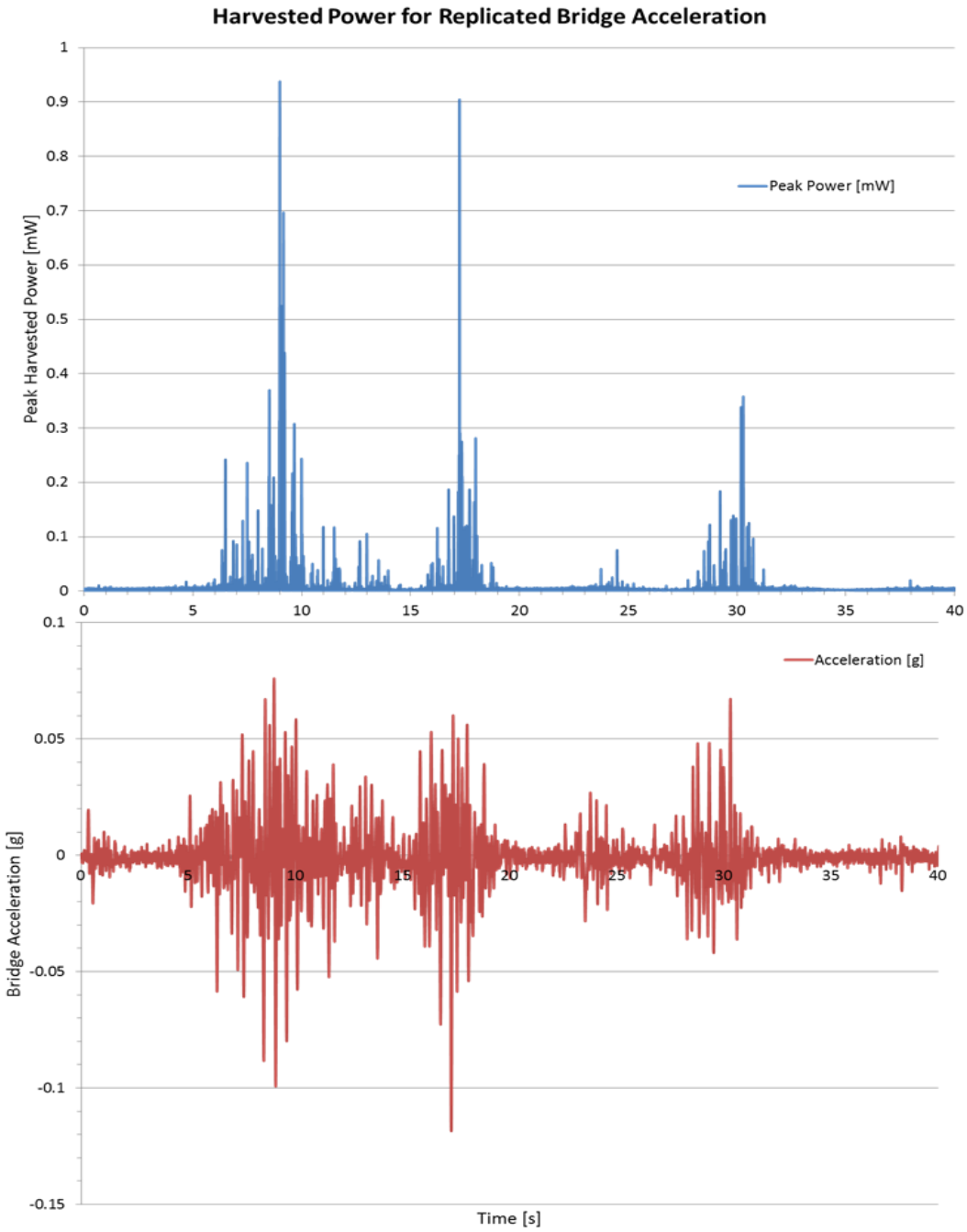

Figure 80. Peak harvested power as excited by a replicated IH-35N over Medina River acceleration profile, for the nonlinear case with load resistance of 14 kΩ.

These results show significantly wider bandwidth for the nonlinear case under swept sinusoidal excitation, as predicted from the literature. The performance under bridge excitation is significantly ($1/3^{rd}$) less than the linear case for the same data sample. This confirms the simulation results of Chapter 5, suggesting the linear case is preferable for bridge vibrations.

6.3: COMPARISON TO SIMULATION AND OTHER WORKS

To gain some preliminary perspective of the previous testing results, simulations were performed with the measured parameters of the constructed prototype, as shown in Figure 81. This simulation uses the measured bridge data from the IH-35N-US-290E direct connector rather than the IH-35N bridge over Medina River, which was used for the laboratory tests. The capability to compare the two with the same dataset is near completion, and will be included in future work to be continued by another student on the team. The average power of the experiment was measured to be 80μW, while the simulated average power of Figure 81 is near 30μW. The long-term average of the harvester presented by (Li, 2008) over 24 hours of bridge excitation is near 53μW. The acceleration levels are much higher for the bridge (Li, 2008) used, but at the same time the power is after rectification and storage by an active system. Although the harvester used in Li's test was designed for 3.11Hz and larger bridge amplitudes, a simulation with the published harvester parameters was performed to gain a rough estimate of the performance on the IH-35N-US-290E bridge (see Figure 82). The average power from this simulation is 2 μW, but without further details of this harvester, the results included in the figure should be considered as unconfirmed. More detailed benchmarking of the harvester prototyped in this thesis to other published works is recommended for future work.

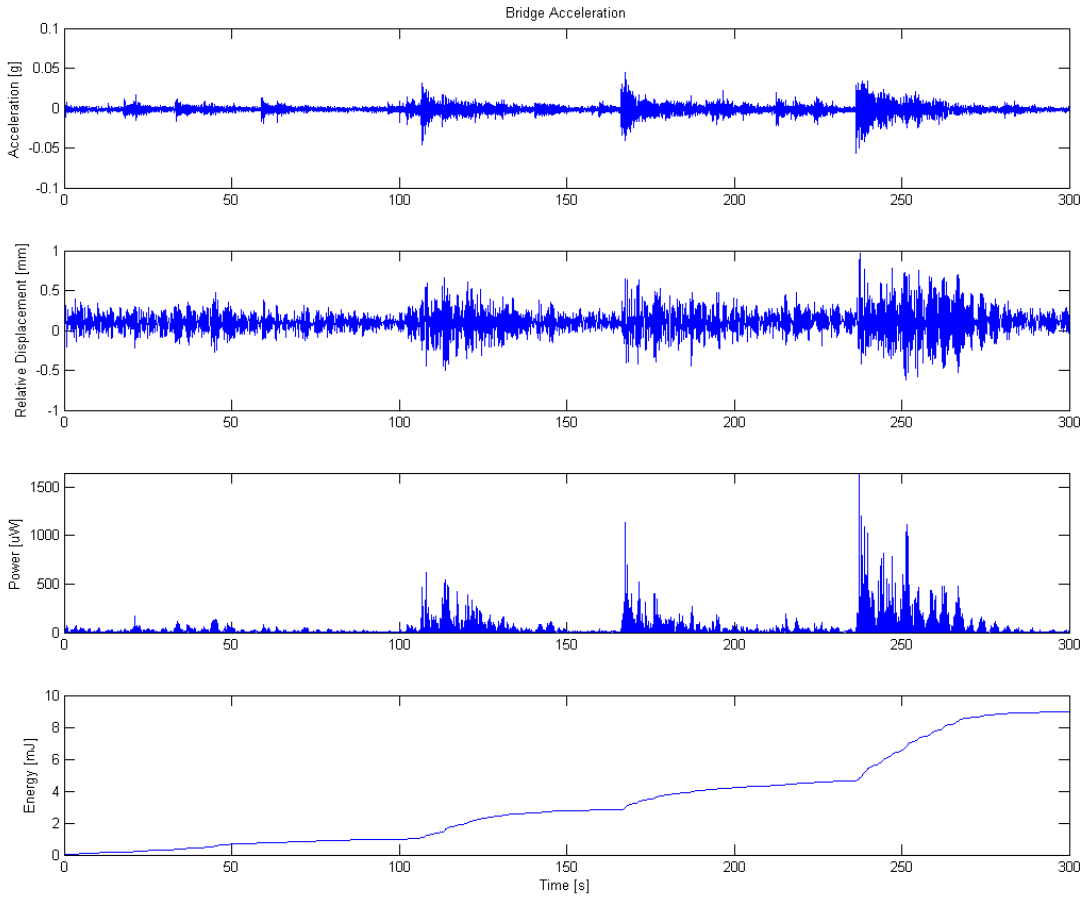

Figure 81. Bridge acceleration, relative displacement (between magnet and coil), peak harvested power, and harvested energy for 300 seconds of IH-35N-US-290E direct connector acceleration for the linear case with actual measured parameters.

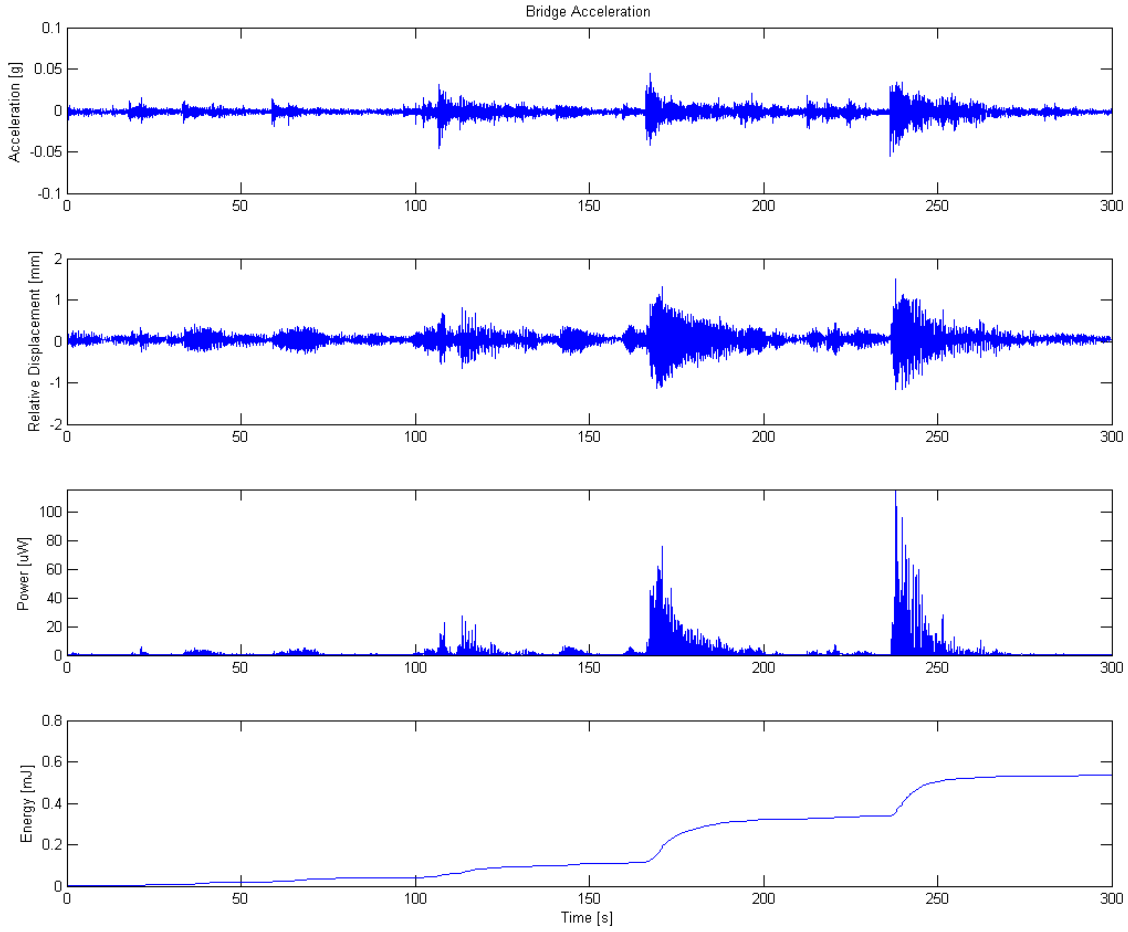

Figure 82. Bridge acceleration, relative displacement (between magnet and coil), peak harvested power, and harvested energy for 300 seconds of IH-35N-US-290E direct connector acceleration for parameters inferred from the harvester of (Li, 2008).

6.4: CHAPTER SUMMARY

The embodied design was constructed by the author and upon completion; the mechanical and electrical damping coefficients, undamped and damped natural frequencies, and spring stiffness were measured. The laboratory setup which was constructed by the author was detailed and then used to perform dynamic testing on the prototype. The significant result is confirmation that the linear case outperforms the nonlinear case for bridge vibration, though by only a factor of 3 rather than 100, as

predicted with the numerical model. The average power harvested by the linear case for the bridge data tested was found to be 80μW. The data used was in the mid-range of acceleration levels, so higher power is attainable even without changes to the harvester. Regardless, this power level is below the target value of 0.5 mW as stated in Chapter 1. For a first round prototype, with many approximations, this is fairly reasonable. The energy harvesting team believes the target value may be reached with refined design and improved equipment, software, and manufacturing capabilities. The harvesting of energy from bridge vibrations, thought to be waste energy, is worthy of further investigation. This investigation should proceed and with the right improvements, is possible to successfully power a WSN node.

Chapter 7: Design Evolution

A beta prototype was designed to use identical internal components as the testing prototype, for the most part, but in a smaller package with added functionality to ease use. Four features pertaining to the harvester enclosure were identified for improvement. They were:

- Quick assembly and disassembly with minimal tooling
- Bridge attachment in two locations with minimal tooling
- Circuit enclosure with easy access
- Quick frequency tuning with minimal tooling

This design is capable of using springs or spring magnets, as it was designed in parallel with the testing of the alpha prototype, before conclusions of the performance were made.

7.1: Conceptual and Embodiment Design

Concept sketches for each option considered are shown in Figures 83-86. For now, the features allowing the harvester to form part of an array of harvesters were not designed and are left for future work. The first prototype is designed for top down assembly by which internal components are inserted into the housing tube and fastened in place from the outside. This proved to be much more time consuming than expected. For the refined prototype the housing is composed of two halves which join along a vertical seam. The two vertical halves are then held together by top and bottom caps. This allows quick access to any internal part while greatly reducing part quantity by incorporating the bearing, coil, and magnet mounting features into the housing as one part. Mounting is eased via integrated clamps which pivot to allow attachment to various bridge dimensions. The customer preferred mounting to the bridge's web stiffener plates and

cross-frames. This is achieved with two clamps which may be oriented to match the bridge's dimensions without the use of any tools, and then tightened. The use of clamps was largely prescribed by the customer requirement that structural modifications to the bridge, adhesives, or magnetic clamps must be avoided. It should be noted that the features allowing the harvester to form part of an array of harvesters were not designed and are left for future work.

The circuit board is desired to be embedded in the back side of the harvester, between the two mounting clamps, with a removable cover plate to protect against debris. The top and bottom end caps serve to mount the bearings and spring magnets, and facilitate adjustment to tune the resonant frequency. The bearing is housed inside of a central post within each cap and held in place by a steel plate. This plate, being ferromagnetic, also serves to hold the spring magnets in place. If desired, the spring magnets may be replaced by helical springs, which would slide over the central post and be compressed between the cap and translating magnet. Internal threads on the caps and external threads on the two housing halves allow the user to tune the frequency up and down by threading the caps in and out, respectively. This feature moves the spring or magnets closer to or further from the translating magnet, changing the stiffness. The threads allow the tuning to be performed easily without tools. In addition, a visual guide could be printed on the housing to allow the user to thread to the desired frequency. The design allows the harvester to be used with the linear or nonlinear case with minimal steps required to change.

The final design is presented in Figures 87-89. A honeycomb structure was added to the front of the housing to allow the project sponsors to see the internal components in motion. In addition, ridges were added to the caps for added grip. Figure 90 shows the harvester in two possible mounting orientations, attached to a cross-frame and web

stiffener plate. The mounting clamp's rotation mechanism may be seen in Figure 91. To adjust the clamps, the user first pulls the clamp away from the harvester, disengaging the teeth, and then rotates to the desired position. When the clamp is released a spring reengages the teeth, locking the clamp in position. A finite element model was used to design the return spring for printing, Figure 92. The force required to disengage the teeth was designed to be 10 lbf, within the comfortable hand force range.

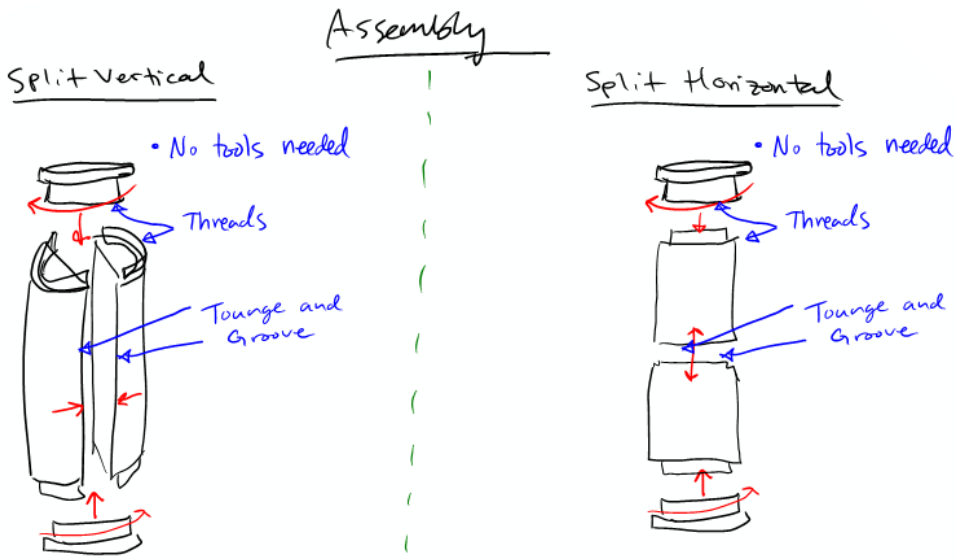

Figure 83. Assembly/disassembly concept sketches, showing vertical and horizontal housing separation.

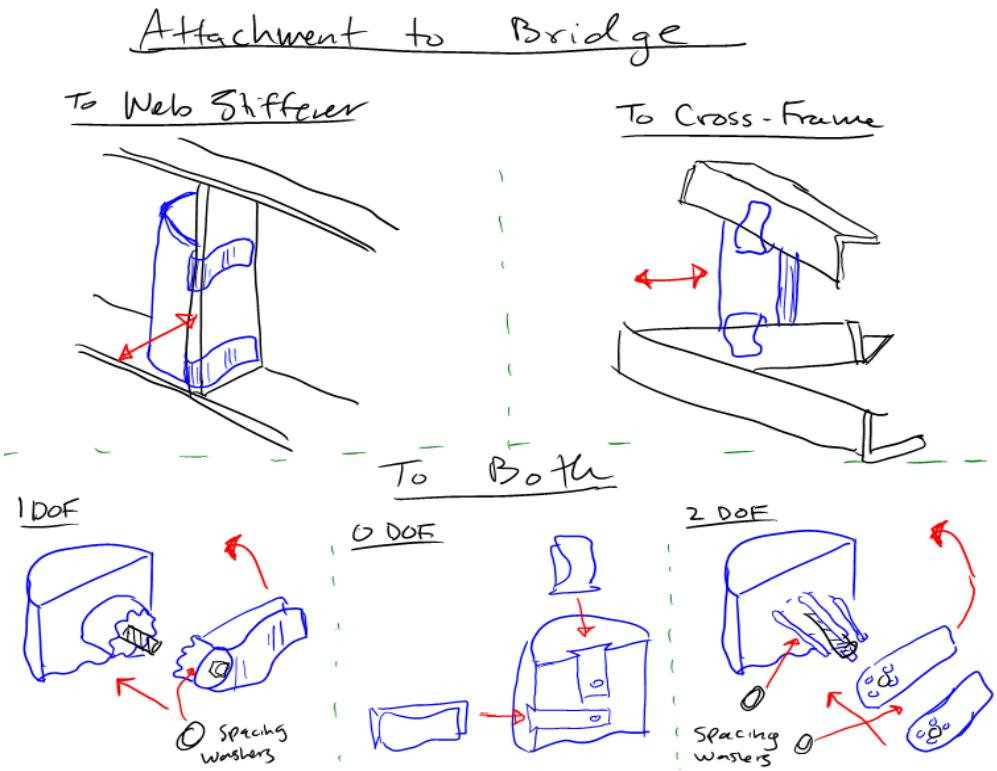

Figure 84. Bridge mounting concept sketches, showing mounting to the web stiffener plate and cross-frame, as well as 0, 1, and 2 degree of freedom adjustment for mounting to both locations.

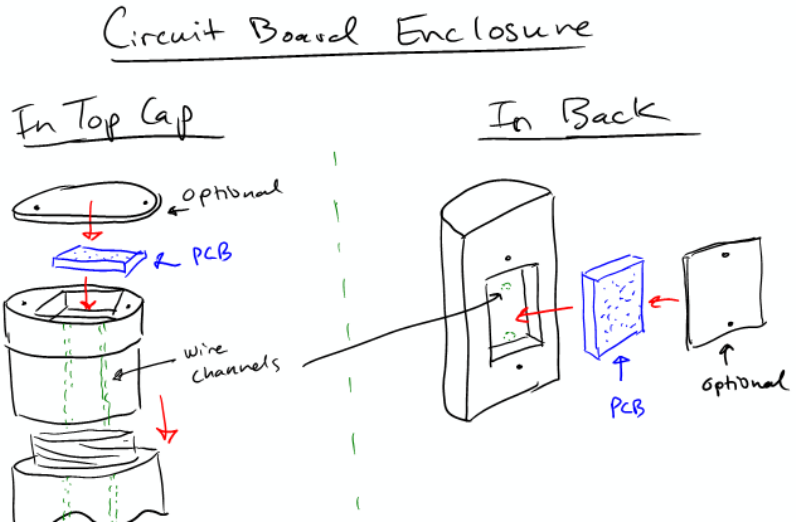

Figure 85. Circuit board enclosure concept sketches.

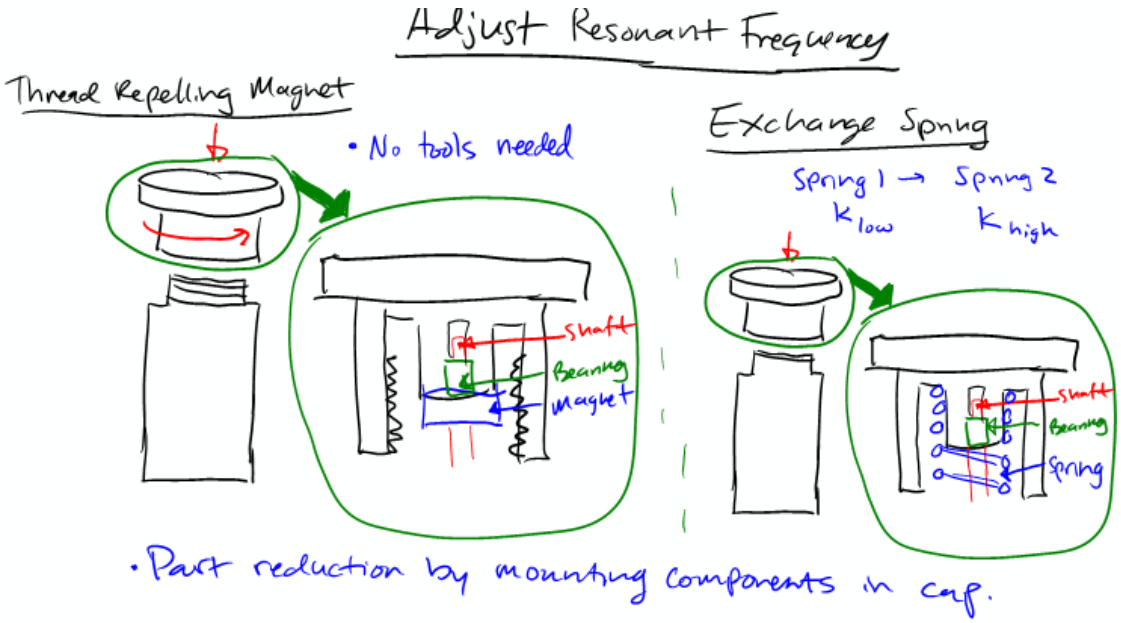

Figure 86. Frequency tuning and magnet/spring interchangeability concept sketches.

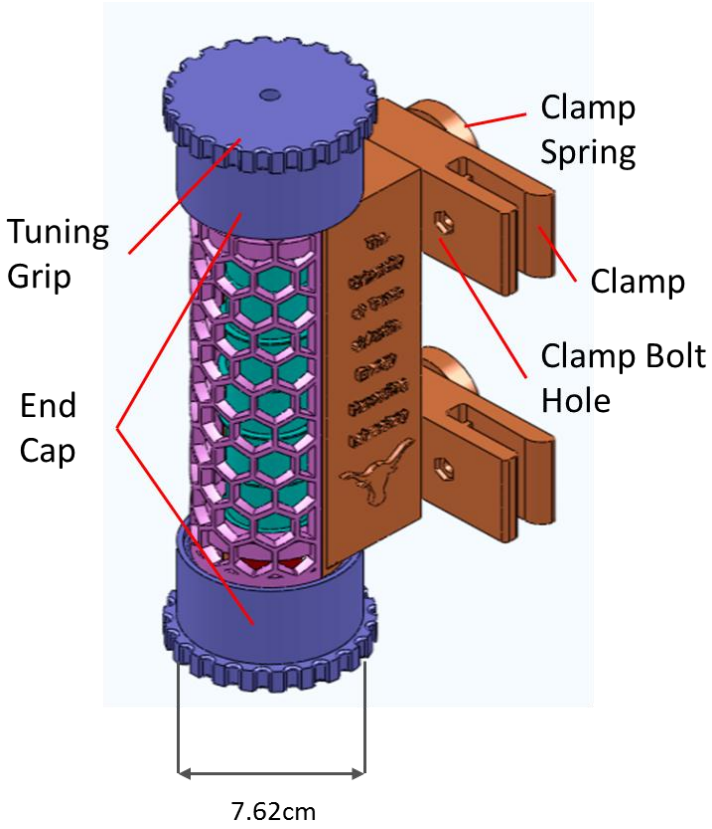

Figure 87. Finished CAD model isometric view.

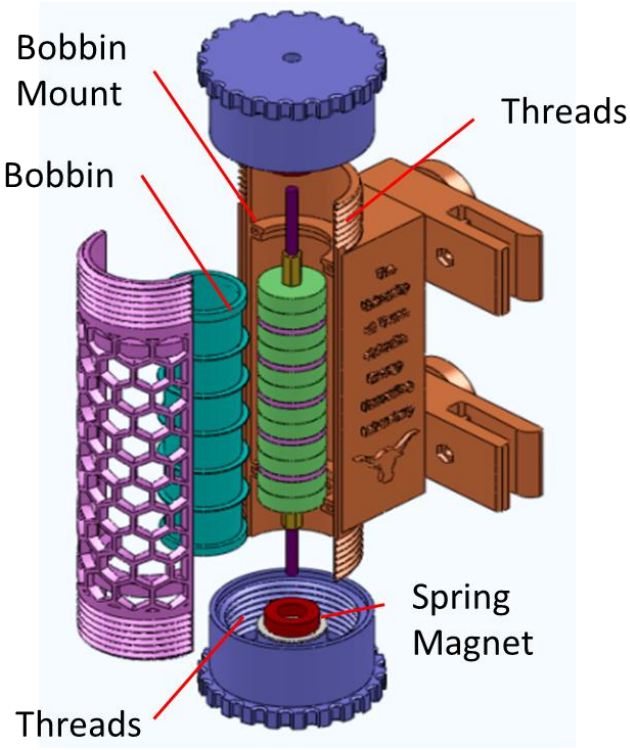

Figure 88. Finished CAD model exploded view.

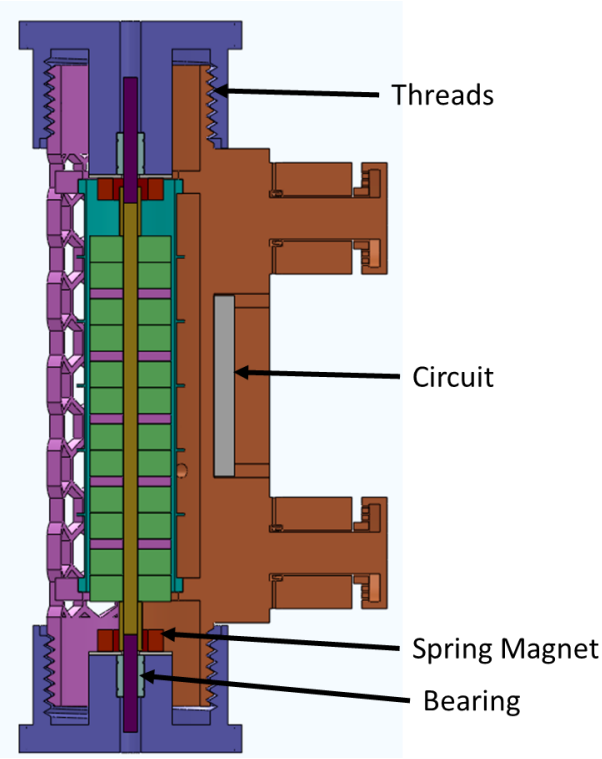

Figure 89. Cross-sectional view of energy harvester, showing threads, bearing, magnet, and circuit mounting.

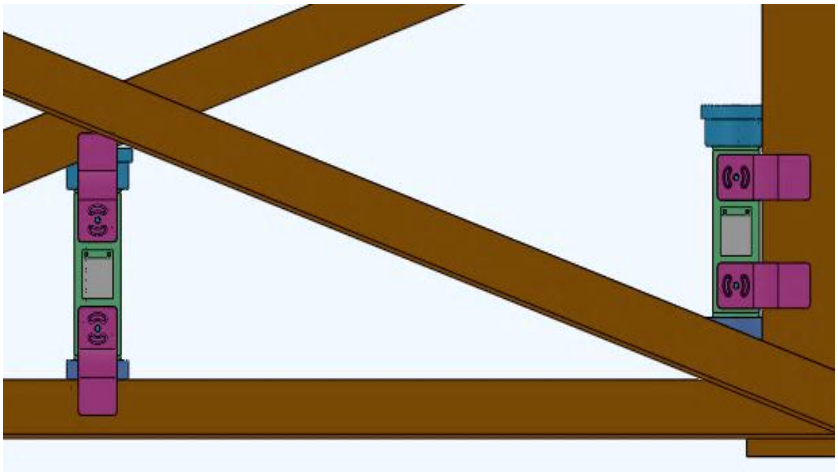

Figure 90. Harvester mounted to cross-frame and web stiffener plate

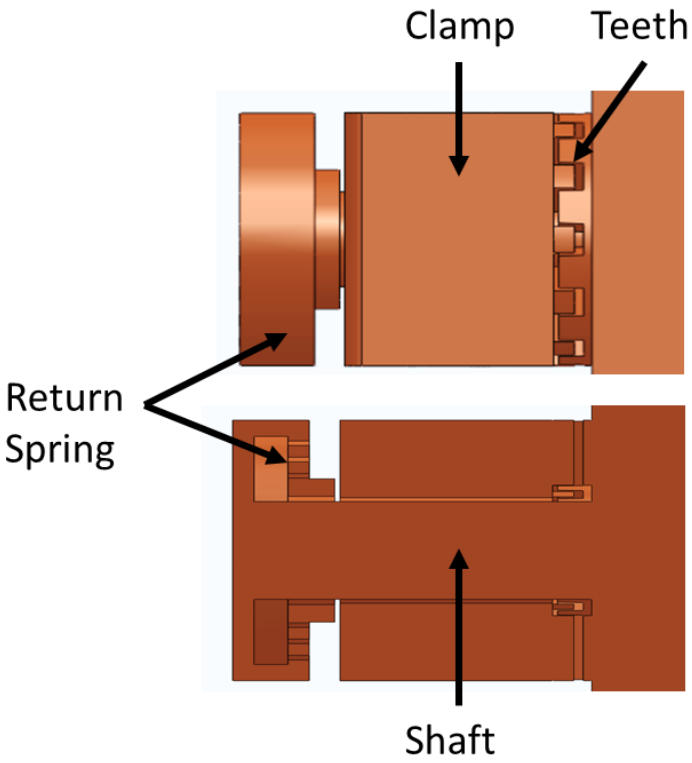

Figure 91. Detail view of the clamp rotation mechanism (top), and cross-sectional view (bottom).

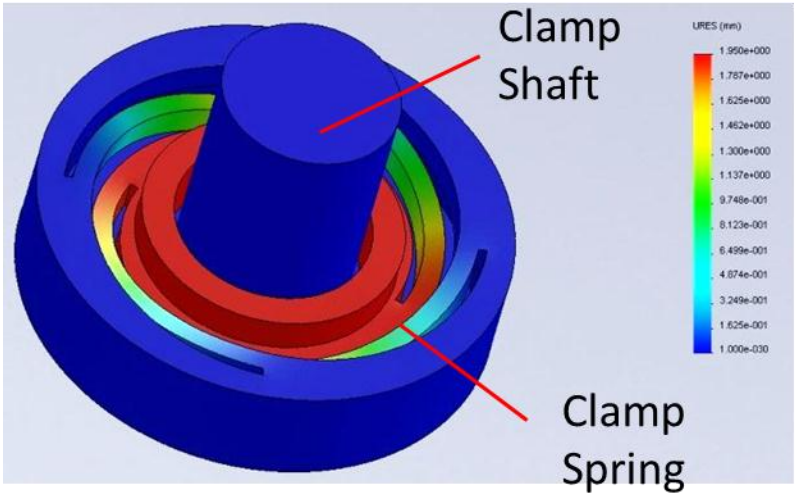

Figure 92. FEA deflection results for the loaded return spring.

7.2: PROTOTYPE FABRICATION AND EXPERIMENTATION

The second prototype was printed using Selective Laser Sintering (SLS) for its fast turnaround time and ability to print complex multifunctional components with structural integrity, Figures 93-94a. To print the components, proper tolerances needed to be specified between all mating components such that there would be no risk of an incorrect fitting. A clearance of 0.5 mm was specified between the mating surfaces of the male and female threads as well as a coarse thread pitch of 5 mm. The shaft outer diameter (inside the clamp) was given a generous clearance of 0.8 mm as well as 0.5 mm for the surfaces of the teeth and 0.5 mm for the tongue and groove fitment of the coil bobbin within the body. The completed CAD model was saved into .STL format, a mesh type format for additive manufacturing (see Figure 94b). A diagnostic was performed on the mesh using the Rhinoceros™ software tool, which found and corrected a few issues.

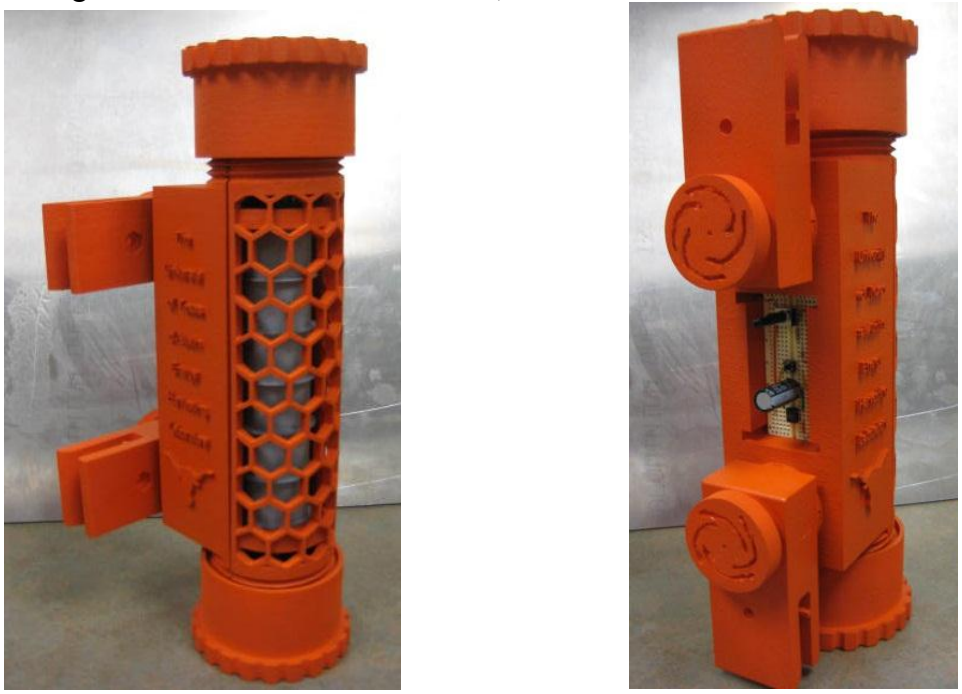

(a) (b)

Figure 93. Finished harvester front isometric view (a), rear isometric view (b).

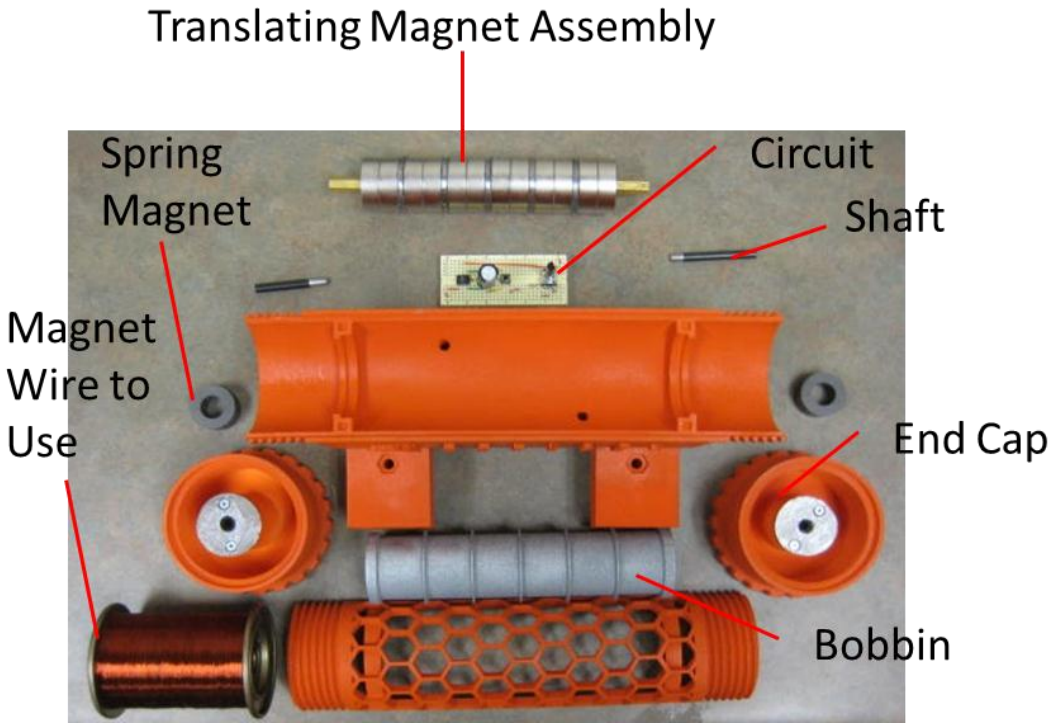

Figure 94. Disassembled components.

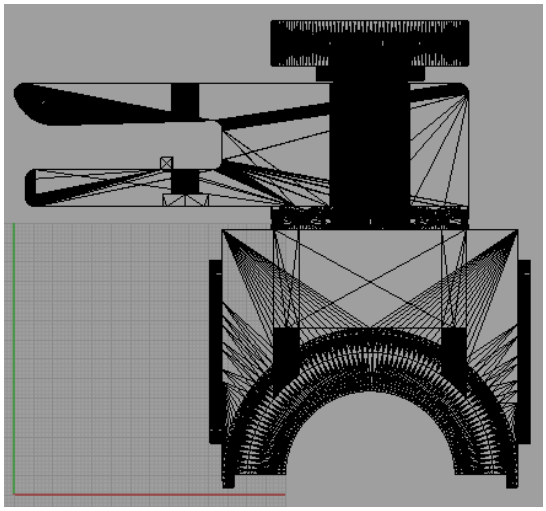

Figure 95. , mesh as viewed in the mesh analysis tool Rhinosceros™ (Robert McNeel & Associates, 2011).

Tolerances are a large hindrance in design for SLS. While traditional manufacturing techniques may achieve linear tolerances, for example, of .05 mm if required, SLS will have considerable difficulty achieving 0.2 mm accuracy. This resulted in excessive clearance in the mounting clamp's interlocking teeth, which would hinder the transfer of kinetic energy from the bridge to the harvester and reduce power output.

The force to disengage the mounting clamp of the refined prototype was measured by attaching two springs and measuring the deflection once the clip was able to be adjusted. The measured force was 11 lbf, close to the model's prediction of 10 lbf. The smooth surface of the clamp caused poor grip, so any future iteration should include a recessed slot for ergonomics. Foam inserts were added to compensate by providing added stiffness to the clamp's spring.

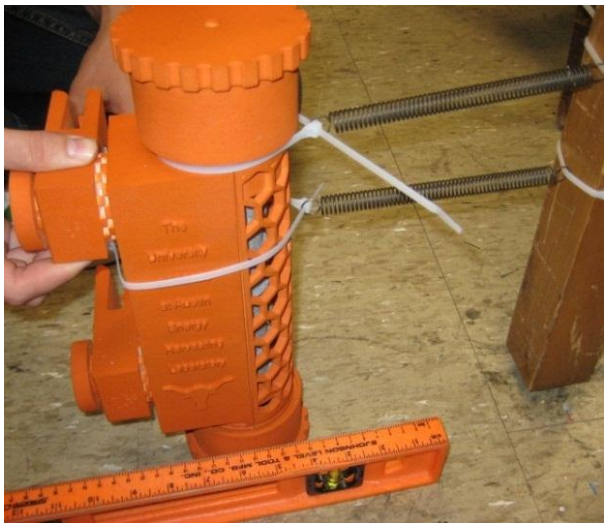

Figure 96. Measurement of force needed to disengage teeth to allow clamp rotation.

7.3: CHAPTER SUMMARY

A beta design was completed which focused on the aspects of bridge mounting, user interaction, tuning of resonant frequency, volume and part reduction, and housing of

circuitry. The effort was completed in parallel with the testing entailed in the previous chapter, before results favoring the linear case were found. To guarantee this effort would not be in vain, the design accommodates the use of springs or spring magnets to satisfy either case. The design was constructed using SLS, and resulted in less than half the total volume of the first prototype, as well as a part reduction of 86% (about half being fasteners), assembly and tuning steps, and added mounting capability, as quantified in Table 15.

Table 15. Quantitative prototype comparison.

Parameter	**Refined Prototype**	**Testing Prototype**
Volume	~200 in^3	~450 in^3
Unique Parts	7	51
Assembly Steps	7	36
Tuning Steps	2	10
Mounting Steps	2-4 Steps (1-5 mins)	No mounting

The use of SLS was primarily to reduce construction time. If this design were to be manufactured, injection molded plastic would replace the SLS parts with minor changes, which would be considered in a design for manufacturing and assembly process.

Chapter 8: Conclusions

8.1: Summary and Conclusions

This thesis began with a description of the need for the project and its organization and purpose. A review of energy harvesting was conducted to understand the technologies available for investigation. A summary of this review is as follows:

Energy harvesting and scavenging is a field with great potential for future mobile, quick-install, and remote applications, enabling growth in wireless sensing applications. There are many energy sources and types of harvesters to consider for any application, and the number is growing rapidly. Solar, wind, and vibration harvesters possess the highest power densities of those reviewed, with solar being most attractive with a power density one order of magnitude above wind and vibration. Vibration harvesting possesses one very important trait—the ability to be sealed from the environment and protected from intentional or accidental damage—whereas solar and wind harvesters must interact with the elements directly. Properly matching the impedance characteristics of the energy conversion mechanism to those of the energy source must not be overlooked, and this requires careful study of the ambient energy source. Furthermore, conditioning and storing the harvested electrical energy are as important to the overall success of the harvester as capturing and converting the energy, so care must be taken in the design of these subsystems. The average number of lifecycles, operating conditions, and self-discharge of storage devices must be considered for successful delivery to the load. Capacitors, ultracapacitors, and lithium-ion batteries are at the top of the storage options, due to their high energy density, easy electrical monitoring, and growing research focus. Ultracapacitors may be used to rapidly collect bursts of energy, and then deliver this energy to a more efficient long-term storage source, such as ceramic capacitors or

lithium-ion batteries. The near future will see solid-electrolyte lithium-ion batteries with increased storage capacity, allowing implementation in energy harvesting applications where their 100,000+ cycle life will help maintenance-free operation for decades.

Several concepts of various types of harvesters were generated following this review and narrowed down to vibration energy harvesting. Within vibration harvesting, the selection of an electromagnetic conversion mechanism was made for its inherent benefits for the application at hand. With this selection, the acceleration time histories of three bridges were recorded and analyzed for spectral content. A summary of the concept generation, selection, and field measurements is as follows:

The key functions a fully evolved energy harvester should perform were identified as: interface with environment, direct energy from environment, separate energy, transform energy, convert energy, store energy in short term, store electrical energy in long term, supply energy to electric load, interface with user, divert debris, theft, vandalism, and adapt to changing environment. Considering these functions, many concepts were generated and organized into a mind-map. Several of these were further developed and sketched, including road hose, wind-belt, reflected solar, expansion joint, electromagnetic vibration, and piezoelectric impact concepts. A few concepts were generated for mounting a generic harvester to the two most-common bridge types: I-girder and box-girder, with a focus on meeting the limiting design constraints set by the project. Patents relating to energy harvesting from bridges and roadways were briefly presented, with the most developed invention harvesting the motions of expansion joints from within the bridge. After review, the author selected vibration harvesting using induction for further development. Harvesting vibrations requires more sophisticated

design, incurring larger risk than solar or wind harvesters, but with greater satisfaction of the project requirements and constraints if successful. To counter this, other students on the project are pursuing solar and wind harvesters in parallel efforts. To characterize the bridge vibrations, accelerations were measured at various positions and times and analyzed in the frequency and time domains. Further measurement and analysis is being performed by a Civil Engineering graduate student on the project, with a focus on temperature and traffic effects. The data presented thus-far shows stable, dominant frequencies in the 1.5-16 Hz range which may be harvested by tuned linear harvesters.

Following this, a detailed literature review of electromagnetic vibration energy harvesters was performed, including methods for tuning resonant frequency, widening bandwidth, and efficiently rectifying, conditioning, and storing the harvested electrical energy. The key points of this review being as follows:

The harvesters found thus far utilized a breadth of compliant members such as helical springs, cantilevered beams, supported beams, and flexible hinges on rigid beams. Others use soft ferromagnetic material such as iron to concentrate the magnetic flux in the region of the coils to give higher induced voltages. A common trend amongst almost all published research in the field is a lack of discussion or justification for the concept selection. Regardless, the key findings of this literature review are:

- *For high peak power output:*
    - *High seismic mass is desired.*
    - *Target high acceleration amplitudes.*
    - *Target high frequencies with sufficient acceleration amplitudes.*
    - *Match harvester and load impedance.*

- *Use Schottky diodes if reverse breakdown voltage is acceptable.*
- *Use a tantalum or ceramic-type capacitor for storage.*
- *If significant benefit, use a switching AC-DC or switching DC-DC converter.*
  - *Use a commercially available system.*
- *Omit cogging/ripple forces and variable reluctance to reduce losses.*

- *For high average power output (robustness):*
  - *Desire wide bandwidth for simultaneous harvesting of multiple frequencies*
    - *Mechanically coupled, nonlinear, arrays, or bistable harvesters seem good for ambient vibration.*
      - *Individual harvesters in an array should be rectified independently to avoid destructive interference.*
  - *Desire passively tunable bandwidth to match specific bridge during installation.*
    - *Tune without introduction of damping by changing length, center of gravity, or tensile axial loading.*
    - *Design for lowest frequency with capability of tuning to higher frequencies.*

In the end, the vibration source's characteristics, the risk vs. reward preferences and budget of the project heavily influence the type of harvester and circuitry which should be used.

Drawing from this review, four electromagnetic vibration energy harvester concepts were generated which include resonant frequency tuning and bandwidth widening methods. The concept including stiffening magnetic stiffness was selected, modeled analytically and numerically, and then designed parametrically. Simulations

were performed to predict the performance of the harvester using the numerical model. More work is needed to expand the capabilities of the numerical model, but preliminary results favor the linear case for bridge vibration as it has better performance under random vibrations. This model was used to size the system and predict its performance, leading to its embodiment.

The embodied design was constructed by the author and upon completion; the mechanical and electrical damping coefficients, undamped and damped natural frequencies, and spring stiffness were measured. The laboratory setup which was constructed by the author was detailed and then used to perform dynamic testing on the prototype, including replicated bridge excitation. The significant result is confirmation that the linear case outperforms the nonlinear case for bridge vibration, though by only a factor of 3 rather than 100, as predicted with the numerical model. The average power harvested by the linear case for the bridge data tested was found to be 80μW. The data used was in the mid-range of acceleration levels, so higher power is attainable even without changes to the harvester. Regardless, this power level is below the target value of 0.5 mW as stated in Chapter 1. For a first round prototype, with many approximations, this is fairly reasonable. The energy harvesting team believes the target value may be reached with refined design and improved equipment, software, and manufacturing capabilities. The harvesting of energy from bridge vibrations, thought to be waste energy, is worthy of further investigation. This investigation should proceed and with the right improvements, is possible to successfully power a WSN node. The harvester performance was then compared to a similar harvester from Clarkson University.

Finally, a beta design was completed which focused on the aspects of bridge mounting, user interaction, tuning of resonant frequency, volume and part reduction, and

housing of circuitry. The effort was completed in parallel with the testing of the first prototype, before results favoring the linear case were found. To guarantee this effort would not be in vain, the design accommodates the use of springs or spring magnets to satisfy either case. The design was constructed using Selective Laser Sintering, and resulted in less than half the total volume of the first prototype, as well as a part reduction of 86% (about half being fasteners), assembly and tuning steps, and added mounting capability.

8.2: FUTURE WORK

The work begun in this thesis will be carried on by another graduate student in the energy harvesting team. Refinements to the numerical model, laboratory setup, and prototype will be conducted to improve the performance of the constructed harvester. These refinements include the installation and use of at least one laser position sensor for accurate measurement of the translating magnet assembly's position and velocity, as well as the electromechanical conversion relationship between this velocity and the coil's open-circuit voltage. Another refinement will include the replacement of the NI CompactDAQ with a NI CompactRIO to make use of its real-time controller. This will allow the precise control of the shaker table acceleration, ensuring that the harvester is excited as desired. With these changes made, it is desirable to test the harvester with a sample of each bridge to fully understand its performance. This will coincide with the refinement of the numerical model to include the more accurately measured parameters, which will then be used to perform further testing without physical experimentation. An improved numerical model will also aide in the refinement of the design to include lower friction and higher electromagnetic coupling. Upon these changes, a prototype should be

fabricated with increased precision to ensure better matching of actual and desired parameters. Rapid prototyping should be used to reduce manufacturing time and complexity, with higher precision bushings or the like used in areas requiring close tolerances. Any areas of potential sliding contact should be coated with a long-lasting lubricant such as Tungsten Disulfide, from a coating service like Boca Bearing ("Boca Bearing," 2011). The coating achieves longer lifetime and lower friction than Teflon, and is ideal for applications where liquid lubricant cannot be reapplied.

Before a large amount of effort is placed in refining the current designs, the generated focused concepts should be reinvestigated and could include renewed focus on bistable harvesters. These perform well for low frequency, random vibrations such as those found on highway bridges, and could lead to significantly higher average power output under real bridge excitation. In this reinvestigation, it would be very beneficial to better understand the customer preferences of peak power vs. average power (robustness), through utility functions, for example.

Finally, the electrical circuitry must be finalized with suggestions made in Chapter 4 serving as inputs. A basic version would include: a Schottky diode full-wave rectifier, a DC-DC voltage regulator, a Tantalum capacitor for long-term, low loss storage, complimented by an ultracapacitor or lithium-ion battery. An improved version would include a switching DC-DC regulator. Some off the shelf products exist from Microstrain (Microstrain, 2011) and AmbioSystems (AmbioSystems, 2011), or can be constructed using integrated circuits from a company such as Linear Technology (Linear Technology, 2011).

Appendix A: Customer Needs Interview

Interviewee(s): Dr. Sharon Wood, Dr. Todd Helwig, Jeremiah Fasl, Matt Reichenbach

1. Concerning the energy harvester, what do you consider the most important aspect of the system?

Power WSN node for 2 week measurement interval w/ samples @ 30Hz for power = 60mW.

2. What do you think the second most important aspect of the energy harvester should be?

No altering bridge for mounting. Prefer mounting to web stiffeners and cross frames.

3. On a scale of 1 to 10, with 10 being the most important, rate the importance of being wear-resistant to environmental factors.

7

4. On a scale of 1 to 10, with 10 being most important, rate the importance of ease of installation.

6

5. On a scale of 1 to 10, with 10 being most important, rate the importance of the cost of the product.

4

6. On a scale of 1 to 10, with 10 being the most important, rate the importance of the life span of the product.

9, has to be better than current batteries.

7. How long do you think a product like this should last?

Minimum of 10 years.

8. How much would you spend to purchase an energy harvesting system such as the one being developed?

For harvester: $600 max, $200 ideal.

9. How often would you be willing to do maintenance on the product?

10 years or more preferred.

10. How often do you expect vandalism/theft to be a problem? What measures need to be taken to prevent vandalism/theft?

If harvester mounted underneath bridge away from the abutments, not much. Mount in location where man-lift is needed for access.

Appendix B: Specification Sheet

Table B-1. Functional requirements.

Demand or Wish	Specification		Test / Verification
Functional Requirements			
★ **D**	Generate long-term energy level of	> 104 Wh/year (375 kJ/year)	analytical models, field testing
★ **D**	Provide power level continuously for 2 weeks of	> 61 mW	analytical models, field testing
W	Provide continuous power for router of	> 207 mW (1.8 kWh/year, 6.5 MJ/year)	analytical models, field testing
W	Provide continuous power to gateway like CompactRio	> 10 W (88 kWh/year, 315 MJ/year)	analytical models, field testing
D	Store enough energy to go two weeks with no harvesting input	> 20 Wh (75 kJ)	analytical models, field testing
★ **D**	Provide DC voltage	6 V DC, constant	analytical models, field testing
D	Provide DC current	200 mA, max pulse	analytical models, field testing
W	Communicate to central node	*lack of power, *malfunction	analytical models, field testing

Table B-2. Design constraints: Geometry, forces, material, and signals.

Demand or Wish	Specification		Test / Verification
Constraints			
Geometry			
D	Dimensions: Volume	< 1 ft3	Engineering drawings
D	Dimensions: Area of largest surface	< 4 ft2	Engineering drawings
W	Width of any module sitting on bottom flange of I-beam	< 5 inches	Engineering drawings
★ **D**	Clearance of bottom of system above bottom of bridge structure	> 0 inches	Engineering drawings
D	Maximum length of wiring connecting system modules	< 10 ft / node	Engineering drawings
Forces			
D	Force needed to detach from bridge	> 100 lb	field testing
D	Torque needed to detach from bridge	> 200 ft-lb	field testing
★ **D**	Protected from forces, impact, and chewing by	ice, hail, gravel, debris, rats/mice and squirrels, birds and bats, bird nests, bird and bat excrement	analytical models, field testing
Material			
D	Resistant to humidity and moisture for	> 10 years	accelerated testing
D	Resistant to damage from temperatures	-20° F - 120° F	manufacturer specs
D	Resistant to corrosion from moisture and acidic substances (bird excrement, pollution) for	> 10 years	accelerated testing
D	Resistant to deterioration from UV rays for	> 10 years	accelerated testing
Signals			
W	EM interference with WSN and other systems from energy harvester	none	manufacturer specs, field testing

Table B-3. Design constraints: Safety, ergonomics, assembly, operation, maintenance, and costs.

Demand or Wish	Specification		Test / Verification
Safety			
D	Will not detach from bridge	(see "Forces")	analytical models, field testing
★ **D**	Does not interfere with clearance of traffic	(see "Geometry")	field testing
★ **W**	Number of parts on driving surface of road	0	Engineering drawings
W	Vandalism/Theft-resistant: tools to access or remove from bridge	ladder or man-lift	field testing
Ergonomics			
D	Weight of complete system	< 20 lb	Engineering drawings
★ **W**	Time to install system	< 1.5 hours	field testing
★ **D**	Skill level to install	general technician or less	field testing
Assembly			
★ **W**	Number of permanent changes to bridge such as welds and drilled holes (drilling into concrete is acceptable if needed)	0	Engineering drawings
D	Number of drilled holes to steel structure	0	Engineering drawings
★ **D**	Locations system can be installed on bridge	*space between steel I-beam girders, *interior and/or exterior of hollow steel box girders	field testing
W	Location system can be installed	Any steel surface, above or below deck, on exterior or interior (e.g. trusses)	field testing
Operation			
D	Service life	> 10 - 15 years	analytical model of power levels, accelerated testing
Maintenance			
★ **W**	Maintenance interval	> 10 years	analytical models, field testing, accelerated testing
D	Maintenance interval	> 5 years	analytical models, field testing, accelerated testing
Costs			
W	Manufacture cost	< $200	Parts list, labor cost
D	Manufacture cost	< $600	Parts list, labor cost

Appendix C: Generated Concepts Mind Map

Figure C-1. Mind map of all generated concepts organized and colored by energy source.

Bibliography

A123 Systems. (2007). A123 Systems. Retrieved January 19, 2011, from http://www.a123systems.com/

Abramovich, H., Harash, E., Milgrom, C., & Amit, U. (2009). Energy Harvesting From Airport Runway.

Advanced Linear Devices. (2011). Advanced Linear Devices. Retrieved April 6, 2011, from http://www.aldinc.com/

Altshuller, G. S. (1984). *Creativity As An Exact Science*. Luxembourg: Gordon and Breach.

AmbioSystems. (2011). AmbioSystems LLC | Home. Retrieved March 28, 2011, from http://www.ambiosystems.com/

American Radio Relay League. (2011). *The ARRL Handbook for Radio Communications*. (American Radio Relay, Ed.) (6th ed.). ARRL.

Amirtharajah, R., & Chandrakasan, a P. (1998). Self-powered signal processing using vibration-based power generation. *IEEE Journal of Solid-State Circuits*, *33*(5), 687-695. doi:10.1109/4.668982

Annalisa Bonfiglio, & Danilo De Rossi (Eds.). (2010). *Wearable Monitoring Systems*. Springer.

Armstrong, B., & Wit, C. C. de. (1995). Friction Modeling and Compensation. *The Control Handbook*. CRC Press.

Arnold, D. P. (2007). Review of Microscale Magnetic Power Generation. *IEEE Transactions on Magnetics*, *43*(11), 3940-3951. doi:10.1109/TMAG.2007.906150

Baxter, L. K. (1996). *Capacitive Sensors: Design and Applications* (p. 320). John Wiley and Sons.

Beeby, S. P., & O'Donnell, T. (2008). Electromagnetic Energy Harvesting. In D. J. Priya, Shashank And Inman (Ed.), *Energy Harvesting Technologies* (pp. 129-161). Springer Publishing Company, Incorporated. doi:10.1007/978-0-387-76464-1

Beeby, S. P., Torah, R. N., Tudor, M J, Glynne-Jones, P., O'Donnell, T., Saha, C. R., & Roy, S. (2007). A micro electromagnetic generator for vibration energy harvesting. *Journal of Micromechanics and Microengineering*, *17*(7), 1257-1265. doi:10.1088/0960-1317/17/7/007

Beeby, S. P., Tudor, M J, & White, N M. (2006). Energy harvesting vibration sources for microsystems applications. *Measurement Science and Technology*, *17*(12), R175-R195. doi:10.1088/0957-0233/17/12/R01

Boca Bearing. (2011). . Retrieved August 26, 2011, from http://www.bocabearings.com/

Bradford, P., & Pabst, S. (2009). Energy Generating Expansion Joint.

Burke, A. (2000). Ultracapacitors: why, how, and where is the technology. *Journal of Power Sources*, *91*(1), 37-50. doi:10.1016/S0378-7753(00)00485-7

von Büren, T., & Tröster, G. (2007). Design and optimization of a linear vibration-driven electromagnetic micro-power generator. *Sensors and Actuators A: Physical*, *135*(2), 765-775. doi:10.1016/j.sna.2006.08.009

Challa, V. R., Prasad, M. G., Shi, Y., & Fisher, F. T. (2008). A vibration energy harvesting device with bidirectional resonance frequency tunability. *Smart Materials and Structures*, *17*(1), 015035. doi:10.1088/0964-1726/17/01/015035

Charnegie, D. (2007). *Frequency Tuning Concpets For Piezoelectric Cantilever Beams and Plates for Energy Harvesting*. *Work*. University of Pittsburgh.

Cheung, Y. K., Au, F. T. K., Zheng, D. Y., & Cheng, Y. S. (1999). Vibration of Multi-Span Non-Uniform Bridges Under Moving Vehicles and Trains By Using Modified Beam Vibration Functions. *Journal of Sound and Vibration*, *228*(3), 611-628. doi:10.1006/jsvi.1999.2423

Cottone, F., Vocca, H., & Gammaitoni, L. (2009). Nonlinear Energy Harvesting. *Physical Review Letters*, *102*(8), 1-4. doi:10.1103/PhysRevLett.102.080601

Crown Audio. (2011). Crown Amplifiers. Retrieved August 8, 2011, from http://www.crownaudio.com/amps.htm

Curry, D. (2008). *Energy Harvesting for Bridge Monitoring*. Clarkson University.

Cymbet. (2011). Cymbet EnerChip Solid State Energy Storage for Thin Film Batteries and Power Management. Retrieved January 19, 2011, from http://cymbet.com/

Danielsson, O. (2003). Design of a Linear Generator for Wave Energy Plant. *Office*, (January).

Dick, B., Fralick, M., Jazo, H., Kerber, M., & Waters, R. (2009). *Powering of wireless sensors through the exclusive use of kinetic energy*. *2009 IEEE Sensors* (pp. 1406-1409). Christchurch: IEEE. doi:10.1109/ICSENS.2009.5398431

Dick, B., Fralick, M., Jazo, H., Kerber, M., Brewer, J., & Waters, R. (2009). *Optimization of kinetic energy harvester for low amplitude vibration*. *2009 IEEE Sensors* (pp. 1840-1843). IEEE. doi:10.1109/ICSENS.2009.5398420

Dierks, E. C. (2011). Xmarks Shared Bookmarks Folder, Literature Review B. Retrieved January 19, 2011, from http://share.xmarks.com/folder/bookmarks/iaJ2yLUUbD

Duderstadt, J. J. (chair). (2005). *Committee to Assess the Capacity of the United States Engineering Research Enterprise, Engineering Research and America's Future: Meeting the Challenge of a Global Economy*. Washington, D.C.: National Academies Press.

Ed Fagan Inc. (2011). Special Purpose Metals and Alloys for High Technology Industries from Ed Fagan Inc. Retrieved August 8, 2011, from http://www.edfagan.com/

El-hami, M., Glynne-Jones, P., White, N. M., & Beeby, S. P. (2000). Design analysis of a self-powered micro-renewable power supply. *International Conference on Electrical Machines 2000 (ICEM)*.

El-hami, M., Glynne-Jones, P., White, N.M., Hill, M., Beeby, S. P., James, E., Brown, A. D., et al. (2001). Design and fabrication of a new vibration-based electromechanical power generator. *Sensors and Actuators A: Physical*, *92*(1-3), 335-342. doi:10.1016/S0924-4247(01)00569-6

Electric-Auto. (2011). Comparison of Different Battery Technologies. Retrieved January 2, 2011, from http://electric-auto.org

Energy Harvesting Forum. (2011). List of Manufacturers. Retrieved January 2, 2011, from http://www.energyharvesting.net/

Federal Highway Administration. (2010). Deficient Bridges by State and Highway System. Retrieved February 14, 2011, from http://www.fhwa.dot.gov/bridge/nbi/defbr10.cfm

Field, T., Energy, O., Begins, H., & Ripen, T. (n.d.). The Field Of Energy Harvesting Begins To Ripen. *Electronic Design*.

Gerl, B. (2007). Piggybanks for Power. *Pictures of the Future: Materials for the Environment: Energy Storage*. Retrieved from http://www.siemens.com/innovation/en/publikationen/publications_pof/pof_fall_2007/materials_for_the_environment/energy_storage.htm

Gieras, J., Oh, J.-H., Huzmezan, M., & Sane, H. (2005). Electromechanical Energy Harvesting System.

Glynne-Jones, P., Tudor, M J, Beeby, S. P., & White, N M. (2004). An electromagnetic, vibration-powered generator for intelligent sensor systems. *Sensors and Actuators A: Physical*, *110*(1-3), 344-349. doi:10.1016/j.sna.2003.09.045

Google. (2010). Google Labs Books Ngram Viewer. Retrieved 2010, from http://ngrams.googlelabs.com/

Harrop, P. (2009). An Introduction to Energy Harvesting. *IDTechEX Report*. IDTechEX. Retrieved from http://www.energyharvestingjournal.com

Helix Wind. (2011). S322 Turbine. Retrieved December 1, 2011, from http://www.helixwind.com

Huggins, R. A. (2010). *Energy Storage*. *Media* (p. 406). Springer.

Humdinger Wind Energy LLC. (2011). Windbelt Innovation: Overview. Retrieved March 7, 2011, from http://www.humdingerwind.com

IDTechEx. (2011). Energy Harvesting Journal. Retrieved March 20, 2011, from http://www.energyharvestingjournal.com

Infinitie Power Solutions. (2010). Infinite Power Solutions. Retrieved January 19, 2011, from http://www.infinitepowersolutions.com/

Jewell, G. W., & Howe, D. (2002). A low-power, linear, permanent-magnet generator/energy storage system. *IEEE Transactions on Industrial Electronics*, *49*(3), 640-648. doi:10.1109/TIE.2002.1005391

Joseph A. Paradiso, T. S. (2005). Energy Scavenging for Mobile and Wireless Electronics. *PERVASIVE Computing*, 18-27. IEEE CS and IEEE Com/Soc.

Khaligh, A., & Onar, O. C. (2009). *Energy Harvesting: Solar, Wind, and Ocean Energy Conversion Systems* (p. 350). Taylor and Francis.

Kotter, D. K., Novack, S. D., Slafer, W. D., & Pinhero, P. (2008). Solar Nantenna Electromagnetic Collectors. *2nd International Conference on Energy Sustainability, ASME* (pp. 1-7).

Labworks. (2011). Labworks Inc.- Vibration Test Products. Retrieved August 8, 2011, from http://www.labworks-inc.com/

Li, H. (2008). *A linear generator powered from bridge vibrations for wireless networks*. Clarkson University.

Li, H., & Pillay, Pragasen. (2007). A Linear Generator Powered from Bridge Vibrations for Wireless Sensors. *2007 IEEE Industry Applications Annual Meeting*, 523-529. Ieee. doi:10.1109/07IAS.2007.85

Li, H., & Pillay, Pragasen. (2008). A Methodology to Design Linear Generators for Energy Conversion of Ambient Vibrations. *2008 IEEE Industry Applications Society Annual Meeting*, 1-8. Ieee. doi:10.1109/08IAS.2008.72

Linear Technology. (2011). Linear Technology - Home Page. Retrieved April 6, 2011, from http://www.linear.com/

MWS Industries. (2011). Copper Magnet Wire Data. Retrieved May 26, 2011, from http://www.mwswire.com/pdf_files/mws_tech_book/copper_magnet_wire_data.pdf

Mann, B. P., & Sims, N. (2009). Energy harvesting from the nonlinear oscillations of magnetic levitation. *Journal of Sound and Vibration*, *319*(1-2), 515-530. doi:10.1016/j.jsv.2008.06.011

Martinez, S. (1978). Highway Turbine.

Microstrain. (2011). Microstrain: Wireless Systems -EH-Link™ Energy Harvesting Wireless Sensor Node. Retrieved March 28, 2011, from http://www.microstrain.com/eh-link.aspx

Mide. (2011). Volture Vibration Energy Harvesters. Retrieved December 1, 2011, from http://www.mide.com

Missouri Department of Transportation. (2011). Bridge Inspection with Snooper. Retrieved March 16, 2011, from http://www.modot.gov/newsroom/archives/2007.htm

Moog Crossbow. (2011). Moog Crossbow: The Smart Sensors Company. Retrieved August 8, 2011, from http://www.xbow.com/

NIST Technology Innovation Program. (2008). *Advanced Sensing Technologies for the Infrastructure: Roads, Highways, Bridges and Water*. *Environmental Protection* (pp. 1-8). Gaithersburg, MD.

National Climatic Data Center. (2011). Online Climate Data Directory. Retrieved March 6, 2011, from http://lwf.ncdc.noaa.gov/oa/climate/climatedata.html

National Instruments. (2011). What is a Wireless Sensor Network? Retrieved March 16, 2011, from http://sine.ni.com

National Transportation Safety Board. (2007). *Highway Accident Report: Collapse of I-35W Highway Bridge Minneapolis, Minnesota August 1, 2007*. *Transportation*. Retrieved from http://www.dot.state.mn.us/i35wbridge/

New Energy Watch. (2011). VAWT Versus HAWT Wind Power. Retrieved January 12, 2011, from http://www.newenergywatch.com

Paloheimo, H., & Omidiora, M. (2009). A Feasibility Study on Compressed Air Energy Storage System for Portable Electrical and Electronic Devices. *2009 International Conference on Clean Electrical Power*, 355-362. Ieee. doi:10.1109/ICCEP.2009.5212029

Perpetuum. (2011). Perpetuum PMG37 Micro-generator. Retrieved December 1, 2011, from http://www.perpetuum.com

Pisano, G. P., & Shih, W. C. (2009). Restoring American Competitiveness. *Harvard Business Review*, (July-August), 114-125.

Pistoia, G. (2005). *Batteries for portable devices* (p. 296). Elsevier.

Priya, S., & Inman, D. J. (Eds.). (2008). *Energy Harvesting Technologies* (1st ed.). Springer. doi:10.1007/978-0-387-76464-1

RITA. (2007). Maps of Structurally Deficient Bridges on the National Highway System. Retrieved March 16, 2011, from http://www.bts.gov/programs/geographic_information_services/maps

Renewable Energy Research Laboratory: University of Massachusetts at Amherst. (2011). Wind Power: Capacity Factor, Intermittency, and what happens when the wind doesn't blow? Amherst. Retrieved from http://www.ceere.org/rerl/about_wind

Retti, K. L. (2007). Multiple Layer Solar Energy Harvesting Composition and Method.

Rincon-Mora, G. A. (2009). Harvesting Microelectronic Circuits. In S. Priya & Daniel J. Inman (Eds.), *Energy Harvesting Technologies* (pp. 287-321). Springer. doi:10.1007/978-0-387-76464-1

Robert McNeel & Associates. (2011). Rhinoceros: NURBS modeling tools for designers. Retrieved August 8, 2011, from http://www.rhino3d.com/rp.htm

Roundy, S., Wright, P. K., & Rabaey, J. M. (2004). *Energy scavenging for wireless sensor networks: with special focus on vibrations* (p. 212). Springer.

Rutman, J. (2004). Magnetic Bearings: Theory and Practice, More or Less... Retrieved January 2, 2011, from http://physics.technion.ac.il/~rutman/jeremy's seminar.html

SAFT. (2007). Saft Batteries. Retrieved January 19, 2011, from http://www.saftbatteries.com/

Saez, M. L. M. (2004). *Energy Harvesting from Passive Human Power*. *Wearable Computers*.

Sazonov, E., Curry, D., & Pillay, P. (2009). Self-Powered Sensors for Monitoring of Highway Bridges. *IEEE Sensors Journal*, *9*(11), 1422-1429. doi:10.1109/JSEN.2009.2019333

Seiko. (2011). Kinetic Watch. Retrieved December 1, 2011, from http://www.seikowatches.com

Shearwood, C., & Yates, R. B. (1997). Development of an electromagnetic microgenerator. *Electronics Letters*, *33*(22), 1883-1884.

Silicon Solar. (2011). Flexible Solar Panels - Consumer Ready Modules - OEM. Retrieved November 1, 2011, from http://www.siliconsolar.com

Silva, C. W. D. (2000). *Vibration: Fundamentals and Practice* (Vol. 0, p. 943). CRC Press.

Smith, R. L. (1978). Road Vehicle-Actuated Air Compressor and System Therefor.

Solar Panel Center. (2011). Types of Solar Panels. Retrieved March 7, 2011, from http://www.solarpanelcenter.net

Spreeman, D., Folkmer, B., Maurath, D., & Manoli, Y. (2006). Tunable Transducer for low frequency vibrational energy scavenging. *Proceedings, EurosensorsXX (Goteborg, Sweeden).*

Starner, T. (1996). Human-powered wearable computing. *IBM Systems Journal*, *35*(3), 618-629. doi:10.1147/sj.353.0618

Stephen, N. (2006). On energy harvesting from ambient vibration. *Journal of Sound and Vibration*, *293*(1-2), 409-425. doi:10.1016/j.jsv.2005.10.003

Sundance Power Systems Inc. (2011). Solar Insolation for U.S. Major Cities. Retrieved March 7, 2011, from http://www.sundancepower.com

Sunforce Products Inc. (2011). Sunforce 400-Watt Wind Generator. Retrieved December 1, 2011, from http://www.sunforceproducts.com

The MathWorks. (2011). Translational Friction: Simulate friction in contact between moving bodies. Retrieved May 25, 2011, from http://www.mathworks.com/help/toolbox/physmod/simscape/ref/translationalfriction.html

Toberman, C. E. (1975). Expressway Power Generating System.

ToolStore. (2011). Faraday Flashlight. Retrieved December 1, 2011, from http://homebuildshoptools.com

Turner-Fairbank Highway Research Center: Federal Highway Administration. (2001). *Reliability of Visual Bridge Inspection*. Retrieved from http://www.tfhrc.gov/pubrds/marapr01/bridge.htm

Ueno, T., Summers, E., Wun-Fogle, M., & Higuchi, T. (2008). Micro-magnetostrictive Vibrator Using Iron-Gallium Alloy. *Sensors and Actuators A: Physical*, *148*(1), 280-284. doi:10.1016/j.sna.2008.08.017

Voltree Power. (2009). Bioenergy Harvester. Retrieved January 12, 2011, from http://voltreepower.com

Wang, B. T.-lo, Huang, D., & Shahawy, M. (1992). Dynamic Response of Multigirder Bridges. *Structural Engineering*, *118*(8), 2222-2238.

Wang, Z. L., & Kang, Z. C. (1998). *Functional and Smart Materials: Structural Evolution and Structure Analysis* (p. 514). Springer.

Weaver, J. M. (2010). Xmarks Shared Bookmarks Folder: Literature Review A. Retrieved January 19, 2011, from http://share.xmarks.com/folder/bookmarks/xAUnqum8uE

Weaver, J. M., Crawford, R. H., & Wood, K. L. (2010). Design of Energy Harvesting Technology: Feasibility For Low-Power Wireless Sensor Networks. *ASME 2010 International Design Engineering Technical Conferences & Computers and Information in Engineering Conference* (pp. 1-10). Montreal: ASME.

Weaver, J. M., Wood, K. L., & Crawford, R. H. (2011). Exploring Innovation Opportunities in Energy Harvesting Using Functional Modeling Approaches. *ASME 2011 International Design Engineering Technical Conferences*. Washington, D.C.

Wikipedia Contributors. (2005). Darrieus Wind Turbine. *Wikipedia, The Free Encyclopedia*. Retrieved March 6, 2011, from http://en.wikipedia.org/wiki/File:Darrieus-windmill.jpg

Williams, C. B., & Yates, R. B. (1996). Analysis of a micro-electric generator for microsystems. *Sensors and Actuators A: Physical*, *52*, 8-11.

Windspire Energy. (2011). Windspire Wind Turbine. Retrieved December 1, 2011, from http://www.windspireenergy.com

Wood, S. L., & Dean, P. K. (2007). *Methodology for the Quantitative Evaluation of the Remaining Fatigue Life of Fracture Critical Bridges*. Austin.

Wu, X., Lin, J., Kato, S., Zhang, K., Ren, T., & Liu, L. (2008). A frequency adjustable vibration energy harvester. *PowerMEMS 2008+ microEMS 2008* (pp. 245-248). Sendai.

Xing, X., Lou, J., Yang, G. M., Obi, O., Driscoll, C., & Sun, N. X. (2009). Wideband vibration energy harvester with high permeability magnetic material. *Applied Physics Letters*, *95*(13), 134103. doi:10.1063/1.3238319

Xue, H., Hu, Y., & Wang, Q.-M. (2008). Broadband piezoelectric energy harvesting devices using multiple bimorphs with different operating frequencies. *IEEE transactions on ultrasonics, ferroelectrics, and frequency control*, *55*(9), 2104-8. doi:10.1109/TUFFC.903

Yang, B., Lee, C., Xiang, W., Xie, J., Han He, J., Kotlanka, R. K., Low, S. P., et al. (2009). Electromagnetic energy harvesting from vibrations of multiple frequencies. *Journal of Micromechanics and Microengineering*, *19*(3), 035001. doi:10.1088/0960-1317/19/3/035001

Yin, X., Fang, Z., Cai, C. S., & Deng, L. (2010). Non-stationary random vibration of bridges under vehicles with variable speed. *Engineering Structures*, *32*(8), 2166-2174. Elsevier Ltd. doi:10.1016/j.engstruct.2010.03.019

Zhu, D., Roberts, S., Tudor, Michael J, & Beeby, S. P. (2008). Closed Loop Frequency Tuning of a Vibration-Based Micro-Generator. *PowerMEMS 2008+ microEMS 2008* (pp. 229-232). Sendai.

Zhu, D., Tudor, Michael J, & Beeby, S. P. (2010). Strategies for increasing the operating frequency range of vibration energy harvesters: a review. *Measurement Science and Technology*, *21*(2). doi:10.1088/0957-0233/21/2/022001

Vita

Eric Carl Dierks was born and raised in Round Rock, Texas and earned his Bachelor of Science in Mechanical Engineering from the University of Texas at Austin in December 2008. Following this he worked for the Institute for Advanced Technology in Austin modeling, simulating, optimizing, and testing battery-inductor pulsed power supplies for electromagnetic rail guns for the United States Army and Navy. There, he also briefly served as a reviewer for Carnegie Mellon's Autonomous Platform Demonstrator robotic program. Upon completion of this thesis he plans to begin work in the engineering design, energy harvesting, or automation fields.

Email: ericcdierks@gmail.com
Phone: (512) 630-6634
Permanent Address: 300 Gladeview Dr. Round Rock, Texas 78681
Online Resume: www.linkedin.com/pub/eric-dierks/a/9a7/9b9

This thesis was typed by Eric Carl Dierks.